8279

THE FREE AIR LASER STRAIN METER

(A Feasibility Study of a New Method of Observing Tectonic Motions)

by

WAYNE HARRY CANNON

B.Sc., University of British Columbia, 1963
M.Sc., University of British Columbia, 1967

A THESIS SUBMITTED IN PARTIAL FULFILMENT OF

THE REQUIREMENTS FOR THE DEGREE OF

DOCTOR OF PHILOSOPHY

in the Department

of

GEOPHYSICS

We accept this thesis as conforming to the required standard

THE UNIVERSITY OF BRITISH COLUMBIA

September, 1970

In presenting this thesis in partial fulfilment of the requirements for an advanced degree at the University of British Columbia, I agree that the Library shall make it freely available for reference and Study. I further agree that permission for extensive copying of this thesis for scholarly purposes may be granted by the Head of my Department or by his representatives. It is understood that copying or publication of this thesis for financial gain shall not be allowed without my written permission.

Department of GEOPHYSICS

The University of British Columbia
Vancouver 8, Canada

Date April 20, 1971

ABSTRACT

Theoretical investigation into the feasibility of making laser strain meter measurements over large distances through the uncontrolled atmosphere indicate that such observations are likely possible with present day technology. The observing device, here-in called a free air laser strain meter, would use laser output at three frequencies, appropriately spaced in the spectrum, coupled with the dispersion of the atmosphere to separate "geometrical" fluctuations from "refractive" fluctuations of the optical path length between the end mirrors of the strain meter. The geometrical fluctuations can be averaged to reveal tectonic changes in distance between the end mirrors.

Theoretical expressions for averaging times, confidence limits, strain sensitivity, accuracy of observations, fringe count rate, fringe visibility, aperture size and laser power are derived in terms of the relevant physical, geophysical, and atmospheric parameters.

Free air laser strain meters, like conventional laser strain meters, appear to be capable of measuring earth strain over distances of several Kms. up to the limit of frequency stability of the laser in the presence of moderate atmospheric turbulence. In the free air laser strain meter the laser frequency stability and not atmospheric effects is the ultimate factor limiting strain sensitivity.

Over distances of several kilometers free air laser strain meters are theoretically able to make strain measurements more sensitively, ($\frac{\delta D}{D} \backsim 10^{-11} - 10^{-12}$) , and more rapidly, (observation interval $\Delta\tau \backsim$ 10 minutes - 1 hour) , than any other device, known or proposed, operating through the uncontrolled atmosphere. The successful operation of free air laser strain meters would represent an improvement over present methods by a factor of $10^3 - 10^4$ in sensitivity of observation. The realization of free air laser strain meters would provide geophysicists in the fields of geodesy and tectonics with a tool of unusual capabilities and as such would be recognized as a major advance.

TABLE OF CONTENTS

	Page
ABSTRACT	ii
LIST OF FIGURES	vii
ACKNOWLEDGEMENTS	viii
CHAPTER I PREFACE	1
CHAPTER II INTRODUCTION	
A. GEODETIC MEASUREMENTS OF TECTONIC MOTIONS	
1. The Geodimeter	4
2. Accuracy of Measurement	5
3. Results	7
B. LASER STRAIN METER MEASUREMENTS OF TECTONIC MOTION	
1. The Laser Strain Meter	9
2. Accuracy of Measurement	13
3. Results	14
C. OUTDOOR OPTICAL INTERFEROMETRY	
1. Y. Väisälä	16
2. K. E. Erickson	18
CHAPTER III FREE AIR LASER STRAIN METERS	
A. CONCEPTION	22
B. THEORY	
1. Separation of "Geometrical" and "Refractive" Optical Path Length Fluctuations	25
2. Statistical Analysis of Free Air Laser Strain Meter Observations to Reveal Tectonic Motions	38

Page

3. Statistical Analysis of Fluctuations in Ray-Path of a Laser Beam Propagating Through a Turbulent Atmosphere

a. The Problem of Random Flights 50

b. Calculation of Probability Density Function for $\epsilon(t)$ 55

c. Calculation of Probability Density Function for $\delta S(\Delta t)$ 67

4. Free Air Laser Strain Meter Observations 70

5. Accuracy of Observations

a. Error Propagation Analysis 74

b. Systematic Errors 80

c. Random Errors 86

d. Accuracy of Fringe Counting 89

C. FRINGE OBSERVATION

1. Degenerating Effects of the Atmosphere on a Laser Beam 93

2. Fraunhofer Diffraction for a Double Rectangular Aperture 96

3. Fringe Visibility 103

4. Fringe Counting Rate 117

D. POWER REQUIREMENTS 120

CHAPTER IV CONCLUSIONS

A. SUMMARY OF RESULTS 130

B. APPLICATIONS OF FREE AIR LASER STRAIN METERS

1. Tectonic Research 138

2. Earthquake Prediction 139

3. Engineering 143

Page

APPENDIX A-1 THE GAS LASER

1. Operating Characteristics 144

2. Frequency Stability 149

APPENDIX A-2 THE REFRACTIVE INDEX OF THE ATMOSPHERE

1. Formula for Refractive Index 154

2. Statistical Properties of Atmospheric Refractive Index 158

APPENDIX A-3 MATHEMATICAL APPENDIX 164

APPENDIX A-4 GEOPHYSICAL AND ATMOSPHERIC PARAMETERS 171

APPENDIX A-5 LIST OF SYMBOLS 177

BIBLIOGRAPHY 180

LIST OF FIGURES

Figure		Page
II-1	Schematic of Conventional Laser Strain Meter	11
II-2	The Väisälä Comparator	17
II-3	The Interferometer of K. E. Erickson	20
III-1	Schematic of a Free Air Laser Strain Meter System	24
III-2	Parameterization of the Atmospheric Ray Paths	26
III-3	Analysis of Free Air Laser Strain Meter Observations	42
III-4	Angular Parameters of Atmospheric Ray-Path	51
III-5	Straight Line Approximation to the Atmospheric Ray-Path	59
III-6	Fraunhofer Diffraction from a Double Rectangular Aperture	97
III-7	Intensity Pattern, I(xy), from Fraunhofer Diffraction Through a Double Rectangular Aperture	101
III-8	Coherence Between Apertures #1 and #2	105
IV-1	Example of Observed Earthquake Strain Percursor	140
A-1-1	Frequency Distribution of Laser Output	147

ACKNOWLEDGEMENTS

I would like to formally acknowledge the encouragement and counsel of Dr. M. W. Ovenden and Dr. D. E. Smylie whose support during this research is greatly appreciated. In addition I would like to thank my colleague, Mr. O. Jensen, for the contribution of many helpful criticisms and suggestions.

I am also grateful to the Department of Geophysics, U.B.C. under Dr. R. D. Russell for financial support during this research. Sincere thanks is owed to Miss J. Kalmakoff for a very able and accurate job of typing.

CHAPTER I

PREFACE

Throughout history advances in man's ability to accurately measure distances both atomic and galactic have resulted in profound changes in his world view. This is illustrated by contrasting the ancient Greeks with that of any of their contemporaries. While other Europeans held that the world was flat with "edges" which were to be avoided the Greeks of the time held the world to be a rigid sphere suspended in the space of the heavens. This enlightenment on behalf of the Greeks is owed to Eratosthenes who measured the radius of the globe in about 240 B.C. [1]. It is no accident that Eratosthenes accomplished this while head of the Library of Alexandria, Egypt, for it was from the Egyptians, who had developed it to resurvey the arable lands of the Nile Valley after its annual flood, that the Greeks learned the science of geodesy.

Modern geodetic measurements can establish the coordinates of any location on the earth's surface to within a circle a few meters in diameter [2]. This advance in accuracy of measurement reveals many undulations in the shape of the geoid and has changed man's view of the planet's interior from static to dynamic.

While it is conceded that on the basis of geologic evidence large tectonic motions have occurred in the earth's crust producing correspondingly large changes of geodetic coordinates, time dependence is not a consideration in most geodetic surveys. Tectonic changes in geodetic coordinates, except in cases of catastrophe, occur at rates small enough to have been of no concern to classical geodesy. However with the development of the laser strain meter and long baseline radio interferometry the observation of tectonic motions in real time both locally and globally is possible [3]. These advances in man's ability to measure distance will once again alter his world view and render geodesy a time dependent discipline.

As part of this general trend this thesis is presented as a proposal to combine the particular advantages of geodimeters, i.e., operating ability over long distances through the uncontrolled atmosphere, with those of the laser strain meter, i.e., high strain sensitivity resulting from the direct interference of photons, to realize a "free air laser strain meter" to be applied to geodetic and tectonic studies. To introduce this thesis and present background information pertinent to its understanding it is necessary to briefly discuss the two methods of observing tectonic motions, the geodetic survey method and the laser strain meter method; and in addition discuss two notable achievements in the field of outdoor optical interferometry.

The presentation of the thesis has been a somewhat difficult task as it draws from several diverse areas of physics. I have chosen to simplify the presentation by including several calculations and supporting arguments in a series of appendices to which the reader can refer if so moved by curiosity or doubt.

CHAPTER II

INTRODUCTION

A. GEODETIC MEASUREMENTS OF TECTONIC MOTIONS

1. The Geodimeter

The geodimeter [4] is an electro-optical distance measuring device which uses the transit time of a light signal between source and receiver to measure distance. The geodimeter emits a collimated light beam whose intensity is modulated at radio frequencies by means of a Kerr cell linked to a crystal oscillator. The light beam is directed to a distant retro-reflecting device and the returned modulated light beam is photo-detected by a receiver on the geodimeter. The total phase difference between the emitted and received modulated light signals is proportional to the round trip distance between geodimeter and reflector. This phase difference is measured electronically to within a multiple of 2π and thus the emitter-receiver distance is determined to within an integral number of wavelengths of the modulated beam. Repeating the measurement at several modulation frequencies reduces the ambiguity in the order number of interference between the emitted and received signal and hence reduces the ambiguity in the emitter-receiver distance. In general, observations at three closely spaced modulation frequencies along with knowledge of the approximate emitter-receiver distance obtained from maps, aerial photographs, or

rougher surveys are sufficient to allow a precise measure of the required distance. Geodimeters can work effectively up to distances of 20-50 km.

2. Accuracy of Measurement

The largest single source of error in all terrestrial electronic distance measurement is the uncertainty in the mean signal propagation velocity due to an uncertainty in the mean group refractive index value of the atmosphere along the propagation path. The mean refractive index value along the beam is often estimated from measurements of atmospheric pressure, temperature and humidity taken at one or more points along the light path. Under favourable meteorological conditions distance measurement reproducible to one or two parts in 10^6 can be made. This corresponds to an error of ±1-2 cm. in a 10 km. distance. More commonly, however, survey closure errors of several parts in 10^6 are encountered [5].

A more sophisticated and potentially more accurate method of measuring the mean refractive index along the light path is through the observation of the relative atmospheric dispersion of two or three different color geodimeter beams. This method reflects a true spatial average of the refractive index along the light path and hence is in principle superior to the method of spot sampling of atmospheric pressure, temperature and humidity.

In the case of dry air the magnitude of the relative dispersion between geodimeter beams of two different colors is proportional to the mean air density and hence the mean refractive index along the light path. The observation of this dispersion gives sufficient information to calculate the spatial average density for dry air and hence the desired mean refractive index. In practice however, the atmosphere contains variable amounts of water vapour with a dispersion different from that of air [A-2]. The two-color dispersion method, by neglecting the presence of water vapour, is subject to errors in the estimated value of mean refractive index of up to several parts in 10^6 depending on atmospheric conditions [7]. This shortcoming of the two-color dispersion method can be reduced by spot sampling the humidity at points along the light path. The two-colour dispersion method supplemented with an independent measurement of the mean humidity along the light beam can in principle provide an estimate of the mean refractive index along the ray path accurate to one part in 10^7 [7].

The addition of a third color will render the dispersion method sensitive to spatial averages along the beam of pressure, temperature, and humidity; thus allowing an estimate of the mean refractive index accurate to 2-3 parts in 10^8 [7]. The three-color dispersion method ignores variations in CO_2 content of the atmosphere, the next most significant atmospheric variable after water vapour. However the variations in

CO_2 content expected to be encountered in the uncontrolled atmosphere are so small as to cause refractive index variations of only one part in 10^9 [21].

A further limitation on the accuracy of geodimeter length measurement is the uncertainty in the light beam modulation frequency. The frequency stability of geodimeter oscillators is approximately one part in 10^7 and so geodimeter measurements to higher accuracies are not possible without a calibration of the instrument against some more accurate oscillator. Since the use of geodimeters to observe tectonic motions requires repeated measurements of a given distance separated by an interval of several months, oscillator stability is an important consideration in such observations.

3. Results

One of the most thorough and extensive programs of measuring tectonic motions by the geodetic survey method has been carried out continuously since 1959 in California by the State of California Department of Water Resources [8]. In a program intended to aid the design and layout of the aquaducts for the two billion dollar California State Water Project a network of over 3000 km. of geodimeter lines has been laid out in a criss-cross fashion over the San Andreas and related fault systems. Geodetic length determinations of these lines are

repeated at intervals of the order of months. Atmospheric refractive index corrections to the geodimeter measurements are made from data obtained by spot sampling of the atmospheric pressure temperature and humidity at points along the geodimeter line. The accuracy of measurement as indicated by closure errors is typically one part in 10^6, although this figure can vary somewhat according to observing conditions.

Movement on the California fault system is found to vary, in a rather complex manner from location to location, from zero to over 4 cm./year. Changes in the rate of fault movement are found to be related to the occurrence of earthquakes within the regions. Anomalous length changes of geodimeter lines generally foreshadow local earthquakes. The result of the California measurements strongly indicate that large movements and high rates of movement precede an earthquake by hours or days and that continuous or near continuous monitoring of suspected earthquake sites could be used to forecast earthquakes and issue short-range warnings.

The development of two-color dispersion laser geodimeter systems has reached the field testing stage [9] and although a complete three-color dispersion system has not yet operated the elements of such a system have been used separately [7]. Such devices can be expected to be capable of automatic and continuous strain monitoring with strain sensitivities of 10^{-7} - 10^{-8} in the near future.

B. LASER STRAIN METER MEASUREMENTS OF TECTONIC MOTIONS

1. The Laser Strain Meter

Laser strain meters generally consist of a unimodal frequency stabilized laser; the output of which is directed into an interferometer whose reflecting elements are fixed to the solid earth. The interferometer is coupled to a readout system which monitors the interference fringe pattern. A change in the length of the interferometer caused by earth strain is accompanied by a change in the order number of the interference; and is measured directly in terms of the wavelength of the laser output by counting fringes. Automatic and continuous monitoring of the interference fringes results in a record of earth strain as a function of time.

Laser strain meters are constructed using both the Michelson and Fabrey-Perot type interferometers. One method of using the Michelson scheme involves the construction of an equal-arm interferometer in which the mirror constituting one arm is not coupled to the earth but held rigid while the mirror constituting the other arm is fixed to the solid earth and is free to respond to earth strain. Any resulting inequalities in the lengths of the arms of the interferometer produce changes in the fringe pattern from which changes in ambient strain conditions are inferred.

The Fabrey-Perot interferometer is most often used in the construction of laser strain meters. In one illustration of the Fabrey-Perot scheme, Fig. II-1, both mirrors are fixed to the solid earth and an evacuated pipe interposed between them leaving only small air gaps at each end. In this scheme the laser beam traverses an evacuated path between the mirrors. This prevents changes in the optical path length between the end mirrors caused by pressure, temperature, and humidity fluctuations from being observed as "apparent" strain, indistinguishable from "real" strain by such an instrument. The air gaps between the end mirrors and the transparent ends of the evacuated pipe are kept as small as possible for the same reason. Most laser strain meters use a retro-reflecting device; often a plane mirror mounted at the focus of a converging lens; as the end element of the Fabrey-Perot resonator. This insures that the beam will always be returned to its proper position on the front element of the Fabrey-Perot etalon in spite of misalignments which occur due to tectonic activity.

When the laser is coupled to the interferometer it is desirable to reduce the light reflected from the optical surfaces of the interferometer back into the laser to a minimum. Allowing reflected light to re-enter the laser can result in the stimulation of unwanted modes of oscillation and must therefore be suppressed. This is generally done in laser strain meters by deliberate slight misalignment of the interferometer surfaces as well as by the use of quarter-wave

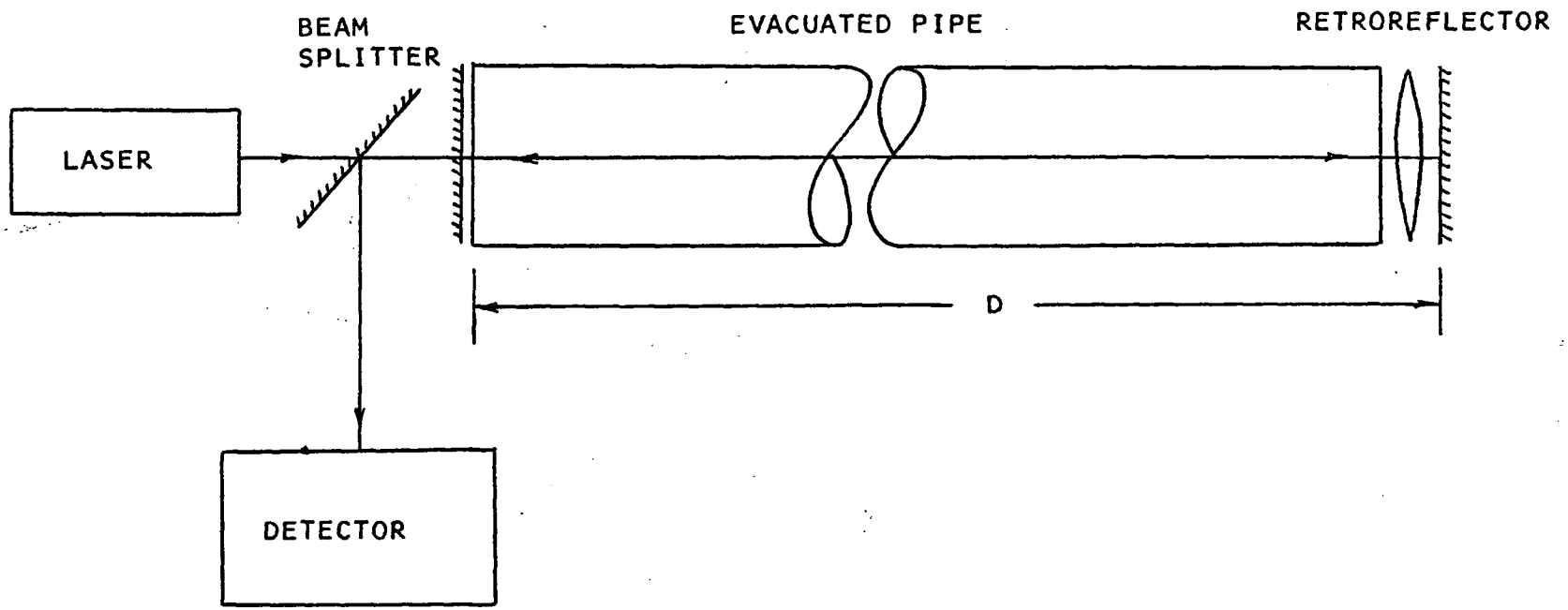

FIG. II-1

SCHEMATIC OF CONVENTIONAL LASER STRAIN METER

coatings. Quarter-wave coatings are effective in suppressing reflections from the optical surfaces because of the high monochromaticity of the laser output.

The fringe counter usually employs two photomultiplier tubes focussed on opposite sides of a fringe. As the fringes move in response to earth strain the output of the photomultiplier becomes unbalanced, the magnitude and sign of the imbalance being a measure of the fringe displacement. A means is provided for the fringe counter to move rapidly to a successive fringe when the fringe displacement reaches a given limit, usually one fringe width. Fringe counters capable of counting to one hundredth part of a fringe and as rapidly as a megacycle have been built.

Two Fabrey-Perot interferometers at right angles provide a set of reference axes relative to which components e_{11} and e_{22} of the strain tensor e_{ij} can be measured. The off diagonal components e_{12} and e_{21} can be measured by introducing a third strain meter oriented at 45° to the first two.

Laser strain meters exhibit some notable and advantageous properties not commonly found in measuring devices. The laser strain meter responds linearly to earth strain over an "infinite" range of amplitude. They also exhibit a flat

amplitude response with zero phase shift over all frequencies of tectonic activity from secular strain (D.C.) up to the highest frequencies observable by the readout system.

2. Accuracy of Measurement

Strain, being defined only at a point, cannot be strictly observed by any extended device. The laser strain meter measures the average strain over an extended region comparable in dimensions to the length of the strain meter arms. Although shortening the arms of the strain meter facilitates a truer measure of point strain it also results in a lower strain sensitivity. In addition the quantity usually of geophysical interest is the ambient strain field which is measured best by a strain meter of considerable extension. For these reasons laser strain meters range in length from a few meters to 1 km.

The accuracy of measurement of laser strain meters is limited mainly by the stability of the laser frequency $S\nu(\tau)$ [A-1, eqn. A-1-4]. If D is the length between the mirrors of a Fabrey-Perot laser strain meter and $\Delta D(\tau)$ is the change in the length D in an interval of time τ ; then the accuracy with which the strain, $\frac{\Delta D(\tau)}{D}$, is determined cannot exceed $S\nu(\tau) = \frac{\delta\nu(\tau)}{\nu}$. Thus laser strain meters presently have short period strain sensitivities as high as one part in 10^{12} [14] and long term strain sensitivities of one part in 10^{10} [15].

3. Results

Laser strain meters are able to observe most all of the seismic activity normally recorded by standard seismic equipment such as earthquake events and microseisms. However because of their flat response to tectonic activity down to zero frequency (secular strain) they have been most useful in studying long term, low frequency tectonic motions. In this regard they are unrivalled and consequently have revealed a variety of tectonic phenomena, some of which are not observable by other devices.

Laser strain meters which are set up straddling known fault zones are able to observe movement on the fault in real time. These measurements reveal that creep on the fault is episodic, appearing periodically with a back-and-forth motion super-imposed on it [14].

Laser strain meters are used to observe tides in the solid earth caused by lunar gravitational attraction. Earth tides are observed to have a 12 hour period with a strain amplitude of about 5 parts in 10^8 [16] which corresponds roughly to a vertical amplitude at the equator of the earth of 30 cm. The amplitude of earth tides is observed by laser strain meters to be about ten times larger than normal in the vicinity of a large fault confirming theoretical predictions of the build up of strain around faults in the earth's crust. Laser strain meters have also been used to observe fundamental modes of oscillation of the earth following large earthquakes.

Tectonic processes which are attributed to local mountain building processes are also observed by laser strain meters located in cordillera regions [16]. These phenomena appear as micro-tremors accompanied by unrecovered step changes in the ambient strain of a few parts in 10^9. Successive strain steps usually have the same sign which is indicative of some cumulative geologic process.

One of the most interesting phenomena revealed by laser strain meters are residual unrecovered strains of the order of parts in 10^8 observed at distances of thousands of km. from earthquake epicentres which appear to be directly associated with the seismic event [17]. Recent evidence suggests that a rapid imposition of strain at teleseismic distances may precede earthquakes by periods ranging from several minutes to several hours. In this regard Vali and Bostrom [15] report observing on a laser strain meter located in Washington State U.S.A. an approximately linear accumulation of strain amounting to 49 parts in 10^9 over a period of 30 minutes preceding a Central American earthquake of magnitude 5.7.

Extending laser strain meters, as they are currently conceived, to lengths of several km. would facilitate a measure of the relative tectonic motion of adjacent crustal blocks of unprecedented accuracy; exceeding the accuracy of the geodetic measurements by a factor of 10^3 - 10^5 depending on the length

of time over which the observation is made. This is not achieved in practice simply because of the technical difficulties and cost involved in constructing evacuated systems several km. in length. The encumberance of the evacuated pipe extending the full distance between the points over which relative displacements are to be measured has limited laser strain meters to lengths of 1 km. or less.

C. OUTDOOR OPTICAL INTERFEROMETRY

The observation of interference between two light beams which have traversed an appreciable distance along separate paths through the uncontrolled atmosphere (free-air) is difficult because of atmospheric turbulence. Fluctuations in atmospheric conditions are accompanied by corresponding fluctuations in refractive index. The atmospheric refractive index fluctuations produce several degenerating effects in the light beams which reduce interference effects to levels which are often below observable limits. In spite of the difficulties inherent in free-air interferometry at optical wavelengths, free-air interferometry has been applied by several workers to problems in geodesy and meteorology. The work of Y. Väisälä and K. E. Erickson is notable in this regard.

1. Y. Väisälä

In 1929, Y. Väisälä [18] developed a light interference comparator capable of measuring geodetic baselines up to lengths of 0.864 km. through the uncontrolled atmosphere

to accuracies which are claimed to be one part in 10^7. The comparator is shown schematically in Fig. II-2.

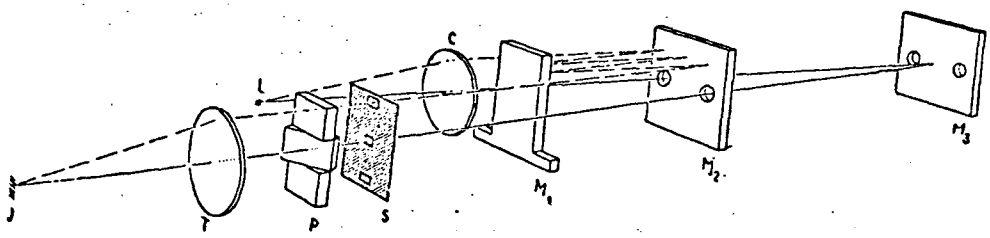

FIG. II-2

THE VAISALA COMPARATOR

Light from a white incandescent source L is collimated by a lens C and directed into two axially aligned Fabrey-Perot resonators defined by pairs of half silvered mirrors M_1M_2 and M_1M_3. White light interference fringes are observed in the telescope T when the two interfering beams have equal optical path lengths. This occurs when the distance M_1M_3 is an integral multiple of the distance M_1M_2. The distance M_1M_2 is established in the field by inserting a quartz gauge block 1 meter in length between the mirrors. A white light source is used for accuracy since white light fringes disappear if the optical path difference between the beams is but a few wavelengths whereas a monochromatic source will produce interference fringes between beams whose path

lengths differ by many millimeters.

The use of the Väisälä comparator ideally involves level terrain with the light beam about 1 meter above the ground. Temperature readings are taken simultaneously with the fringe observations at several points along the light path. The markers between which the comparator measures distance are usually set in large concrete blocks, buried underground for stability. The comparator can be used in any weather for distances of up to 0.1 km. but night-time observations are needed for long baseline work.

The Väisälä comparator has been used to establish several standard geodetic baselines around the world: Argentina 0.480 km.; the Netherlands 0.576 km.; Germany 0.864 km. and Finland 0.864 km.

2. K. E. Erickson

Erickson (19) has used free-air interferometry to investigate the accuracy with which optical length comparison can be made without close control or sampling of the atmosphere. Erickson's theoretical proposal involves the observation of channel spectrum interference between white light beams which have traversed different paths through free-air in the comparator. Erickson's theory indicates the possibility of establishing the order numbers of interference for fringes of the spectrum by counting the number of fringes in the channel

spectrum separating three standard wavelengths. Knowing the order numbers of interference for each of these three points in the channel spectrum and the refractivity formula for the atmosphere he is then able to calculate the contribution to the interference order arising out of purely geometrical path differences between the beams. It was hoped that this method applied to a device such as a Väisälä comparator would facilitate accurate determinations of geodetic baselines by optical means not requiring any measurement of atmospheric parameters along the light path.

Erickson's theory requires the relative refractivity of the atmosphere to be independent of atmospheric conditions. This condition does not hold for variable amounts of water vapour in the atmosphere. As a consequence of this Erickson's method involving three wavelengths does not facilitate free-air length comparisons much more accurate than those achieved by the Väisälä comparator, one part in 10^7, and requires a measure of atmospheric water vapour content along the light paths. However, it should be noted that Erickson's method extended to four wavelengths can cope with atmospheric variations in water vapour content. This involves determining the order of interference at a fourth point in the channel spectrum and extending the spectral range far into the ultraviolet.

To demonstrate the practicability of his theory Erickson constructed a free-air interferometer, shown schematically in Fig. II-3.

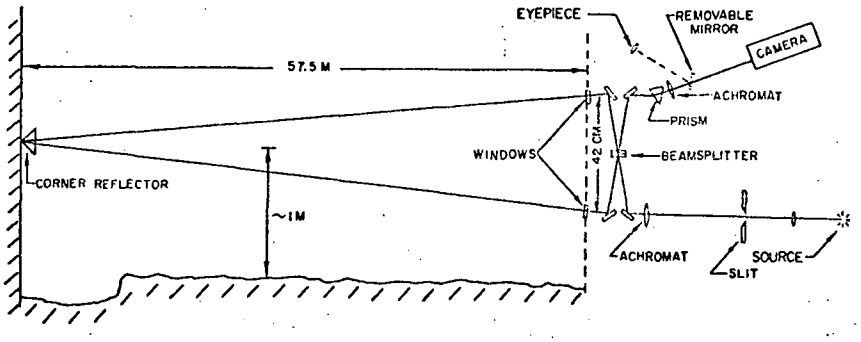

FIG. II-3

THE INTERFEROMETER OF K. E. ERICKSON

Radiation from the white light source is divided by the beam splitter and each fraction of the beam is sent in opposite directions around an outdoor path of total length 0.115 km. The channel spectrum interference pattern is recorded photographically by a camera. The beams were within 1.5 meters of the ground over their entire path where atmospheric conditions are normally least favourable. Under conditions too poor to obtain a channel spectrum the fringes remained visible but were unsteady and warped. Under good conditions the fringes were visible continuously and long, unbroken records of fringe motion were obtained. The aperture

of Erickson's interferometer was of the order of 3 cm. across. It was noted that under very unfavourable conditions the small scale atmospheric refractive index inhomogeneities were sufficiently intense to destroy phase coherence across the aperture causing the interference fringes to rapidly appear and disappear. This effect was observable in photographs of the fringes taken at 64 frames per second. Erickson concludes that good channel spectrum fringes could be obtained over distances of 0.5 km. or more.

CHAPTER III

FREE AIR LASER STRAIN METERS

A. CONCEPTION

The free air laser strain meter is a conception for extending laser strain meter measurements to distances of several kilometers or more through the uncontrolled atmosphere. There are two principle impediments to the realization of free air laser strain meters. The first is the difficulty of observing interference between optical signals which have traversed an appreciable distance along separate paths of a turbulent atmosphere. The second is the difficulty of interpreting any interference fringes observed in terms of tectonic displacements.

The difficulty of interpretation can be overcome by the use of three lasers of different frequencies. The dispersion of the atmosphere at optical frequencies will allow the separation of the fluctuations in optical path length between the end mirrors into "refractive" and "geometric" contributions. Tectonic activity can be revealed by filtering the data and observing any trends in the series of path length fluctuations.

It is proposed to overcome the difficulty of observing interference fringes by the use of a "double rectangle" interferometer and restricting the area of acceptance of the rectangular aperture to a "coherence patch" size. Light from

laser sources is no more immune to the degenerating effects of atmospheric turbulence than optical radiation from any other source, however, lasers offer the advantages of large spatial and temporal coherence at the output and high intensity both of which will be useful in minimizing observation difficulties.

One physical arrangement for a free air laser strain meter, which makes no claim to being optimal, is shown in Fig. III-1. It consists of three frequency stabilized lasers L_1 , L_2 and L_3 with frequencies ν_1 , ν_2 , ν_3 respectively whose outputs are combined by mirrors M_1 , M_2 , M_3 and directed by mirror M_4 to a retro-reflecting mirror M_6 at a distance D . A portion of the combined original output of the three lasers is transmitted by M_4 and directed into a prism p_1 . In a similar manner a portion of the combined return beam is directed by mirror M_5 located at O into a prism p_2 . The prisms separate the wavefronts into three optical channels which bring them to interfere in pairs at rectangular diffracting apertures I_1 , I_2 and I_3 are fringe counters C_1 , C_2 and C_3 . The fringe counts in a series of continuous consecutive intervals are the raw data from which tectonic changes in the length D are calculated by the readout system.

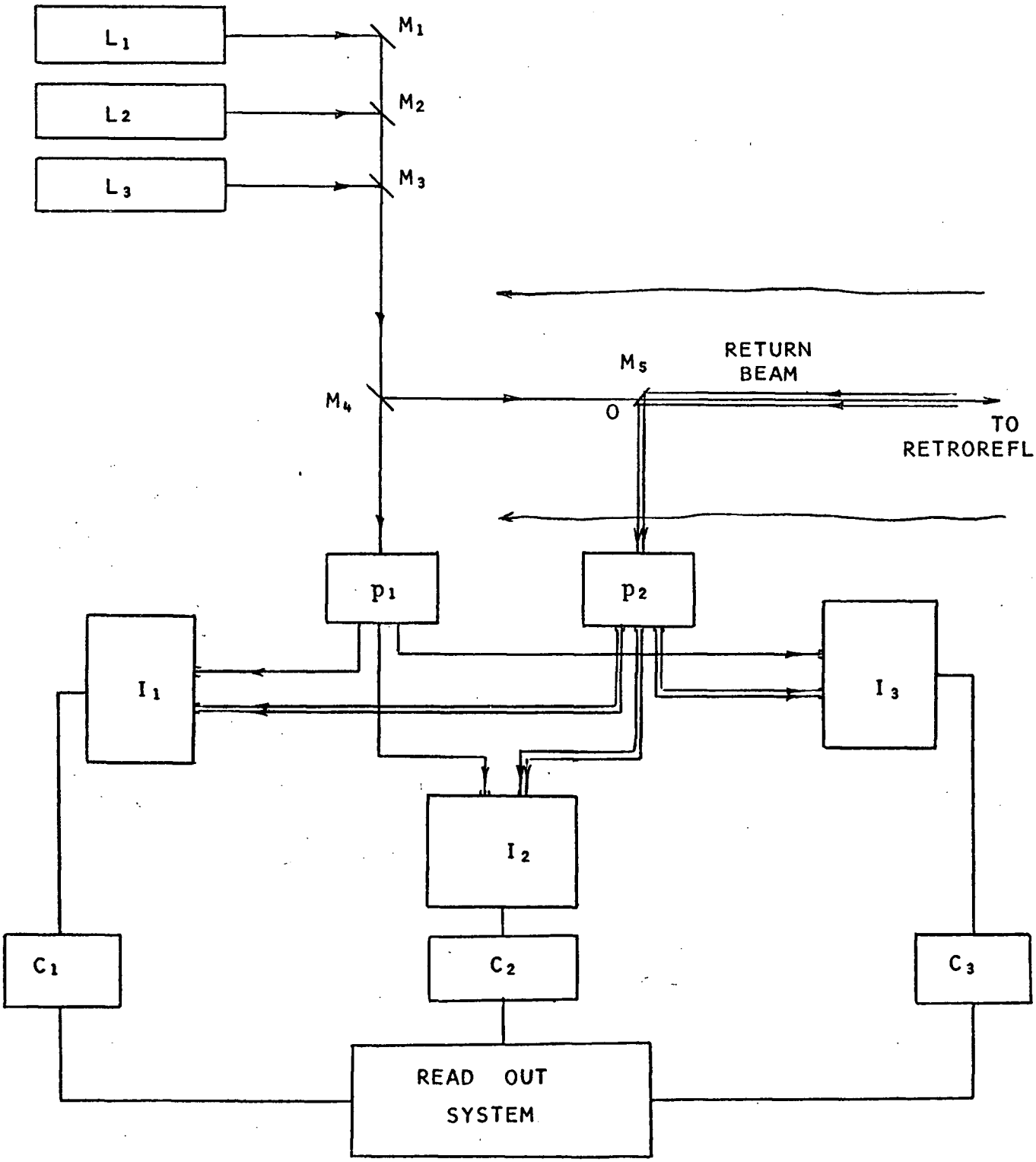

FIG. III-1

SCHEMATIC OF A FREE AIR LASER STRAIN METER SYSTEM

B. THEORY

1. Separation of "Geometrical" and "Refractive" Optical Path Length Fluctuations

Consider cartesian coordinate axes, Fig. III-2, with the origin at O , Fig. III-1, oriented so that the x-axis points in the direction of the retro-reflecting mirror M_6 at a distance $D(t)$. The parametric curves $\vec{C}_{\lambda_i}(\ell, t_1)$ and $\vec{C}_{\lambda_i}(\ell, t_2)$ represent the geometrical atmospheric paths, to the retro-reflector and back, at times t_1 and t_2 respectively, of a single ray of wavelength λ_i $i = 1, 2, 3$ of the combined output beam.

$$\vec{C}_{\lambda_i}(\ell, t) = \frac{d\vec{R}_{\lambda_i}(\ell, t)}{d\ell} \qquad \text{(B-1-1)}$$

where

$$\vec{R}_{\lambda_i}(\ell, t) = X_{\lambda_i}(\ell, t)\hat{i} + Y_{\lambda_i}(\ell, t)\hat{j} + Z_{\lambda_i}(\ell, t)\hat{k}$$

is the position vector of an oriented element $d\vec{C}_{\lambda_i}$ of the ray-path $\vec{C}_{\lambda_i}(\ell, t)$ and ℓ is a parameter, $0 \leq \ell \leq D(t)$, proportional to distance along the x-axis; $\hat{i}$, $\hat{j}$, $\hat{k}$ are unit vectors along the x , y and z axes respectively.

Fig. III-2 shows the atmospheric ray-paths taken by single rays of the combined laser beam at times t_1 and t_2 respectively. The individual rays of each wavelength λ_i $i = 1, 2, 3$ are shown as taking separate but closely spaced ray-paths at times t_1 and t_2 due to atmospheric dispersion. The "mean ray-path" $\vec{C}(\ell, t)$ is also indicated

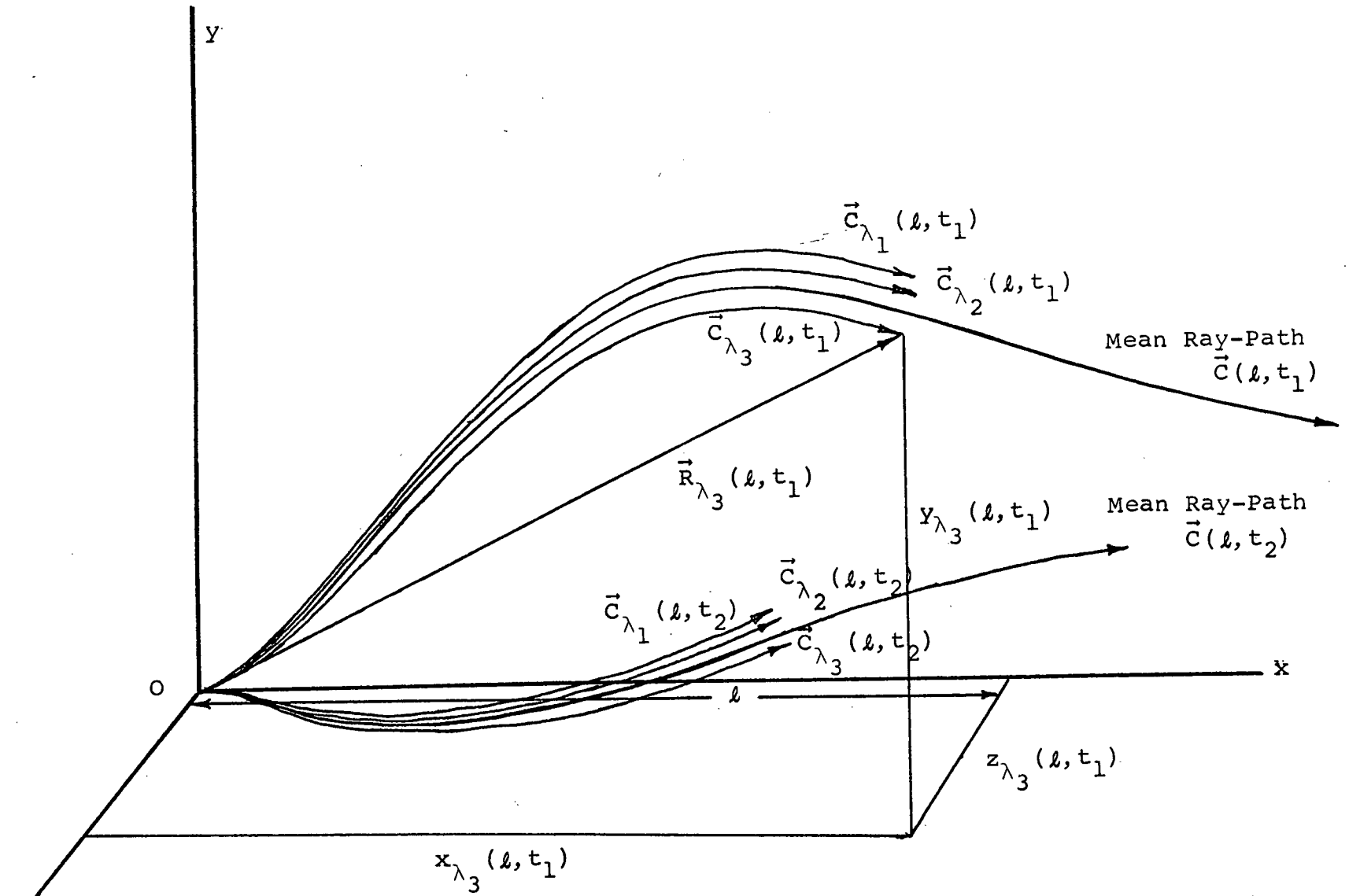

FIG. III-2

PARAMETERIZATION OF THE ATMOSPHERIC RAY-PATHS

in each case.

The arc length of the curves $\vec{C}_{\lambda_i}(\ell, t)$ is $S_{\lambda_i}(\ell)$ given by

$$S_{\lambda_i}(t) = \int_0^{D(t)} \left[\vec{C}_{\lambda_i}(\ell, t) \cdot \vec{C}_{\lambda_i}(\ell, t) \right]^{1/2} d\ell$$

Let

$$S_{\lambda_i}(\ell, t) = \left[\vec{C}_{\lambda_i}(\ell, t) \cdot \vec{C}_{\lambda_i}(\ell, t) \right]^{1/2}$$

be a parameterized differential arc length segment of the geometrical curve $\vec{C}_{\lambda_i}(\ell, t)$ representing the ray-path between the end mirrors of the strain meter for radiation of wavelength λ_i at time t.

Then:

$$S_{\lambda_i}(t) = \int_0^{D(t)} S_{\lambda_i}(\ell, t)\, d\ell \qquad \text{(B-1-2)}$$

At every point $\vec{R}_{\lambda_i}(\ell, t)$ along the ray-path the atmospheric refractive index for radiation of wavelength λ_i has the value $n_{\lambda_i}(\vec{R}_{\lambda_i}(\ell, t))$. The optical path length for a ray of wavelength λ_i travelling from O (mirror M_5) to the retro-reflector (mirror M_6) and back is $L_{\lambda_i}(t)$.

$$L_{\lambda_i}(t) = 2 \int_0^{D(t)} n_{\lambda_i}(\vec{R}_{\lambda_i}(\ell, t)) S_{\lambda_i}(\ell, t)\, d\ell \qquad \text{(B-1-3)}$$

Here it has been assumed that the retro-reflector simply returns the ray back along its incoming path. This assumption is a good one for purposes of this analysis since the refractive index conditions are virtually unchanged over time intervals comparable to the transit time of a photon between mirrors M_5 and M_6. It should be emphasized, however, that this assumption is not necessary for the development of this analysis and could be dispensed with, resulting in a slightly more difficult mathematical treatment but no significant difference in the end results.

The net change in optical path length for radiation of wavelength λ_i between times t_1 and t_2 is $\delta L_{\lambda_i}(t_1 t_2)$

$$\delta L_{\lambda_i}(t_1 t_2) = 2 \int_0^{D(t_2)} n_{\lambda_i}\left(\vec{R}_{\lambda_i}(\ell, t_2)\right) S_{\lambda_i}(\ell, t_2)\, d\ell - 2 \int_0^{D(t_1)} n_{\lambda_i}\left(\vec{R}_{\lambda_i}(\ell, t_1)\right) S_{\lambda_i}(\ell, t_1)\, d\ell \qquad \text{(B-1-4)}$$

Now the refractive index $n_{\lambda_i}(\vec{R}_{\lambda_i})$ is given by

$$n_{\lambda_i}\left(\vec{R}_{\lambda_i}(\ell, t)\right) = 1 + f(\lambda_i)\, F\left[P(\vec{R}_{\lambda_i}(\ell,t)), T(\vec{R}_{\lambda_i}(\ell,t))\right] + g(\lambda_i) G\left[p(\vec{R}_{\lambda_i}(\ell,t)),\ T(\vec{R}_{\lambda_i}(\ell,t))\right]$$

where $P(\vec{R}_{\lambda_i}(\ell,t))$, $T(\vec{R}_{\lambda_i}(\ell,t))$, and $p(\vec{R}_{\lambda_i}(\ell,t))$ are the partial pressure of "dry air", temperature, and partial pressure of water vapour at position $\vec{R}_{\lambda_i}$ along the ray-path of wavelength λ_i $i = 1, 2, 3$ respectively [A-2, eqn. A-2-6] .

Substituting the formula for refractive index into eqn. B-1-4 results in eqn. B-1-5

$$\delta L_{\lambda_i}(t_1 t_2) = 2\left[\int_o^{D(t_2)} S_{\lambda_i}(\ell,t_2)d\ell - \int_o^{D(t_1)} S_{\lambda_i}(\ell,t_1)d\ell\right]$$

$$+2f(\lambda_i)\left[\int_o^{D(t_2)} F\left[P(\vec{R}_{\lambda_i}(\ell,t_2)),\ T(\vec{R}_{\lambda_i}(\ell,t_2))\right]S_{\lambda_i}(\ell,t_2)d\ell\right.$$

$$\left.-\int_o^{D(t_1)} F\left[P(\vec{R}_{\lambda_i}(\ell,t_1)),\ T(\vec{R}_{\lambda_i}(\ell,t_1))\right]S_{\lambda_i}(\ell,t_1)d\ell\right]$$

$$+2g(\lambda_i)\left[\int_o^{D(t_2)} G\left[p(\vec{R}_{\lambda_i}(\ell,t_2)),\ T(\vec{R}_{\lambda_i}(\ell,t_2))\right]S_{\lambda_i}(\ell,t_2)d\ell\right.$$

$$\left.-\int_o^{D(t_1)} G\left[p(\vec{R}_{\lambda_i}(\ell,t_1)),\ T(\vec{R}_{\lambda_i}(\ell,t_1))\right]S_{\lambda_i}(\ell,t_1)d\ell\right]$$

$$i = 1, 2, 3 \qquad \text{(B-1-5)}$$

Eqn. B-1-5 can be written

$$\delta L_{\lambda_1}(t_1t_2) = U_{\lambda_1}(t_1t_2) + f(\lambda_1)V_{\lambda_1}(t_1t_2) + g(\lambda_1)W_{\lambda_1}(t_1t_2)$$

$$\delta L_{\lambda_2}(t_1t_2) = U_{\lambda_2}(t_1t_2) + f(\lambda_2)V_{\lambda_2}(t_1t_2) + g(\lambda_2)W_{\lambda_2}(t_1t_2) \qquad \text{(B-1-6)}$$

$$\delta L_{\lambda_3}(t_1t_2) = U_{\lambda_3}(t_1t_2) + f(\lambda_3)V_{\lambda_3}(t_1t_2) + g(\lambda_3)W_{\lambda_3}(t_1t_2)$$

where

$$U_{\lambda_i}(t_1t_2) = 2\left[\int_0^{D(t_2)} S_{\lambda_i}(\ell,t_2)\,d\ell - \int_0^{D(t_1)} S_{\lambda_i}(\ell,t_1)\,d\ell\right]$$

$$V_{\lambda_i}(t_1t_2) = 2\left[\int_0^{D(t_2)} F\left[P(\vec{R}_{\lambda_i}(\ell,t_2)),T(\vec{R}_{\lambda_i}(\ell,t_2))\right] S_{\lambda_i}(\ell,t_2)\,d\ell - \int_0^{D(t_1)} F\left[P(\vec{R}_{\lambda_i}(\ell,t_1)),T(\vec{R}_{\lambda_i}(\ell,t_1))\right] S_{\lambda_i}(\ell,t_1)\,d\ell\right]$$

$$W_{\lambda_i}(t_1t_2) = 2\left[\int_0^{D(t_2)} G\left[p(\vec{R}_{\lambda_i}(\ell,t_2)),T(\vec{R}_{\lambda_i}(\ell,t_2))\right] S_{\lambda_i}(\ell,t_2)\,d\ell - \int_0^{D(t_1)} G\left[p(\vec{R}_{\lambda_i}(\ell,t_1)),T(\vec{R}_{\lambda_i}(\ell,t_1))\right] S_{\lambda_i}(\ell,t_1)\,d\ell\right] \qquad \text{(B-1-7)}$$

Suppose for the moment the small differences between the individual rays forming the triplet of rays at time t_1 and t_2, $\vec{c}_{\lambda_i}(\ell, t_1)$ and $\vec{c}_{\lambda_i}(\ell, t_2)$, can be ignored and the triplet of rays in eqn. B-1-5 can be replaced by a "mean ray-path", $\vec{C}(\ell, t_1)$ and $\vec{C}(\ell, t_2)$, at times t_1 and t_2 respectively.

$$\vec{C}(\ell, t) = \frac{d\,\vec{R}(\ell, t)}{d\,\ell}$$

where

$$\vec{R}(\ell, t) = \frac{1}{3}\left\{\left(\sum_{i=1}^{3} x_{\lambda_i}(\ell, t)\right)\hat{i} + \left(\sum_{i=1}^{3} y_{\lambda_i}(\ell, t)\right)\hat{j} + \left(\sum_{i=1}^{3} z_{\lambda_i}(\ell, t)\right)\hat{k}\right\} .$$

This definition of the "mean ray-path" is such that the mean ray is geometrically centered in the triplet of rays.

Substituting the mean ray-path for the individual ray-paths in each case in eqn. B-1-7 yields eqn. B-1-8

$$\delta L_{\lambda_1}(t_1 t_2) = U(t_1 t_2) + f(\lambda_1)V(t_1 t_2) + g(\lambda_1)W(t_1 t_2)$$

$$\delta L_{\lambda_2}(t_1 t_2) = U(t_1 t_2) + f(\lambda_2)V(t_1 t_2) + g(\lambda_2)W(t_1 t_2)$$

$$\delta L_{\lambda_3}(t_1 t_2) = U(t_1 t_2) + f(\lambda_3)V(t_1 t_2) + g(\lambda_3)W(t_1 t_2)$$

(B-1-8)

where

$$U(t_1 t_2) = 2\left[\int_0^{D(t_2)} S(\ell, t_2)\, d\ell - \int_0^{D(t_1)} S(\ell, t_1)\, d\ell\right]$$

$$V(t_1 t_2) = 2\left[\int_0^{D(t_2)} F\left[P(\vec{R}(\ell, t_2)), T(\vec{R}(\ell, t_2))\right] S(\ell, t_2)\, d\ell - \int_0^{D(t_1)} F\left[P(\vec{R}(\ell, t_1)), T(\vec{R}(\ell, t_1))\right] S(\ell, t_1)\, d\ell\right] \quad \text{(B-1-9)}$$

$$W(t_1 t_2) = 2\left[\int_0^{D(t_2)} G\left[p(\vec{R}(\ell, t_2)), T(\vec{R}(\ell, t_2))\right] S(\ell, t_2)\, d\ell - \int_0^{D(t_2)} G\left[p(\vec{R}(\ell, t_1)), T(\vec{R}(\ell, t_1))\right] S(\ell, t_1)\, d\ell\right]$$

and of course

$$S(\ell, t) = \left[\vec{C}(\ell, t) \cdot \vec{C}(\ell, t)\right]^{1/2}$$

$$S(t) = \int_0^{D(t)} S(\ell t)\, d$$

Eqns. B-1-8 can be expressed in matrix form

$$\begin{pmatrix} \delta L_{\lambda_1}(t_1 t_2) \\ \delta L_{\lambda_2}(t_1 t_2) \\ \delta L_{\lambda_3}(t_1 t_2) \end{pmatrix} = \begin{pmatrix} 1 & f(\lambda_1) & g(\lambda_1) \\ 1 & f(\lambda_2) & g(\lambda_2) \\ 1 & F(\lambda_3) & g(\lambda_3) \end{pmatrix} \begin{pmatrix} U(t_1 t_2) \\ V(t_1 t_2) \\ W(t_1 t_2) \end{pmatrix} \quad \text{(B-1-10)}$$

The inhomogeneous terms in eqns. B-1-10 , $\delta L_{\lambda_i}(t_1 t_2)$, $i = 1 , 2 , 3 ,$ are equal to the net change in optical path length in the interval $\Delta t = t_2 - t_1$ of a single ray of wavelength λ_i traversing the distance between the end mirrors of the free air laser strain meter. The inhomogeneous terms in eqns. B-1-10 are proportional to the net fringe counts observed. If λ_1 , λ_2 , and λ_3 are the wavelengths "in vacuo" of the radiation from lasers L_1 , L_2 , and L_3 respectively and if $C_{\lambda_1}(t_1 t_2)$, $C_{\lambda_2}(t_1 t_2)$ and $C_{\lambda_3}(t_1 t_2)$ are the net fringe counts in the interval $\Delta t = t_2 - t_1$ observed in the interference patterns formed by diffracting apertures I_1 , I_2 , and I_3 respectively, then

$$\delta L_{\lambda_1}(t_1 t_2) = \lambda_1 C_1(t_1 t_2)$$

$$\delta L_{\lambda_2}(t_1 t_2) = \lambda_2 C_2(t_1 t_2) \qquad \text{(B-1-11)}$$

$$\delta L_{\lambda_3}(t_1 t_2) = \lambda_3 C_3(t_1 t_2)$$

The matrix of coefficients in eqns. B-1-10 are known from the refractive index formula for the atmosphere.

The unknowns $V(t_1 t_2)$ and $W(t_1 t_2)$ are associated with changes in the optical path length of the ray in the interval $\Delta t = t_2 - t_1$ which are mainly refractive in origin. Non-zero values of $V(t_1 t_2)$ and $W(t_1 t_2)$ arise mainly from changes in the atmospheric parameters of pressure, temperature and humidity along the ray path.

The unknown $U(t_1 t_2)$, however, is equal to the change in geometrical length of the mean ray-path between the end mirrors of the strain meter in the interval $\Delta t = t_2 - t_1$, as can be seen from its definion in eqns. B-1-9.

It should perhaps be emphasized that the substitution of the mean ray-path $\vec{C}(\ell, t)$ for the triplet of ray paths $\vec{C}_{\lambda_i}(\ell, t)$ in eqns. B-1-7 does not manifest itself as a physical approximation in the measurement process. It merely defines mathematically a "mean ray" in terms of a triplet of rays. The "mean ray", so defined, is no more or

less of an abstraction and hence no more or less "real" than any of the members of the ray triplet. Thus it follows that the mean ray (or more to the point, fluctuations in the mean ray) is as adequate as any for use in making physical observations provided a means of measuring it is available.

A measure of the net fluctuations in the geometrical length of the mean ray is provided by a solution of the eqns. B-1-10 and the existence of this measure is guaranteed by the non-singular nature of the matrix of coefficients.

It can be shown that $U(t_1t_2)$ is made up of contributions from two unrelated effects. From eqn. B-1-9

$$U(t_1t_2) = 2\left[\int_0^{D(t_1)} (S(\ell,t_2)-S(\ell,t_1))d\ell + \int_{D(t_1)}^{D(t_2)} S(\ell,t_2)d\ell\right] \qquad \text{(B-1-12)}$$

which can be written

$$U(t_1t_2) = \delta S(t_1t_2) + 2\delta D(t_1t_2) \qquad \text{(B-1-13)}$$

where

$$\delta S(t_1t_2) = 2\int_0^{D(t_1)} (S(\ell,t_2) - S(\ell,t_1))d\ell \qquad \text{(B-1-14)}$$

and

$$2\delta D(t_1t_2) = 2\int_{D(t_1)}^{D(t_2)} S(\ell,t_2)d\ell \qquad \text{(B-1-15)}$$

At this point in the analysis the necessary approximation will be made that

$$2\,\delta D(t_1 t_2) \cong 2\left[D(t_2) - D(t_1) \right] \qquad \text{(B-1-16)}$$

This is tantamount to assuming that the mean ray-path never deviates strongly from the straight line path between the end mirrors and that the arc length of the mean ray-path between subsequent positions of the retro-reflector (which differ due to tectonic activity) can be approximated by the straight line distance.

That this is a good approximation is borne out experimentally by observations of stellar images in astronomical telescopes in which the r.m.s. value of the fluctuations in the angle of arrival of the ray is about 1"-2" of arc or roughly 10^{-5} rad. [25, P. 225]. Theoretical predictions by Chernov [26, P.17] for r.m.s. fluctuations in the angle of arrival of a light ray after horizontal transmission through the earth's atmosphere of a distance of 10 km. yields a somewhat larger value of the order of 10^{-3} rad. However the error in the value of the net fluctuation in geometrical length of the mean ray-path introduced by this assumption varies as the cosine of the angle of arrival of the ray at the retro-reflector and is likely to be much less than one part in 10^6.

In eqn. B-1-13, $\delta S(t_1 t_2)$ is a random con-

tribution to the net fluctuation in geometrical path length of the mean ray which varies rapidly with time resulting from differences in the choice of atmospheric ray-paths taken between the end mirrors M_5 and M_6 at times t_1 and t_2 .

In eqn. B-1-13, $2\delta D(t_1 t_2)$ is a contribution to the net fluctuation in the total geometrical path length of the mean ray arising out of tectonic changes in distance D between the end mirrors M_5 and M_6 . As such $2\delta D(t_1 t_2)$ contains contributions from the entire spectrum of tectonic motions from high frequency seismic activity on down to earth tides and secular crustal deformations. All of these contributions to $2\delta D(t_1 t_2)$, with the exception of secular crustal deformation, by definition; go to zero when averaged over sufficiently long time intervals.

It is ideally desirable to "filter" a series of continuous consecutive observations of $U(t_i t_{i-1})$ $i = 1, 2, 3 \ldots n$

$$U(t_i t_{i-1}) = \delta S(t_i t_{i-1}) + 2\delta D(t_i t_{i-1})$$

to remove the effects of the atmospheric contribution $\delta S(\tau)$ revealing the tectonic changes in distance $\delta D(\tau)$. The next section will deal with the statistical analysis of free air laser strain meter observations to reveal tectonic motions.

2. Statistical Analysis of Free Air Laser Strain Meter Observations to Reveal Tectonic Motions

The data from free air laser strain meter observations consists of continuous consecutive sampled values of the fluctuations of the geometrical length of the mean ray between the end mirrors of the strain meter, $U(t_i, t_{i-1})$ $i = 1, 2, 3 \ldots n$. There are undoubtedly many ways to process this data in order to filter out the atmospheric contributions to the fluctuations in geometrical ray-path length. The filtering could be done optimally, in the Weiner sense, with knowledge of the power spectra of both the atmospheric fluctuations in geometrical ray-path length and of earth strains. The observed power spectrum of earth strains from periods of 2.35 hours to 4 sec. has been published by Vali [39] but to the author's knowledge, no observations of the power spectrum of geometrical fluctuations in atmospheric ray path length have been made. Another alternative is a least squares fit of a curve to the entire set of data.

The method of data analysis presented in this section is a rather simple one and while making no claim to be optimum, serves to illustrate the relationship between the confidence level of the observations of tectonic motion and the relevant physical, geographical and atmospheric parameters.

Let $\epsilon(t)$ be the extra distance, over the

straight line distance, that a photon travels when traversing the mean ray-path from mirror M_5 to mirror M_6 and back at time t.

$$\epsilon(t) = 2\left[S(t) - D(t) \right] \qquad \text{(B-2-1)}$$

ϵ (t) is a random variable with probability density function $P_{\epsilon(t)}(\beta)$, $0 \leq \beta \leq \infty$. The expected value (ensemble average) of ϵ (t) is given by

$$\overline{\epsilon(t)} = \int_0^\infty \beta P_{\epsilon(t)}(\beta)\beta$$

The random variable $\delta S(t_1 t_2)$ in eqn. B-1-13 is related to $\epsilon(t)$ by

$$\delta S(\Delta t) = \epsilon(t_2) - \epsilon(t_1) \qquad \text{(B-2-2)}$$

where

$$\Delta t = t_2 - t_1 \quad .$$

The random variable $\delta S(\Delta t)$ has probability density function $P_{\delta S}(\beta)$, $-\infty \leq \beta \leq \infty$. The expected value of $\delta S(\Delta t)$ is given by

$$\overline{\delta S(\Delta t)} = \int_{-\infty}^{\infty} \beta \, P_{\delta S}(\beta) d\beta$$

$$\overline{\delta S(\Delta t)} = \overline{\epsilon(t)} - \overline{\epsilon(t)}$$

$$\overline{\delta S(\Delta t)} = 0 \qquad \text{(B-2-3)}$$

Let $\left\{ U(\Delta t_i) \right\} = \left\{ \delta S(\Delta t_i) + 2\delta D(\Delta t_i) \right\}$ $i = 1, 2, 3 \ldots n$ be a sequence of continuous consecutive sampled observations of the fluctuations in geometrical length of the mean ray path $U(\Delta t)$ in the intervals $\Delta t_i = t_i - t_{i-1}$. Define $X(\tau_r)$ to be the net fluctuation in geometrical ray-path length in the interval $\tau_r = \sum_{i=1}^{r} \Delta t_i$, $0 \leq r < n$. Thus

$$X(\tau_r) = \sum_{i=1}^{r} U(\Delta t_i)$$

$$X(\tau_r) = \sum_{i=1}^{r} \delta S(\Delta t_i) + 2 \sum_{i=1}^{r} \delta D(\Delta t_i)$$

In this context "t" is an absolute time variable and "τ" is a relative time variable. $\tau = 0$ at the beginning of the free air laser strain meter observations.

It will be assumed that the values $X(\tau_r)$ $r = 1, 2, 3 \ldots n$ represent sampled values, at intervals Δt of a continuous, differentiable function $X(\tau)$. This is tantamount to assuming that changes in geometric length of the mean ray-path caused by both atmospheric fluctuations and tectonic motions are continuous and "smooth". A hypothetical plot of $X(\tau_r)$ vs. τ is shown in Fig. III-3. It consists of broad band tectonic contributions $2\delta D(\Delta t_i)$ to the fluctuations in geometric ray-path length "contaminated" by large amplitude atmospheric "noise", with mean value zero.

Let $2\delta D_1$ be the average value of $X(\tau_i)$ over the first in sample points $\tau_1 \tau_2 \ldots \tau_m$, where m is an even integer of fixed value, corresponding to an interval of length $\Delta\tau$ centred about $\tau_{\frac{m}{2}}$

$$\Delta\tau = m\Delta t \qquad \text{(B-2-4)}$$

In general, if the entire length of observations of $X(\tau)$ represented by the sampled values $X(\tau_i)$, $i = 1, 2, 3 \ldots n$, is divided up into q intervals each of length $\Delta\tau = m\Delta t$ (where m is an even integer of fixed value and $n = mq$) then; $2\delta D_k$ $k = 1, 2, 3 \ldots q$ is the average value of $X(\tau_i)$ over the m sample points of the k^{th} interval corresponding to times τ_i $i = m(k-1) + 1$, $m(k-1) + 2 \ldots m(k-1) + m$, centred about $\tau_{m(k-1/2)}$.

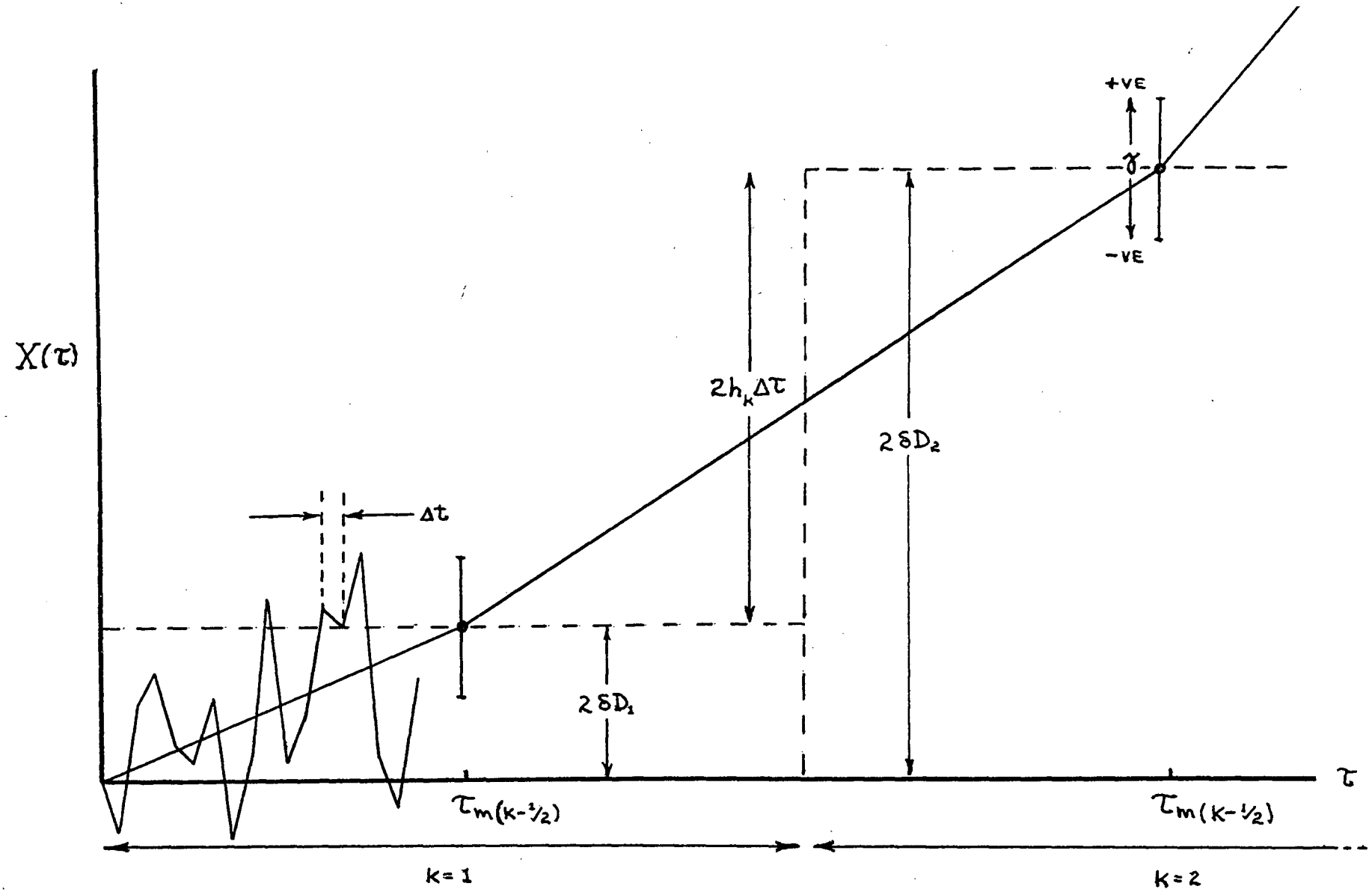

FIG. III-3

ANALYSIS OF FREE AIR LASER STRAIN METER OBSERVATIONS

A curve fitted to a plot of $2\delta D_k$ vs. $\tau_{m(k-1/2)}$ as shown in Fig. III-3, will reveal actual tectonic changes in the straight line distance D between the end mirrors of the strain meter providing

$$|\gamma| \leq 2\left[\delta D_{k+1} - \delta D_k\right] \qquad k = 1, 2, 3 \ldots q$$

where γ, represented in Fig. III-3 by the error bars, is the expected difference or "error" between the sample mean of m samples of $\delta S(\Delta t)$ and the population mean $\overline{\delta S(\Delta t)} = 0$. The tectonic changes in length between the end mirrors of the strain meter will be observed with a "signal-to-noise ratio" of s or better if

$$|\gamma| \leq \frac{2\left[\delta D_{k+1} - \delta D_k\right]}{s} \qquad s > 1 \qquad \text{(B-2-5)}$$

The residual of the averaged atmospheric fluctuation in geometrical ray-path length, γ, is a monotonically decreasing function of the averaging interval $\Delta\tau = m \Delta t$. It is necessary to select an averaging interval $\Delta\tau$ long enough that $|\gamma|$ is less, by a factor s, the signal-noise ratio, than the expected difference in the distance between the end mirrors of the strain meter in the same interval. Thus the averaging interval is clearly dependent in general on

the statistics of the atmospheric fluctuations in geometrical ray-path length as well as the spectrum of tectonic activity.

The following observation should be noted regarding knowledge of $X(\tau)$ as afforded by free air laser strain meter observations. Firstly, the sampling of $X(\tau)$ at intervals $\Delta\tau$ will alias fluctuations in the geometrical length of the mean ray whose frequencies exceed $\frac{1}{2\Delta\tau}$. This folding of the spectrum about the Nyquist frequency will alias fluctuations with frequencies $1/\Delta\tau$, $2/\Delta\tau$, $3/\Delta\tau$ ... back to d.c. Tectonic contributions $2\delta D(\tau)$ to fluctuations in the geometrical ray-path length at these frequencies are assuredly of very small amplitude, however no such assurance can be given regarding the atmospheric contributions $\delta S(\tau)$. However the central limit theorem states that γ (the mean of $\delta S(\tau)$ averaged over an interval $\Delta\tau = m\Delta t$) is a random variable, gaussian distributed about the population mean, $\overline{\delta S(\tau)} = 0$, with standard deviation given by $2\sqrt{\frac{\overline{\delta s^2}}{m}}$ regardless of the high frequency spectral distribution of $\delta S(\tau)$ providing the sampled values of $\delta S(\tau)$ are independent. Independent samples of the random variable $\delta S(\tau)$ can be assured if the sampling interval $\Delta\tau$ is greater than the period of the lowest frequency components in the spectrum of $\delta S(\tau)$.

Secondly, the reconstruction of the curve revealing tectonic changes in length $2\delta D(\tau)$ from the "sampled" values $2\delta D_k$ at intervals of $\Delta\tau$ can be accomplished by the use of many sophisticated "holds". For purposes of this analysis

it will be assumed that a simple "polygonal hold" is used. This is equivalent to a piece-wise straight line approximation to $2\delta D(\tau)$.

Let

$$2h_k = \frac{2\left[\delta D_{k+1} - \delta D_k\right]}{\Delta\tau} \qquad k = 1, 2, 3 \ldots q$$

Then h_k is the linear rate of change of the distance D between the end mirrors of the strain meter in the interval $\Delta\tau = \tau_{m(k+1/2)} - \tau_{m(k-1/2)}$. An observed change in the distance D, $\delta D_{k+1} - \delta D_k$, in the interval $\Delta\tau = \tau_{m(k+1/2)} - \tau_{m(k-1/2)}$ will be called "significant at a signal-noise ratio s" and duly attributed to tectonic processes if

$$|\gamma| \leq \frac{2|h_k|\Delta\tau}{s} \qquad k = 1, 2, 3 \ldots q \qquad \text{(B-2-6)}$$

otherwise the observation will be called "insignificant at a signal-noise ratio s" and it will be assumed that no "significant" tectonic change in the distance D has occurred in that interval.

By the central limit theorem the probability density function for γ the residual of the average of m samples of the atmospheric fluctuations in ray-path length δS, is gaussian about zero with standard deviation

$$2\sqrt{\frac{\overline{\delta S^2}}{m}}$$

$$P_\gamma(\beta) = \left[\frac{m}{2\pi\,\overline{\delta S^2}}\right]^{1/2} \exp - \left[\frac{\beta^2}{2\,\frac{\overline{\delta S^2}}{m}}\right]$$

(B-2-7)

where $\overline{\delta S^2}$ is the variance of δS

$$\overline{\delta S^2} = \int_{-\infty}^{\infty} \beta^2 P_{\delta S}(\beta)\, d\beta$$

Let $\eta(|\xi|)$, $0 \le \eta(|\xi|) \le 1$, be the probability that $|\gamma| \le \frac{2 h_k \Delta\tau}{s}$ after averaging over m samples of δS

$$\eta(|\xi|) = 2\int_0^{\frac{2|h_k|\Delta\tau}{s}} P_\gamma(\beta)\, d\beta$$

In this sense $\eta(|\xi|)$ is the "confidence level" of the observation of the tectonic change in distance. $\eta(|\xi|)$ is the probability that an observation of tectonic motion which has been called "significant" (as it represents a change in the distance D, $\delta D_{k+1} - \delta D_{k-1}$ for which $|\gamma| \le \frac{2|h_k|\Delta\tau}{s}$)

is in fact "genuinely significant". The larger the choice of $|\xi|$ the less likely is the possibility of the modulus of the average of m samples of δS exceeding $|\gamma|$ and the larger the confidence in the observation.

The following change of variable

$$\gamma' = \gamma\sqrt{\frac{m}{\delta S^2}} \qquad \text{(B-2-8)}$$

in eqn B-2-7 defines a probability density function for γ' which is gaussian with parameters zero and one.

$$P_{\gamma'}(\beta) = \frac{1}{\sqrt{2\pi}} \exp - \left[\frac{\beta^2}{2}\right] \qquad \text{(B-2-9)}$$

Let $\eta'|\xi'|$ be the probability that $|\xi'| \leq \frac{2|h_k|\Delta\tau}{s}\sqrt{\frac{m}{\delta S^2}}$ after averaging over m samples of δS.

$$\eta'(|\xi'|) = 2\int_0^{\frac{2|h_k|\Delta\tau}{s}\sqrt{\frac{m}{\delta S^2}}} P_{\gamma'}(\beta)\,d\beta \qquad \text{(B-2-10)}$$

Clearly $\eta'(|\xi'|) = \eta(|\xi|)$. Thus $\eta'(|\xi'|)$ is the "confidence level" of the laser strain meter observation and $|\xi'|$ is the confidence parameter. The confidence level is related by definition to the confidence parameter by

$$\eta(|\xi'|) = \operatorname{erf}\left(\frac{|\xi'|}{\sqrt{2}}\right) \qquad \text{(B-2-11)}$$

It follows from eqns B-2-9 and B-2-10 , [A-3-4] , that

$$\eta'|\xi'| = \operatorname{erf}\left[\frac{1}{\sqrt{2}} \quad \frac{2|h_k|\Delta\tau}{s}\sqrt{\frac{m}{\delta s^2}}\right] \qquad \text{(B-2-12)}$$

It further follows from eqns. B-2-11 and B-2-12 that

$$|\xi'| = \frac{2|h_k|\Delta\tau}{s}\sqrt{\frac{m}{\delta s^2}} \qquad \text{(B-2-13)}$$

where $|\xi'|$ is the value of the confidence parameter appropriate to the required confidence level of observation.

Eqns B-2-12 and B-2-13 relate the confidence level of a free air laser strain meter observation to the length of the observing interval, the modulus of the mean rate of change of distance between the end mirrors of the strain meter and the r.m.s. fluctuations in geometrical ray-path length. The dependence of the confidence level of the

tectonic observations on the mean square fluctuations in geometrical ray-path length $\overline{\delta S^2}$ requires a theoretical expression for $\overline{\delta S^2}$, the derivation of which is the subject for the next section.

This is an interesting problem in its own right with many perplexing physical and philosophical aspects. However for those who are prepared to accept the final mathematical result of section 3, eqn. B-3-14, this section can be considered a digression from the subject of free air laser strain meters. Such readers need only familiarize themselves with the definition of the symbols involved in eqn. B-3-14 and proceed to section 4.

3. Statistical Analysis of Fluctuations in Ray-Path of a Laser Beam Propagating Through a Turbulent Atmosphere

a) The Problem of Random Flights

Eqn. B-2-2 shows that the random variable $\delta S(\Delta t)$ is simply related to the random variable $\epsilon(t)$

$$\delta S(\Delta t) = \epsilon(t_2) - \epsilon(t_1) \qquad \text{(B-2-2)}$$

and hence the statistics of $\delta S(\Delta t)$ are determined by the statistics of $\epsilon(t)$. Now $\epsilon(t)$, eqn. B-2-1, can be expressed as

$$\epsilon(t) = 2 \int_0^{D(t)} \left[1 - \cos\alpha(\ell, t)\right] S(\ell, t) d\ell \qquad \text{(B-3-1)}$$

where $S(\ell, t) = \left[\vec{C}(\ell, t) \cdot \vec{C}(\ell, t) \right]^{1/2}$ is a random variable, the parameterized differential arc length segment of the ray at time t as a function of ℓ and $\alpha(\ell, t)$ is the total 3-dimensional angle between the x-axis and the ray-path at time t as a function of ℓ . The probability density function $P_{\delta S}(\beta)$ is determined by the probability density function $P_{\epsilon}(\beta)$ where $\tau(t)$ is given by eqn. B-3-1.

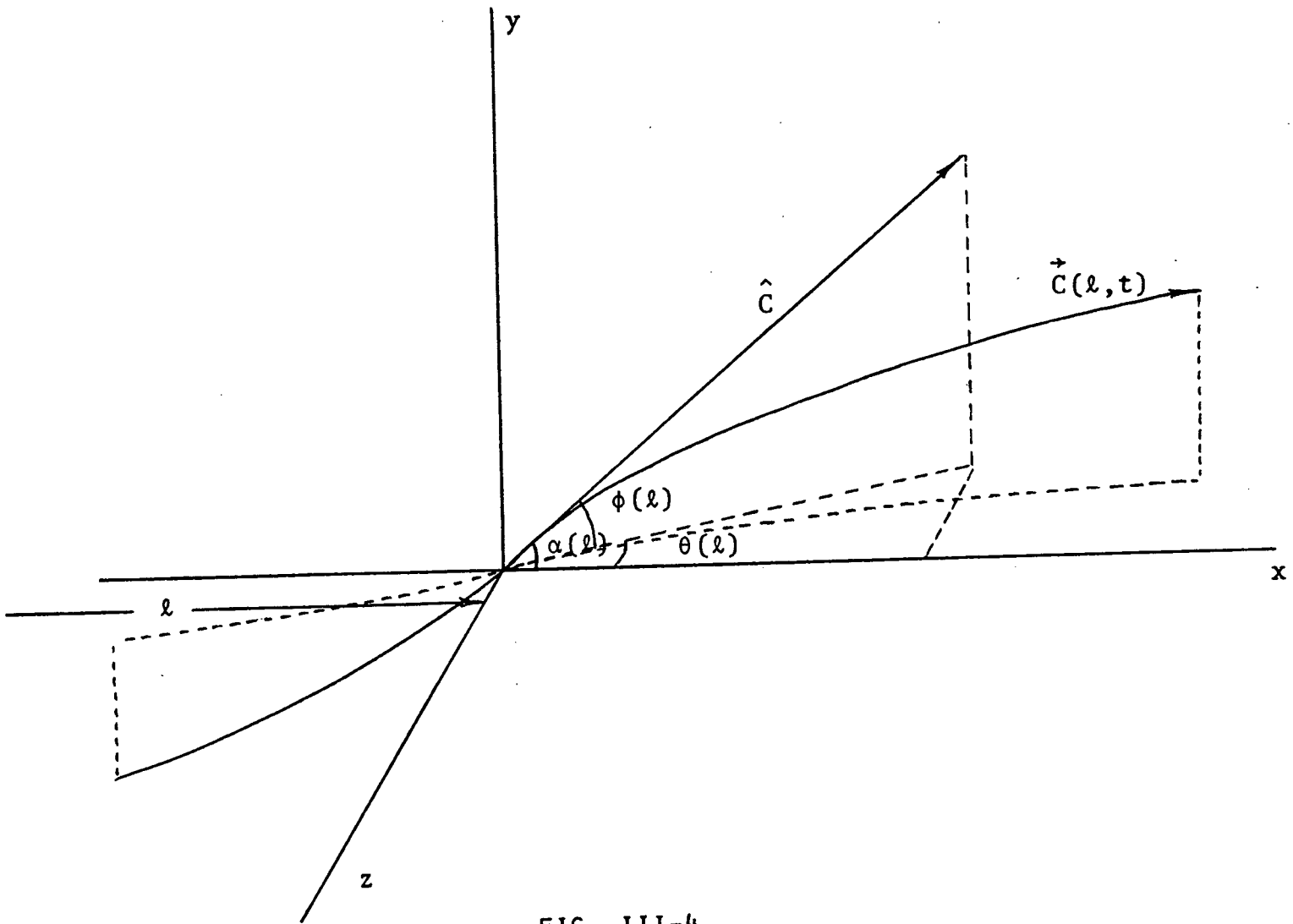

FIG. III-4

ANGULAR PARAMETERS OF ATMOSPHERIC RAY-PATH

It has been pointed out by Wang and Uhlenbeck [33] that the derivation of the probability density function for a random variable $z(t)$

$$z(t) = \int K(\ell,t)y(\ell)d\ell$$

where $K(\ell,t)$ is a given kernel and $y(\ell)$ a random variable with known probability density function other than gaussian is an unsolved problem in the theory of Brownian motion.

It is clear from eqn. B-3-1 that the problem of the derivation of the probability density function for $\varepsilon(t)$ is a member of this class. However a solution for $\varepsilon(t)$ is obtainable if the atmospheric ray-path can be approximated by a series of straight lines. When cast in this approximating form the problem is easily soluble by methods of analysis developed by theoreticians working on problems of Brownian Motion and in particular "the problem of random flights".

The problem of random flights is to calculate the probability that a particle, initially at the origin, will occupy a given volume element of space after a finite number of arbitrary displacements whose probability density functions are known. The solution to this problem is due originally to A. A. Markov and has been generalized to n-dimension by Chandrasekhar [27].

A problem pertinent to the feasibility of free air laser strain meters is to calculate the probability density function for the total path length travelled by a particle engaged in random flight after the particle has achieved a given straight line total displacement from its initial position. Although this problem is related to the problem of random flights it appears that neither Markov nor Chandrasekhar investigated it.

To begin the problem of calculating the distribution of atmospheric ray-path lengths of a single ray of a laser beam it is necessary to assume that the atmospheric refractive index fluctuations can be divided into two classes depending on their scale. One class, characterized by scales of dimension ℓ_o or larger, causes deflection of the laser beam as a whole while preserving the structure of the wave front; whereas the other class, characterized by scales of dimension less than ℓ_o, causes internal degradation of the laser beam such as "crumbling of the wave front" and fluctuations in intensity and phase coherence across the beam while preserving the beam's direction of travel. This assumption immediately permits one to approximate the ray-path over a straight line total distance D by a series of straight line segments of length ℓ_o, where $\ell_o << D$.

Over distances of the order ℓ_o or less it is assumed that a single ray may undergo many rapid fluctuations in direction about its initial direction but that its mean direction is constant; whereas over distances larger than ℓ_o it is assumed that a single ray may experience many large fluctuations in direction which add appreciably to its total path length.

The assumption that the ray-path can be characterized by a length ℓ_o such that for distances larger than ℓ_o the fluctuations in direction of the ray are essential whereas for distances smaller than ℓ_o they are trivial and can be ignored is both drastic and curious. Support for making such an assumption comes from the theory of Brownian motion where an exactly analogous assumption is made concerning velocities (rather than displacements) of Brownian particles.

It is fundamental to the theory of Brownian motion [27] to assume that there exists a time scale Δt such that for intervals of time $\tau<\Delta t$ the velocity $\vec{u}$ of a Brownian particle is essentially constant whereas its acceleration $\frac{d\vec{u}}{dt}$ can suffer many and possibly large fluctuations; whereas for intervals of time $\tau>\Delta t$ the velocity $\vec{u}$ of a Brownian particle can vary appreciably. This assumption restricts the validity of the theoretical predictions to times $\tau >> \Delta t$. The justification for this assumption in the case of Brownian motions comes solely from the success of the theoretical predictions.

b) Calculation of the Probability Density Function for $\epsilon(t)$

We shall begin by assuming gaussian probability density functions for the azimuth θ and elevation ϕ of the unit tangent vector $\hat{C}$ to the ray-path $\vec{C}(\ell, t)$, Fig. III-4

$$P_\theta(\beta) = \frac{1}{\sqrt{2\pi\,\overline{\theta^2}}} \exp\left[-\frac{\beta^2}{2\theta^2}\right] \qquad -\infty \leq \beta \leq \infty$$

$$P_\phi(\beta) = \frac{1}{\sqrt{2\pi\,\overline{\phi^2}}} \exp\left[-\frac{\beta^2}{2\phi^2}\right] \qquad -\infty \leq \beta \leq \infty$$

Beckmann (22) has pointed out that regardless of the detailed distribution of the microscale fluctuations in refractive index, the fluctuations in direction of the ray will be gaussian distributed by the Central Limit Theorem.

Chernov (26, P. 22) assuming a gaussian auto-correlation function of refractive index fluctuations on a micro-scale $C_{\mu\mu}(r) = \exp\left[-r^2/r_o^2\right]$ has also derived the above prob ability density functions $P_\theta(\beta)$ and $P_\phi(\beta)$ and shown that for isotropic atmosphere turbulence

$$\overline{\theta^2} = \overline{\phi^2} \quad \frac{2\sqrt{\pi}\,\overline{\mu^2}\,\ell}{r_o}$$

where r_o is the "inner scale" of turbulence, $\overline{\mu^2}$ the mean square refractive index fluctuation and the formulae is valid for propagation distances $\ell >> r_o$, measured along the ray-path.

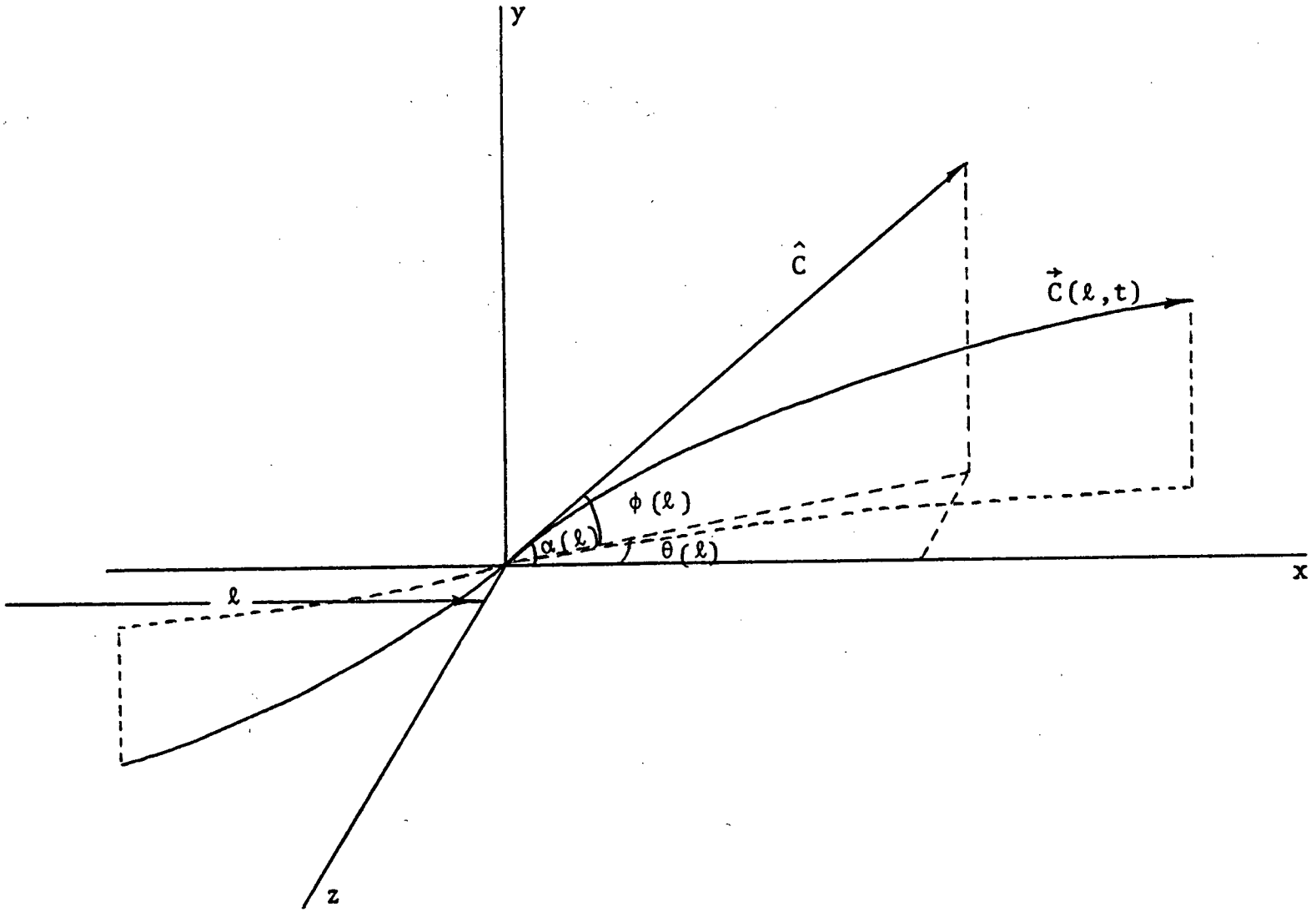

FIG. III-4

ANGULAR PARAMETERS OF ATMOSPHERIC RAY-PATH

The total angle α between the ray and the "straight line path" or the extension of the initial direction of propagation, represented by the x-axis in Fig. III-4, is given by

$$\cos \alpha = \cos \theta \cos \phi$$

If α, θ, and ϕ are all small angles then

$$1 - 1/2\, \alpha^2 = (1-1/2\, \theta^2)\,(1-1/2\phi^2)$$

$$\alpha^2 = \theta^2 + \phi^2$$

The probability density functions for θ^2 and ϕ^2 can be readily calculated (A-3-1)

$$P_{\theta 2}(\beta) = \frac{1}{\sqrt{2\pi\ \beta^2\ \overline{\theta^2}}} \exp\left[-\frac{\beta^2}{2\overline{\theta^2}}\right] \qquad 0 \leqslant \beta \leqslant \infty$$

$$P_{\phi 2}(\beta) = \frac{1}{\sqrt{2\pi\beta^2\ \overline{\phi^2}}} \exp\left[-\frac{\beta^2}{2\ \overline{\phi^2}}\right] \qquad 0 \leqslant \beta \leqslant \infty$$

and the probability density function for α^2, $P_{\alpha 2}(\gamma)$,

$$P_{\alpha 2}(\gamma) = P_{\theta 2}(\beta) \otimes P_{\phi 2}(\beta)$$

where "Ø" symbolizes convolution. $P_{\alpha 2}(\beta)$ can be readily calculated (A-3-2) to be

$$P_{\alpha 2}(\beta) = \frac{1}{\overline{\alpha^2}} \exp -\left[\frac{\beta}{\overline{\alpha^2}}\right] \qquad 0 \quad \beta \quad \infty \qquad \text{(B-3-2)}$$

where

$$\overline{\alpha^2} = \frac{4\sqrt{\pi}\,\overline{\mu^2}}{r_o} .$$

Consider the atmospheric ray-path $\vec{C}(\ell, t)$ between mirrors M_5 and M_6 and back of a free air laser strain meter to be approximated by straight line segments of length ℓ_o and let α_k be the total angle between the straight line path, represented by the x-axis, and the k^{th} segment of the ray-path $k = 1 , 2 , 3 \ldots n$, Fig. III-5.

The extra distance, over the straight line distance, travelled by the ray on the k^{th} segment of its path during its to-and-fro journey between the end mirrors is $\Delta\epsilon_k$

$$\Delta\epsilon_k = 2\left[\ell_o - \ell_k\right] \qquad k = 1 , 2 , 3 \ldots . n$$

$$\Delta\epsilon_k = 2\left[\ell_o - \ell_o \cos \alpha_k\right]$$

If α_k is a small angle

$$\cos \alpha_k = 1 - 1/2 \; \alpha_k^2$$

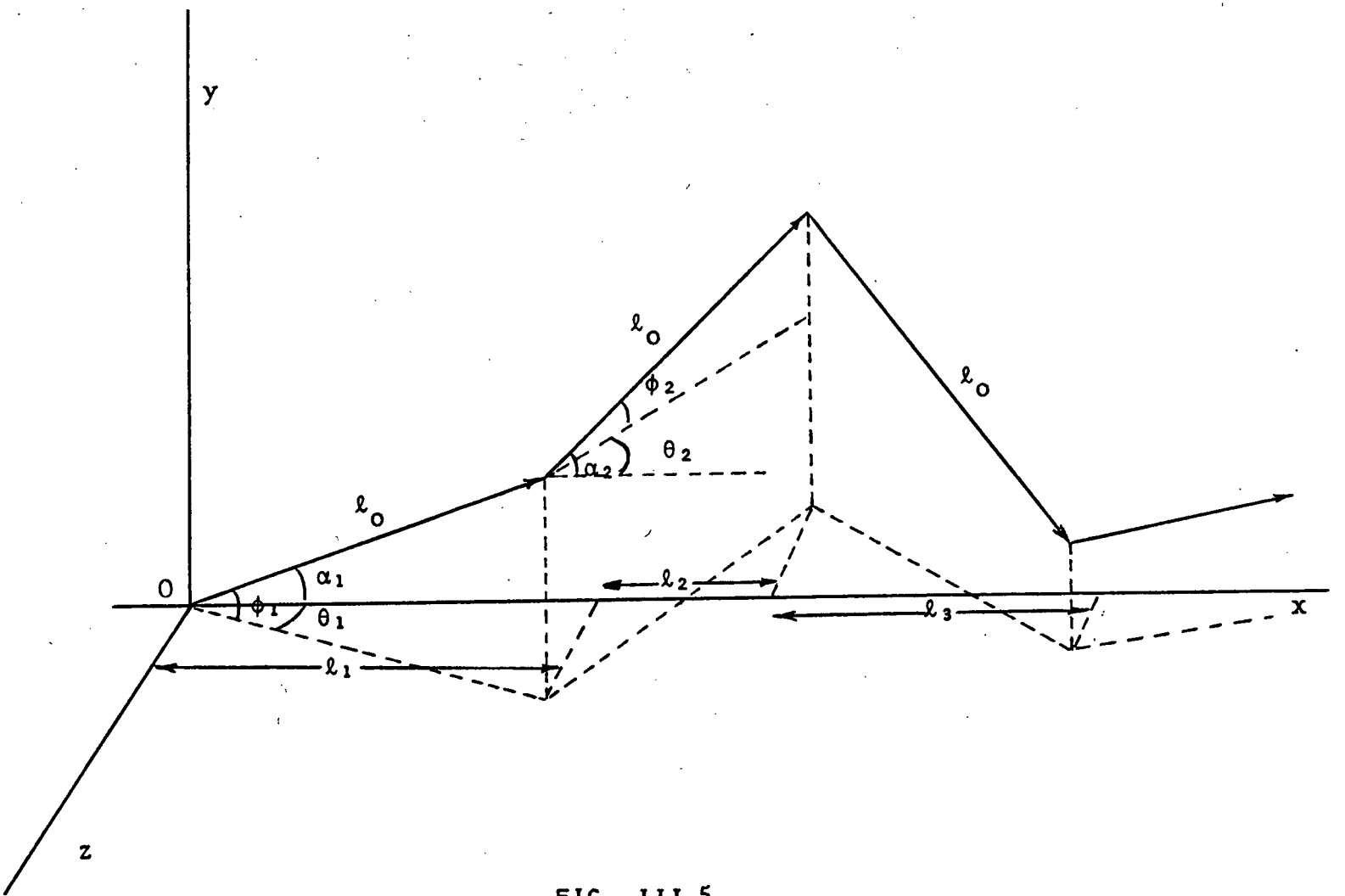

FIG. III-5

STRAIGHT LINE APPROXIMATION TO THE ATMOSPHERIC RAY-PATH

$$\Delta\epsilon_k = \ell_o \alpha_k^2 \qquad k = 1, 2, 3 \ldots n.$$

The total extra path length, over the straight line distances, travelled by the ray is

$$\epsilon = \sum_{k=1}^{n} \Delta\epsilon_k = \sum_{k=1}^{n} \ell_o \alpha_k^2$$

The problem of calculating the probability distribution for ϵ, the extra path length, as opposed to calculating its mean square value is complicated by the fact that integrals (or summations) taken along the curved ray-path cannot be replaced by integrals (or summations) along the straight line path as is frequently done in problems of this sort.

Thus with the curved ray-path approximated by straight line segments of length ℓ_o ; the deflections in azimuth and elevation, θ_k and ϕ_k , refer to the angles between the present direction of the k^{th} line segment and the extension of the $k\text{-}1^{th}$ line segment. The total deflection in azimuth and elevation, Θ_k and Φ_k , relative to the extension of the initial direction of propagation (or the x-axis) is given

$$\Theta_k = \theta_1 + \theta_2 + \theta_3 + \ldots + \theta_k$$

$$\Phi_k = \phi_1 + \phi_2 + \phi_3 + \cdots \phi_k$$

Since each angle θ_k and ϕ_k is a gaussian random variable with variance $\overline{\theta^2}$ and $\overline{\phi^2}$; it follows that Θ_k and Φ_k are gaussian random variables with variances given by

$$\overline{\Theta_k^2} = k\,\overline{\theta^2}$$

$$\overline{\Phi_k^2} = k\,\overline{\phi^2}$$

As before the small angle approximation holds and the total angle between the k^{th} segment of the ray-path and the straight line path, α_k , is related to the total azimuthal and elevation angles Θ_k and Φ_k by

$$\alpha_k^2 = \Theta_k^2 + \Phi_k^2$$

Thus α_k^2 has a probability density function

$$P_{\alpha_k^2}(\beta) = \frac{1}{\alpha_k^2} \exp\left[-\frac{\beta}{\alpha_k^2}\right]$$

where

$$\overline{\alpha_k^2} = \overline{\Theta_k^2} + \overline{\Phi_k^2} = k(\theta^2 + \phi^2)$$

$$\overline{\alpha_k^2} = k\,\overline{\alpha_o^2}$$

and k is the number of deflections.

If the turbulence is assumed to be isotropic, then

$$\overline{\theta^2} = \overline{\phi^2}$$

and

$$\alpha_o^2 = \frac{4\sqrt{\pi}\,\overline{\mu^2}\,\ell_o}{r_o}$$

Given the probability density function for α_k^2, $P_{\alpha_k^2}(\beta)$, it follows immediately that the probability density function for $\Delta\epsilon_k = \ell_o \alpha_k^2$, $P_{\Delta\epsilon_k}(\beta)$, is given by

$$P_{\Delta\epsilon_k}(\beta) = \frac{1}{\ell_o \overline{\alpha_k^2}} \exp\left[-\frac{\beta}{\ell_o \overline{\alpha_k^2}}\right] \qquad \text{(B-3-3)}$$

It is clear that since $\epsilon = \sum_{k=1}^{n} \Delta\epsilon$ that the probability density function for ϵ will be given by the convolution of a series of n inhomogeneous probability density functions $P_{\Delta\epsilon_k}(\beta)$, each differing by the parameter $\overline{\alpha_k^2}$

$$P_\epsilon(\gamma) = P_{\Delta\epsilon_1}(\beta) \otimes P_{\Delta\epsilon_2}(\beta) \otimes \ldots \otimes P_{\Delta\epsilon_n}(\beta)$$

This is an exceedingly awkward solution and can only be given in terms of a series summation, the length of the sum varying with the distance D. We shall instead derive an approximate solution and justify it by the following arguments.

The solution to the corresponding homogeneous

problem is simple and was derived by Markov and Chandrasekhar. It should be noted that the above problem is "quasi-homogeneous" in the sense that all members of the set of n probability density functions are of the same mathematical form - an exponential - and differ only among themselves by different values of the parameter $\overline{\alpha_k^2}$. If consecutive fluctuations in the ray direction can be considered uncorrelated (this does not imply independence - for they are dependent) then the variance of the probability distribution function for ϵ is the sum of the variances for the random variables $\Delta\epsilon_k$ which make up its sum.

Thus we shall obtain an approximate probability density function for $\epsilon(t)$ by convolving n homogeneous exponentials together to obtain the mathematical form of $P_{\epsilon(t)}(\beta)$ and then scale it appropriately by insisting that the variance of $P_{\epsilon(t)}(\beta)$ by equal to the sum of the variances of $\Delta\epsilon_k$ $k = 1, 2, 3 \ldots n$.

The convolution of a homogeneous set of n exponential probability density functions can be easily done using the Faltung Theorem. If

$$P_{\Delta\epsilon}(\beta) = \frac{1}{a} \exp\left[-\frac{\beta}{\alpha}\right]$$

is a member of the set and

$$Q_{\Delta\epsilon}(s) = \int_0^\infty \exp(-s\beta)\, P_{\Delta\epsilon}(\beta)\, d\beta \qquad \text{(B-3-4)}$$

as its Laplace transform then

$$Q_{\Delta\epsilon}(s) = \frac{1}{a}\left[\frac{1}{s+\frac{1}{a}}\right]$$

(See Appendix A-3-3)

By the Faltung Theorem the Laplace transform of $P_\epsilon(\beta)$ is $Q_\epsilon(s)$ where

$$Q_\epsilon(s) = \frac{1}{a^n}\left[\frac{1}{s+\frac{1}{a}}\right]^n \qquad (B-3-5)$$

This is a tabulated Laplace transform and has inversion $P_\epsilon(\beta)$ given by

$$P_\epsilon(\beta) = \frac{\beta^{n-1}}{a^n\,(n-1)!}\exp\left[-\frac{\beta}{a}\right]$$

The free parameter "a" shall be fixed by the condition on the variance of $P_\epsilon(\beta)$.

The variance of $P_{\Delta\epsilon_k}(\beta)$ is given by the integral

$$\overline{\Delta\epsilon_k^2} = \int_0^\infty \frac{\beta^2}{k\ell_o\,\overline{a^2}_o}\exp\left[-\frac{\beta}{k\ell_o\,\overline{a^2}_o}\right]d\beta$$

which can be shown (29, P. 317) to be

$$\overline{\Delta \epsilon_k^2} = 2 \left(k \ell_o \overline{\alpha_o^2}\right)^2$$

Therefore the sum of the variances is given by

$$\sum_{k=1}^{n} \overline{\Delta \epsilon_k^2} = 2 \left(\ell_o \overline{\alpha_o^2}\right)^2 \sum_{k=1}^{n} K^2$$

$$\sum_{k=1}^{n} \overline{\Delta \epsilon_k^2} = 2 \left(\ell_o \overline{\alpha_o^2}\right)^2 \frac{n(n+1)(2n+1)}{6}$$

which for large n can be approximated by

$$\sum_{k=1}^{n} \overline{\Delta \epsilon_k^2} = \frac{n^3}{3} \left(\ell_o \alpha_o^2\right)^2 .$$

The variance of $P_\epsilon(\beta)$ is given by the integral

$$\epsilon^2 = \int_o^\infty \frac{\beta^{n+1}}{a^n (n-1)!} \exp\left[-\frac{\beta}{a}\right] d\beta$$

which can be shown (29, P. 317) to be

$$\overline{\epsilon^2} = a^2 \, n(n+1)$$

which for large n can be approximated by

$$\overline{\epsilon^2} = a^2 \, n^2$$

We shall insist that $\overline{\epsilon^2} = \sum_k \overline{\Delta\epsilon_k^2}$

so

$$a^2 n^2 = \frac{n^3}{3} \left(\ell_o \overline{\alpha_o^2} \right)^2$$

Therefore

$$a = \frac{\sqrt{n}\, \ell_o \overline{\alpha_o^2}}{\sqrt{3}}$$

which gives a probability density function for $\epsilon(t)$

$$P_{\epsilon(t)}(\beta) = \left(\frac{3}{n}\right)^{n/2} \frac{\beta^{n-1}}{\left(\ell_o \overline{\alpha_o^2}\right)^n (n-1)!} \exp\left[- \frac{\sqrt{3}\beta}{\ell_o \overline{\alpha_o^2}} \right]$$

where

$$\overline{\alpha_o^2} = \frac{4\sqrt{\pi}\, \mu^2\, \ell_o}{r_o} \qquad \text{(B-3-6)}$$

and since the ray never deviates strongly from the straight line path

$$n \cong \frac{D}{\ell_o} \qquad \text{(B-3-7)}$$

Setting

$$\frac{\sqrt{3}}{\sqrt{n}\, \ell_o\, \alpha_o^2} = q \qquad \text{(B-3-8)}$$

the probability density function for $\epsilon(t)$ can be written

$$P_{\epsilon(t)}(\beta) = \frac{q^n\, \beta^{n-1}}{(n-1)!} \exp\left[- q\beta \right] \qquad o \leq \beta \leq \infty$$

(B-3-9)

c) Calculation of the Probability Density Function for $\delta S(\Delta t)$

The change in geometrical ray-path length $\delta S(\Delta t)$ is a random variable given by

$$\delta S(\Delta t) = \varepsilon(t_2) - \varepsilon(t_1)$$

and has probability density function $P_{\delta S}(\gamma)$, $-\infty \leq \gamma \leq \infty$, where

$$P_{\delta S}(\gamma) = P_{\varepsilon_2}(\beta) \otimes P_{\varepsilon_1}(-\beta)$$

$$P_{\delta S}(\gamma) = \int_{-\infty}^{\infty} P_{\varepsilon_2}(\beta) P_{\varepsilon_1}(\beta-\gamma)\, d\beta \qquad \text{(B-3-10)}$$

However since $P_{\delta S}(\gamma)$ is not defined for negative values of the argument eqn. B-3-10 must be considered separately for $\gamma > 0$ and $\gamma < 0$

1. $\gamma > 0$ $\qquad P_{\delta S}(\gamma) = \int_{\gamma}^{\infty} P_{\varepsilon_2}(\beta) P_{\varepsilon_1}(\beta-\gamma)\, d\beta \qquad \text{(B-3-11)}$

2. $\gamma < 0$ $\qquad P_{\delta S}(\gamma) = \int_{0}^{\infty} P_{\varepsilon_2}(\beta) P_{\varepsilon_1}(\beta-\gamma)\, d\beta$

Since $\varepsilon(t_1)$ and $\varepsilon(t_2)$ are identically distributed random variables it is obvious that $P_{\delta S}(\gamma)$ is an even function of γ so considering only the case $\gamma > 0$ and

substituting eqn. B-3-7 into eqn. B-3-11

$$P_{\delta S}(\gamma) = \left[\frac{q^n}{(n-1)!}\right]^2 \int_{\gamma}^{\infty} \beta^{n-1}(\beta-\gamma)^{n-1}\exp[-q\beta]\exp[-q(\beta-\gamma)]d\beta$$

$$P_{\delta S}(\gamma) = \left[\frac{q^n}{(n-1)!}\right]^2 \exp[q\gamma] \int_{\gamma}^{\infty} [\beta(\beta-\gamma)]^{n-1}\exp[-2q\beta]d\beta$$

This is a tabulated integral [29] and

$$P_{\delta S}(\gamma) = \left[\frac{q}{2}\right]^{n+\frac{1}{2}} \frac{2}{\Gamma(n)\sqrt{\pi}} \gamma^{n-\frac{1}{2}} K_{n-\frac{1}{2}}(q\gamma) \quad , \quad \gamma > 0$$

where $\Gamma(n)$ is the gamma function and $K_{n-\frac{1}{2}}$ is the modified Bessel function of order $n-\frac{1}{2}$. Since $P_{\delta S}(\gamma)$ is even it follows that

$$P_{\delta S}(\gamma) = \left(\frac{q}{2}\right)^{n+\frac{1}{2}} \frac{2}{\Gamma(n)\sqrt{\pi}} |\gamma|^{n-\frac{1}{2}} K_{n-\frac{1}{2}}(q|\gamma|) \qquad \text{(B-3-12)}$$

$$, \; -\infty \leq \gamma \leq \infty$$

The variance $\overline{\delta S^2}$ is given by

$$\overline{\delta S^2} = \int_{-\infty}^{\infty} \gamma^2 P_{\delta S}(\gamma)d\gamma$$

where $P_{\delta S}(\gamma)$ is given by eqn. B-3-12

$$\overline{\delta S^2} = 2 \int_0^\infty \gamma^2 \, P_{\delta S}(\gamma) d\gamma$$

$$\overline{\delta S^2} = \left[\frac{q}{2}\right]^{n+\frac{1}{2}} \frac{4}{\Gamma(n)\sqrt{\pi}} \int_0^\infty |\gamma|^{n+\frac{3}{2}} \, K_{n-\frac{1}{2}}(q|\gamma|) d\gamma$$

This is also a tabulated integral [29] and

$$\overline{\delta S^2} = \frac{2n}{q^2} \qquad \text{(B-3-13)}$$

Substituting eqns. B-3-6, B-3-7, and B-3-8 into eqn. B-3-13 gives

$$\overline{\delta S^2} = \frac{32\pi(\bar{\mu}^2)^2 \ell_o^2 D^2}{3r_o^2} \qquad \text{(B-3-14)}$$

4. Free Air Laser Strain Meter Observations

Substituting eqns. B-3-14 and B-2-4 into eqn. B-2-13 yields

$$|\xi'| = \frac{2\,|h_k|\,r_o}{s\,\mu^2\,\ell_o D}\sqrt{\frac{3\,\Delta\tau^3}{32\pi\,\Delta t}} \qquad \text{(B-4-1)}$$

Eqn. B-4-1 is a relationship between the observation time "$\Delta\tau$" required to observe, with a specified confidence level "η" and signal-noise ratio "s" and in the presence of mean square atmospheric refractive index fluctuations "μ^2", a tectonic change in distance assumed to be proceeding at a linear rate "h_k" and the distance "D" over which the observation is to be made. The quantities "r_o", "ℓ_o", and "Δt" are essentially atmospheric constants equal numerically to the "inner scale of turbulence", the "outer scale of turbulence", and the "correlation time for atmospheric ray-paths", respectively. The magnitude of the confidence parameter, "$|\xi'|$", appropriate for the specified confidence level "η" is given by eqn. B-2-11.

Solving eqn. B-4-1 explicitly for $\Delta\tau$ yields

$$\Delta\tau = \left[\frac{32\pi\,\Delta t}{3}\right]^{1/3}\left[\frac{s\,\mu^2\,\ell_o\,D\,|\xi'|}{2\,|h_k|\,r_o}\right]^{2/3} \qquad \text{(B-4-2)}$$

Choosing

$$D = 5 \text{ km } (5\times10^{5} \text{ cm.})$$

$$r_o = 1 \text{ cm.}$$

$$\ell_o = 10^{3} \text{ cm.}$$

$$|h_k| = 1 \text{ cm./year } (3.17\times10^{-8} \text{ cm/sec})$$

$$10^{-14} \leq \overline{\mu^2} \leq 10^{-12}$$

$$\Delta t = 2\times10^{-1} \text{ sec}$$

$$s = 2$$

(For a discussion concerning the appropriate magnitude of the above physical quantities - see Appendix A-4)

Then

$$55\ |\xi'|^{2/3} \text{ sec} \leq \Delta\tau \leq 1.25 \times 10^{3}\ |\xi'|^{2/3} \text{ sec.} \qquad \text{(B-4-3)}$$

depending on the value of the mean square refractive index fluctuations.

Evaluating eqn. B-4-3 for a 99 percent confidence level of observation requires the confidence parameter $|\xi'|$ to equal 2.58. At a 99 percent confidence level of observation it follows that

$$104 \text{ sec} \leq \Delta\tau \leq 2.35 \times 10^{3} \text{ sec.} \qquad \text{(B-4-4)}$$

Thus eqn. B-4-4 indicates that under conditions of weak atmospheric turbulence, $\overline{\mu^2} \sim 10^{-14}$, a free air laser strain meter has a probability of 0.99 of observing, over a distance of 5 km. and with a signal-noise ratio of 2:1, a tectonic change in distance proceeding linearly at a rate of

1 cm/year in 104 seconds (1.73 minutes) of observing time.

If D is changing at the rate of 1 cm/year the net change in D in 104 seconds is $\delta D = 3.29 \times 10^{-6}$ cm. The resulting strain sensitivity of the free air laser strain meter under such conditions would be

$$\frac{\delta D}{D} = \frac{3.29 \times 10^{-6}}{5 \times 10^{5}}$$

$$\frac{\delta D}{D} = 6.6 \times 10^{-12} \qquad \text{(B-4-5)}$$

This strain sensitivity exceeds the limit of presently attainable laser frequency stabilities for such intervals (12).

Under moderate-to-intense atmospheric turbulence, $\overline{\mu^2} \sim 10^{-12}$, the free air laser strain meter can make the same observation at a 99 percent confidence level in 2.35×10^{3} seconds (39 minutes). At a rate of 1 cm/year the displacement occurring in 2.35×10^{3} seconds is $\delta D = 7.45 \times 10^{-5}$ cm. The resulting strain sensitivity of the free air laser strain meter under such conditions would be

$$\frac{\delta D}{D} = \frac{7.45 \times 10^{-5}}{5 \times 10^{5}}$$

$$\frac{\delta D}{D} = 1.5 \times 10^{-10} \qquad \text{(B-4-6)}$$

This strain sensitivity corresponds to presently attainable

laser frequency stabilities for such intervals (12).

Viewed in another manner these results indicate that a free air laser strain meter could make "sampled observations" of tectonic changes in distance proceeding at rates of 1 cm/year or better over a distance of 5 km. with samples measurements occurring every 1.73 minutes in the presence of weak atmospheric turbulence and every 39 minutes in the presence of moderate-to-intense atmospheric turbulence.

In the free air laser strain meter there are several factors limiting the distance over which observations can be made. Among these are: atmospheric degeneration of phase coherence and subsequent loss of fringe visibility, increase of atmospheric modulation of the laser frequency and subsequent jitter in the fringe pattern, and the frequency stability of the laser itself. It will be seen in Chapter III, Section C that given sufficient laser power and sufficiently fast fringe counters the limiting effects of the atmosphere can be made arbitrarily small, however, the laser frequency stability places an intrinsic limit on the system.

If the laser frequency stability as a function of operating time τ is $\frac{\delta\nu(\tau)}{\nu}$ then a "coherence time" $\delta t(\tau)$ can be defined as

$$\delta t(\tau) = \frac{1}{\delta \nu(\tau)} \qquad \text{(B-4-7)}$$

A necessary operating condition for a free air laser strain meter is that

$$2D \ll c\ \delta t\ (\tau) \qquad \text{(B-4-8)}$$

$\delta t(\tau)$ decreases monotonically with increasing τ and all else being equal, $\Delta\tau$ increases monotonically with D. Thus an arbitrary increase in the observing distance D, even if permitted by other constraints, would lead eventually to a violation of condition B-4-8. Thus the limiting condition on observing distance imposed by the coherence length of the laser is

$$2D \ll \frac{c}{\delta \nu\ (\Delta\tau)}$$

$$\Delta\tau = \left[\frac{32\pi\ \Delta t}{3}\right]^{1/3} \left[\frac{s\ \overline{\mu^2}\ \ell_o\ D\ |\Xi'|}{2\ |h_k|\ r_o}\right]^{2/3}$$

5. Accuracy of Observation

a. Error Propagation Analysis

The major source of error in free air laser strain meter observations is due to uncertainties in the elements of the matrix of coefficients coupled with observational errors in the inhomogeneous terms in eqn. B-1-10. Inaccuracies in these quantities will result in incorrect values for the solutions of $U(\Delta\tau)$, the fluctuations in geometrical ray-path length. The "observational eqns." - eqns. B-1-10

$$\begin{pmatrix} \delta L_{\lambda_1} \\ \delta L_{\lambda_2} \\ \delta L_{\lambda_3} \end{pmatrix} = \begin{pmatrix} 1 & f(\lambda_1) & g(\lambda_1) \\ 1 & f(\lambda_2) & g(\lambda_2) \\ 1 & f(\lambda_3) & g(\lambda_3) \end{pmatrix} \begin{pmatrix} U \\ V \\ W \end{pmatrix}$$

can be written

$$\begin{pmatrix} \overline{\delta L_{\lambda_1}} + q_1 \\ \overline{\delta L_{\lambda_2}} + q_2 \\ \overline{\delta L_{\lambda_3}} + q_3 \end{pmatrix} = \begin{pmatrix} 1 & \overline{f(\lambda_1)} + \epsilon_{12} & \overline{g(\lambda_1)} + \epsilon_{13} \\ 1 & \overline{f(\lambda_2)} + \epsilon_{22} & \overline{g(\lambda_2)} + \epsilon_{23} \\ 1 & \overline{f(\lambda_3)} + \epsilon_{32} & \overline{g(\lambda_3)} + \epsilon_{33} \end{pmatrix} \begin{pmatrix} \overline{U} + p_1 \\ \overline{V} + p_2 \\ \overline{W} + p_3 \end{pmatrix}$$

where the "barred" quantities refer to the exact values and q , ϵ , and p are their absolute errors.

The observational eqn. B-1-10 can be written

$$\underline{L} = \underline{\underline{C}}\,\underline{X}$$

where

$$\underline{L} = \begin{pmatrix} \overline{\delta L_{\lambda_1}} + q_1 \\ \overline{\delta L_{\lambda_2}} + q_2 \\ \overline{\delta L_{\lambda_3}} + q_3 \end{pmatrix}$$

$$\underline{X} = \begin{pmatrix} \overline{U} + p_1 \\ \overline{V} + p_2 \\ \overline{W} + p_3 \end{pmatrix}$$

$$\underline{\underline{C}} = \begin{pmatrix} 1 & \overline{f(\lambda_1)} + \epsilon_{12} & \overline{g(\lambda_1)} + \epsilon_{13} \\ 1 & \overline{f(\lambda_2)} + \epsilon_{22} & \overline{g(\lambda_2)} + \epsilon_{23} \\ 1 & \overline{f(\lambda_3)} + \epsilon_{32} & \overline{g(\lambda_3)} + \epsilon_{33} \end{pmatrix}$$

The "exact" eqn. can be written

$$\underset{\sim}{L} = \underset{\sim}{\underline{\underline{C}}}\,\underset{\sim}{X}$$

where

$$\underset{\sim}{L} = \begin{pmatrix} \overline{\delta L}_{\lambda_1} \\ \overline{\delta L}_{\lambda_2} \\ \overline{\delta L}_{\lambda_3} \end{pmatrix}$$

$$\underset{\sim}{\underline{X}} = \begin{pmatrix} \overline{U} \\ \overline{V} \\ \overline{W} \end{pmatrix}$$

$$\underline{\underline{\tilde{C}}} = \begin{pmatrix} 1 & \overline{f(\lambda_1)} & \overline{g}(\lambda_1) \\ 1 & \overline{f(\lambda_2)} & \overline{g}(\lambda_2) \\ 1 & \overline{f(\lambda_3)} & \overline{g}(\lambda_3) \end{pmatrix}$$

Now

$$\underline{X} = \underset{\sim}{\underline{X}} + \underline{p}$$

$$\underline{L} = \underset{\sim}{\underline{L}} + \underline{q}$$

$$\underline{\underline{C}} = \underline{\underline{E}}\,\underline{\underline{\tilde{C}}}$$

where

$$\underline{p} = \begin{pmatrix} p_1 \\ p_2 \\ p_3 \end{pmatrix}$$

$$\underline{q} = \begin{pmatrix} q_1 \\ q_2 \\ q_3 \end{pmatrix}$$

$$\underline{\underline{E}} = \underline{\underline{I}} + \underline{\underline{\nu}} \begin{pmatrix} 1 + \nu_{11} & \nu_{12} & \nu_{13} \\ \nu_{21} & 1 + \nu_{22} & \nu_{23} \\ \nu_{31} & \nu_{32} & 1 + \nu_{33} \end{pmatrix}$$

and it is assumed that $\nu_{ij} \ll 1$.

By substitution it follows that the observational eqns

$$\underline{X} = \underline{\underline{C}}^{-1} \underline{L}$$

can be written

$$\tilde{\underline{X}} + \underline{p} = (\underline{\underline{E}}\,\tilde{\underline{\underline{C}}})^{-1} (\tilde{\underline{L}} + \underline{q})$$

$$\tilde{\underline{X}} + \underline{p} = \tilde{\underline{\underline{C}}}^{-1} \underline{\underline{E}}^{-1} (\tilde{\underline{L}} + \underline{q})$$

but

$$\underline{\underline{E}}^{-1} = \underline{\underline{I}} - \underline{\underline{\nu}}$$

so

$$\underline{\tilde{X}} + \underline{p} = \underline{\underline{\tilde{C}}}^{-1} (\underline{\underline{I}} - \underline{\underline{\nu}}) (\underline{\tilde{L}} + \underline{q})$$

and dropping terms of the order of $\underline{\underline{\nu}}\ \underline{q}$

$$\underline{\tilde{X}} + \underline{p} = \underline{\underline{\tilde{C}}}^{-1} \underline{\tilde{L}} + \underline{\underline{\tilde{C}}}^{-1} (\underline{q} - \underline{\underline{\nu}} \underline{\tilde{L}})$$

Therefore one can identify

$$\underline{p} = \underline{\underline{\tilde{C}}}^{-1} (\underline{q} - \underline{\underline{\nu}} \underline{\tilde{L}})$$

The column vector $\underline{p}$ representing absolute errors in the unknown U , V , and W can be decomposed into systematic and random errors

$$\underline{p} = \underline{p}_{syst} + \underline{p}_{rand}$$

where

$$\underline{p}_{syst} = - \tilde{\underline{\underline{C}}}^{-1} \underline{\nu} \tilde{\underline{\underline{L}}} \qquad \text{(B-5-1)}$$

$$\underline{p}_{rand} = \tilde{\underline{\underline{C}}}^{-1} \underline{q} \qquad \text{(B-5-2)}$$

b. Systematic Errors

The systematic errors in the matrix of coefficients manifest themselves as a "scaling" by a constant factor of the observed rate of tectonic motion and cannot be eliminated except by more accurate knowledge of the dispersion formula for the atmosphere. An estimate of the magnitude of this scaling can be made based on present knowledge of the dispersion formula for the atmosphere.

From eqn. B-5-1

$$p_{i\ syst} = - \tilde{C}^{-1}_{ij} \nu_{jk} \tilde{L}_k \quad .$$

The only systematic errors affecting the measurement are the errors in $\overline{U}$, the fluctuation in geometrical ray-path length, given by p_1

$$p_{1\ syst} = - \sum_{j=1}^{3} \sum_{k=1}^{3} \tilde{C}^{-1}_{1j} \nu_{jk} \tilde{L}_k \qquad \text{(B-5-3)}$$

This calculation requires values for the elements of the matrix $\underline{\underline{\nu}}$.

The elements of the matrix $\underline{\underline{\nu}}$ are related to the errors in the matrix of coefficients by definition

$$\underline{\underline{C}} = (\underline{\underline{I}} + \underline{\underline{\nu}}) \underline{\underline{\tilde{C}}}$$

which gives rise to nine equations in nine unknowns.

$$1 + \nu_{11} + \nu_{12} + \nu_{13} = 1$$

$$\nu_{21} + 1 + \nu_{22} + \nu_{23} = 1$$

$$\nu_{31} + \nu_{32} + 1 + \nu_{33} = 1$$

$$\nu_{12} \left[\bar{f}(\lambda_2) - \bar{f}(\lambda_1) \right] + \nu_{13} \left[\bar{f}(\lambda_3) - \bar{f}(\lambda_1) \right] = \epsilon_{12}$$

$$-\nu_{21} \left[\bar{f}(\lambda_2) - \bar{f}(\lambda_1) \right] + \nu_{23} \left[\bar{f}(\lambda_3) - \bar{f}(\lambda_2) \right] = \epsilon_{22}$$

$$-\nu_{32} \left[\bar{f}(\lambda_2) - \bar{f}(\lambda_2) \right] - \nu_{31} \left[\bar{f}(\lambda_3) - \bar{f}(\lambda_1) \right] = \epsilon_{32}$$

$$\nu_{12} \left[\bar{g}(\lambda_2) - \bar{g}(\lambda_1) \right] + \nu_{13} \left[\bar{g}(\lambda_3) - \bar{g}(\lambda_1) \right] = \epsilon_{13}$$

$$-\nu_{21} \left[\bar{g}(\lambda_2) - \bar{g}(\lambda_1) \right] + \nu_{23} \left[\bar{g}(\lambda_3) - \bar{g}(\lambda_2) \right] = \epsilon_{23}$$

$$-\nu_{32} \left[\bar{g}(\lambda_3) - \bar{g}(\lambda_2) \right] - \nu_{31} \left[\bar{g}(\lambda_3) - \bar{g}(\lambda_1) \right] = \epsilon_{33}$$

Solving the first set of three equations for $\nu_{11}, \nu_{22}, \nu_{33}$, reduces

them to a set of six equations.

$$\nu_{12}\ \Delta_1 + \nu_{13}\ \Delta_2 = \epsilon_{12}$$

$$\nu_{12}\ \delta_1 + \nu_{13}\ \delta_2 = \epsilon_{13}$$

$$-\nu_{21}\ \Delta_1 + \nu_{23}\ (\Delta_2 - \Delta_1) = \epsilon_{22}$$

$$\nu_{21}\ \delta_1 + \nu_{23}\ (\delta_2 - \delta_1) = \epsilon_{23}$$

$$-\nu_{32}\ (\Delta_2 - \Delta_1) - \nu_{31}\ \Delta_2 = \epsilon_{32}$$

$$-\nu_{32}\ (\delta_2 - \delta_1) - \nu_{31}\ \delta_2 = \epsilon_{33}$$

where

$$\Delta_1 = f(\lambda_2) - f(\lambda_1)$$

$$\Delta_2 = f(\lambda_3) - f(\lambda_1)$$

$$\delta_1 = g(\lambda_2) - g(\lambda_1)$$

$$\delta_2 = g(\lambda_3) - g(\lambda_1)$$

The solutions to the nine equations are

$$\nu_{11} = \frac{\epsilon_{13}(\Delta_2-\Delta_1) - \epsilon_{12}(\delta_2-\delta_1)}{\Delta_1\ \delta_2 - \Delta_2\ \delta_1}$$

$$\nu_{12} = \frac{\epsilon_{12}\,\delta_2 - \epsilon_{13}\,\Delta_2}{\Delta_1\,\delta_2 - \Delta_2\,\delta_1}$$

$$\nu_{13} = \frac{\epsilon_{13}\,\Delta_1 - \epsilon_{12}\,\delta_1}{\Delta_1\,\delta_2 - \Delta_2\,\delta_1}$$

$$\nu_{21} = -\frac{\epsilon_{22}(\delta_2-\delta_1) - \epsilon_{23}(\Delta_2-\Delta_1)}{\Delta_1(\delta_2-\delta_1) - \delta_1(\Delta_2-\Delta_1)}$$

$$\nu_{22} = \frac{\epsilon_{22}\,\delta_2 - \epsilon_{23}\,\Delta_2}{\Delta_1(\delta_2-\delta_1) - \delta_1(\Delta_2-\Delta_1)}$$

$$\nu_{23} = \frac{\epsilon_{23}\,\Delta_1 - \epsilon_{22}\,\delta_1}{\Delta_1(\delta_2-\delta_1) - \delta_1(\Delta_2-\Delta_1)}$$

$$\nu_{31} = -\frac{\epsilon_{33}(\Delta_2-\Delta_1) - \epsilon_{32}(\delta_2-\delta_1)}{\delta_2(\Delta_2-\Delta_1) - \Delta_2(\delta_2-\delta_1)}$$

$$\nu_{32} = -\frac{\epsilon_{32}\,\delta_2 - \epsilon_{33}\,\Delta_2}{\delta_2(\Delta_2-\Delta_1) - \Delta_2(\delta_2-\delta_1)}$$

$$\nu_{33} = \frac{\epsilon_{32}\,\delta_1 - \epsilon_{33}\,\Delta_1}{\delta_2(\Delta_2-\Delta_1) - \Delta_2(\delta_2-\delta_1)}$$

Choosing laser wavelengths $\lambda_1 = 10\ \mu$, $\lambda_2 = 0.5\ \mu$, $\lambda_3 = 0.3\ \mu$, it follows from the dispersion formula for the atmosphere (A-2 eqns. A-2-7 and A-2-8) that $\Delta_1 = 1.804 \times 10^{-6}$, $\Delta_2 = 5.384 \times 10^{-6}$, $\delta_1 = 2.265 \times 10^{-6}$, $\delta_2 = 6.297 \times 10^{-6}$. The refractive index formula claims an accuracy of one part in 10^9 (20) in which case ϵ_{ij} are of the order of 1×10^{-9} randomly distributed about zero.

Thus from the above solutions it follows that

$$\nu_{ij} \sim 2 \times 10^{-3} \qquad \text{(B-5-4)}$$

and are also randomly distributed about zero.

From eqn. B-5-3 it follows that the systematic error in $U(\Delta t)$ is $p_{1\ syst}$

$$\begin{aligned} P_{1\ syst} = {} & \hat{C}_{11}^{-1} \left(\nu_{11} \delta L_{\lambda_1} + \nu_{12} \delta L_{\lambda_2} + \nu_{13} \delta L_{\lambda_3} \right) \\ & + \hat{C}_{12}^{-1} \left(\nu_{21} \delta L_{\lambda_1} + \nu_{22} \delta L_{\lambda_2} + \nu_{23} \delta L_{\lambda_3} \right) \\ & + \hat{C}_{13}^{-1} \left(\nu_{31} \delta L_{\lambda_1} + \nu_{32} \delta L_{\lambda_2} + \nu_{33} \delta L_{\lambda_3} \right) \end{aligned} \qquad \text{(B-5-5)}$$

However the exact solution for $U(\Delta t)$ is given by

$$U(\Delta t) = \tilde{C}_{11}^{-1} \delta L_{\lambda_1} + \tilde{C}_{12}^{-1} \delta L_{\lambda_2} + \hat{C}_{13}^{-1} \delta L_{\lambda_3}$$

Thus the exact value of the fluctuation in geometrical ray-path length $U(\Delta t)$ gets scaled by the systematic errors to a value of $U(\Delta t) + p_{1\ syst}$. The scaling factor is given by the ratio

$$\frac{U(\Delta t) + p_{1\ syst}}{U(\Delta t)}$$

The scaling factor can be estimated by assuming that to a first order (neglecting dispersion) the fluctuations in optical path length are all equal for wavelengths λ_1, λ_2 and λ_3. Thus

$$\delta L_{\lambda_1} \cong \delta L_{\lambda_2} \cong \delta L_{\lambda_3}$$

and

$$p_{1\ syst} \cong \hat{C}_{11}^{-1}\ \delta L_{\lambda_1}\ (\nu_{11} + \nu_{12} + \nu_{13})$$

$$+ \tilde{C}_{12}^{-1}\ \delta L_{\lambda_2}\ (\nu_{21} + \nu_{22} + \nu_{23})$$

$$+ \tilde{C}_{13}^{-1}\ \delta L_{\lambda_3}\ (\nu_{31} + \nu_{32} + \nu_{33})$$

If it is assumed, on the basis of eqn. B-5-4, that the ν_{ij} are drawn from a gaussian distribution about zero with standard deviation of the order of 2×10^{-3} then $p_{1\ syst}$ can be estimated to be

$$p_{1\ syst} = \pm 2\sqrt{3} \times 10^{-3} \left[\tilde{C}_{11}^{-1}\ \delta L_{\lambda_1} + \tilde{C}_{12}^{-1} \delta L_{\lambda_2} + \tilde{C}_{13}^{-1} \delta L_{\lambda_3}\right]$$

and the scaling factor is given by

$$\frac{U(\Delta t) + p_{1\ syst}}{U(\Delta t)} = \frac{1 \pm 2\sqrt{3}x10^{-3}}{1}$$

$$\frac{U(\Delta t) + p_{1\ syst}}{U(\Delta t)} = 1.0 \pm 0.00346 \quad .$$

Since this scaling factor is present in each determination of $U(\Delta t)$ it will also be present in their mean and so will be reflected in the observed tectonic motions.

In other words, present day knowledge of the atmospheric dispersion would result in systematic errors in the observed tectonic motions of the order of $\pm 0.3\%$.

c. Random Errors

The random errors in free air laser strain meter observations are the result of inaccuracies in the fringe count. Keeping the random errors below a maximum acceptable level will place limitations on the accuracy to which fringes must be counted.

From eqn. B-5-2

$$p_{i\ rand} = \tilde{C}^{-1}_{ij}\ q_j$$

The only random errors affecting the measurement are the errors in U , the fluctuation in geometrical ray-path length, given

by

$$p_{1\ rand} = \sum_{j=1}^{3} \tilde{C}_{1j}^{-1}\, q_j$$

If fringes are counted on each channel to $\pm \epsilon$ parts of a fringe, then

$$q_j = \pm \epsilon_j\, \lambda_j$$

and

$$p_{1\ rand} = \pm \epsilon_1 \tilde{C}_{11}^{-1} \lambda_1 \pm \epsilon_2 \tilde{C}_{12}^{-2} \lambda_2 \pm \epsilon_3 \tilde{C}_{13}^{-3} \lambda_3 \qquad \text{(B-5-6)}$$

The worst case occurs when all ϵ_j have the same sign. Thus

$$p_{1\ rand} \leqslant \epsilon \left[\tilde{C}_{11}^{-1} \lambda_1 + \tilde{C}_{12}^{-1} \lambda_2 + \tilde{C}_{13}^{-1} \lambda_3 \right]$$

If wavelengths $\lambda_1 = 10\,\mu$, $\lambda_2 = 0.5\ \mu$, $\lambda_3 = 0.3\ \mu$ are chosen

$$p_{1\ rand} \leqslant \epsilon \lambda_3 \left[33.3\ \tilde{C}_{11}^{-1} + 1.66\ \tilde{C}_{12}^{-1} + \tilde{C}_{13}^{-1} \right] \qquad \text{(B-5-7)}$$

Now

$$\tilde{C}_{ij}^{-1} = \frac{\text{cof.}\left[\tilde{C}_{ji}\right]}{\det.\left[\tilde{C}_{ij}\right]}$$

and from the definition of $\tilde{C}_{ij}$ it follows that

$$\underset{\sim}{C}^{-1}_{11} = 1 + \frac{\bar{g}(\lambda_1)\left[\Delta_1-\Delta_2\right] + f(\lambda_1)\left[\delta_2-\delta_1\right]}{\Delta_1\,\delta_2 - \Delta_2\,\delta_1}$$

$$\underset{\sim}{C}^{-1}_{12} = \frac{\bar{g}(\lambda_1)\,\Delta_2 - \bar{f}(\lambda_1)\,\delta_2}{\Delta_1\,\delta_2 - \Delta_2\,\delta_1}$$

$$\underset{\sim}{C}^{-1}_{13} = \frac{\bar{f}(\lambda_1)\,\delta_1 - \bar{g}(\lambda_1)\,\Delta_1}{\Delta_1\,\delta_2 - \Delta_2\,\delta_1}$$

and using the above wavelengths and dispersion formula for the atmosphere (A-2 eqns A-2-7 and A-2-8) it follows that

$$\underset{\sim}{\bar{g}}(\lambda_1) \cong 6.487 \times 10^{-5} \qquad \underset{\sim}{\bar{f}}(\lambda_1) \cong 7.749 \times 10^{-5}$$

$$\bar{g}(\lambda_2) \cong 6.714 \times 10^{-5} \qquad \bar{f}(\lambda_2) \cong 7.930 \times 10^{-5}$$

$$\bar{g}(\lambda_3) \cong 7.180 \times 10^{-5} \qquad \bar{f}(\lambda_3) \cong 8.288 \times 10^{-5}$$

and so

$$\tilde{C}^{-1}_{11} \cong -93.7$$

$$\tilde{C}^{-1}_{12} \cong 163.5$$

$$\tilde{C}^{-1}_{13} \cong -68.8$$

Substituting these figures into eqn. B-5-7 gives

$$p_{1\ \mathrm{rand}} \leqslant 8.74 \times 10^{-2}\,\epsilon \ \text{cm.}$$

d. Accuracy of Fringe Counting

The proposed method of observation of the free air laser strain meter relies on averaging a series of continuous consecutive observations of the net fluctuations in the geometrical ray-path length to reduce the atmospheric effects (which have a long term mean of zero) to "insignificant" levels. The quantity "γ" represented by the error bars in Fig. III-3 is the expected difference or "error" between the sample mean of M samples of the atmospheric fluctuation in geometrical ray-path length, $\delta S(\Delta t)$, and its population mean, $\overline{\delta S}(\Delta t) \equiv 0$. The exact value of δS is contaminated by the effects of both systematic and random errors

$$\delta S_{obs} = \delta S_{exact} + p_{1\ syst} + p_{1\ rand} \quad .$$

The systematic errors are inherent in the observing method and can be combined with δS_{exact} to give δS_{atmos}

$$\delta S_{obs} = \delta S_{atmos} + p_{1\ rand} \quad .$$

The quantity $\overline{\delta S^2}$ appearing in eqn. B-2-13 should ideally be $\overline{\delta S^2_{atmos}}$ but will in the course of free air laser strain meter observations be substituted for by $\overline{\delta S^2_{obs}}$.

$$\overline{\delta S^2_{obs}} = \overline{\delta S^2_{atmos}} + \overline{p_1^2}_{rand}$$

In order to permit this it is necessary that

$$\overline{p_{1\ rand}^2} \ll \overline{\delta S_{atmos}^2}.$$

$$\overline{p_{1\ rand}^2} = \overline{(\pm \epsilon_1 \tilde{C}_{11}^{-1} \lambda_1 \pm \epsilon_2 \tilde{C}_{12}^{-1} \lambda_2 \pm \epsilon_3 \tilde{C}_{13}^{-1} \lambda_3)^2}$$

If the fringe observation errors are assumed to be uncorrelated in each channel with a mean value of zero then

$$\overline{p_{1\ rand}^2} = \overline{(\epsilon_1 \tilde{C}_{11}^{-1} \lambda_1)^2} + \overline{(\epsilon_2 \tilde{C}_{12}^{-1} \lambda_2)^2} + \overline{(\epsilon_3 \tilde{C}_{13}^{-1} \lambda_3)^2}$$

Using the above values for λ_1 , λ_2 , and λ_3

$$\overline{p_{1\ rand}^2} = \epsilon^2 \lambda_3^2 \left[(33.3\ \tilde{C}_{11}^{-1})^2 + (1.66\ \tilde{C}_{12}^{-1})^2 + (\tilde{C}_{13}^{-1})^2\right]$$

and using the above values for $\tilde{C}_{11}^{-1}$, $\tilde{C}_{12}^{-1}$ and $\tilde{C}_{13}^{-1}$

$$\overline{p_{1\ rand}^2} = 8.83 \times 10^{-3}\ \epsilon^2\ cm^2 \qquad \text{(B-5-8)}$$

The value of $\overline{\delta S_{atmos}^2}$ is given by eqn. B-3-14 to be

$$\overline{\delta S^2_{atmos}} = \frac{32\pi\,(\overline{\mu^2})^2\,\ell_o^2 D^2}{3\,r_o^2}$$

Taking

$$\overline{\mu^2} = 10^{-12}$$

$$\ell_o = 10^3 \text{ cm}$$

$$D = 5 \times 10^5 \text{ cm}$$

$$r_o = 1 \text{ cm}$$

(For a discussion concerning the appropriate magnitude of these quantities - see Appendix A-4)

$$\overline{\delta S^2_{atmos}} = 8.39 \times 10^{-6} \text{ cm}^2$$

If it is required that

$$\overline{p^2_{1\,rand}} \ll \overline{\delta S^2_{atmos}}$$

then

$$8.83 \times 10^{-3}\ \epsilon^2 \ll 8.39 \times 10^{-6}$$

$$\epsilon^2 \ll 10^{-3}$$

or

$$\epsilon \approx 10^{-2}$$

Thus it is seen that counting fringes to an accuracy of $\pm 10^{-2}$ parts of a fringe is sufficient to facilitate free air laser strain meter observations over a distance of 5 km in the presence of moderate atmospheric turbulence.

Present methods of fringe observation in conventional laser strain meters are accurate to small fractions of a fringe. The 1 km. long laser strain meter in the Cascade Tunnel of the Stevens Pass in the state of Washington, U.S.A. counts fringes to an accuracy of $\pm 10^{-2}$ parts of a fringe (39). A small laser strain meter has been designed by Salisbury and Gangi (42) which is capable of measuring strains of one part in 10^{10} over a distance of 1 meter. This strain meter operates with an 0.6328μ He - Ne laser and such measurements correspond to fringe observations of $\pm 3.06 \times 10^{-4}$ parts of a fringe. Moreover it is claimed (39) that the fluctuations in the number of photons in the laser output due to inherent noise characteristics of the laser are so low that measurements accurate to $\pm 10^{-5}$ parts of a fringe are practical.

C. FRINGE OBSERVATION

1. Degenerating Effects of the Atmosphere on a Laser Beam

The degenerating effects of a turbulent atmosphere on a laser beam propagating through it can be roughly divided into two classes; "whole beam" effects and "internal" effects, depending on whether the effect is primarily caused by turbulence scales larger or smaller than ℓ_o . "Whole beam effects" include:

(1) Deviations of direction of the entire beam - "quivering".

(2) Lateral displacements of the entire beam - "spot dancing".

(3) Fluctuations in cross-sectional area of the entire beam - "breathing".

The whole beam effects are those which contribute to the extra ray-path length over the straight line distance, $\varepsilon(t)$, and hence to $\delta S(\Delta t)$. Whole beam effects produce fluctuations in the transit time of the beam and in the case of laser output manifest themselves as a frequency modulation.

Since an electromagnetic disturbance can be described as a complex scalar function of position defined by an amplitude and a phase (if polarization effects are ignored) it follows that the remaining "internal" degenerating atmospheric effects

can be divided into two sub-classes - "amplitude effects" and "phase effects". "Amplitude effects" can be described as:

(4) Fluctuations in intensity of various regions within the beam - "boiling".

"Phase effects" can be described as:

(5) Fluctuations in transit time between individual rays of the beam producing "crumbling of the wave front" or "phase fluctuations" over the beam's cross section.

For the operation of a free air laser strain meter only effects (4) and (5) are potentially troublesome.

Since the atmospheric refractive index, even under the most turbulent conditions, is a continuous function of position, it follows that the fronts of constant phase, which can be assumed to be plane at the exit pupil of the laser, always remain connected surfaces in space as the beam propagates through the atmosphere. Thus a laser beam propagating through a turbulent atmosphere can be described as being "locally coherent". This is intended to describe the fact that surrounding any given point on a front of constant phase there exists a "coherence patch" over which the phase front can be approximated, to any desired accuracy, by a plane. The dimensions of the coherence patch decrease monotonically with increasing specified degree of coherence and with increasing distance of propagation. If the portion of the incoming wavefront incident on the diffracting apertures in

the interferometers I_1 , I_2 and I_3 , Fig. III-1, has dimensions comparable to a region of high coherence, then interference fringes with a correspondingly high visibility will result.

Thus by sufficiently restricting the diffracting aperture and correspondingly increasing the power output of the laser a free air laser strain meter can be made to operate in a condition unperturbed by the degenerating effects of atmospheric turbulence.

2. Fraunhofer Diffraction from a Double Rectangular Aperture

The interferometers I_1 , I_2 and I_3 of a free air laser strain meter, Fig. III-1, will consist of double rectangular diffracting apertures. The optical system will be arranged so that light transmitted by mirror M_4 is incident on rectangular aperture #1 and light from the retroreflector off mirror M_5 is incident on rectangular aperture #2. It is assumed that the aperture dimensions are equal and small enough to ensure reasonable coherence across the aperture. It is further assumed that the airy disc of the optical channel preceding the diffracting aperture is large enough to ensure the existence of a region of the wavefront for interference which is unperturbed by diffraction of the optical channel. The light incident on aperture #1 with angular frequency ω_1 and the light incident on aperture #2, having traversed the turbulent atmosphere, will be partially coherent and have instantaneous angular frequency ω_2 , $\omega_2 \neq \omega_1$. The instantaneous frequency ω_2 varies randomly, with mean value ω_1 , due to the effective frequency modulation imposed on the laser beam by the turbulent atmosphere.

Consider two rectangular diffracting apertures #1 and #2, Fig. III-6, in the $\xi\eta$-plane and assume that the optical disturbance can be represented by a continuous single valued

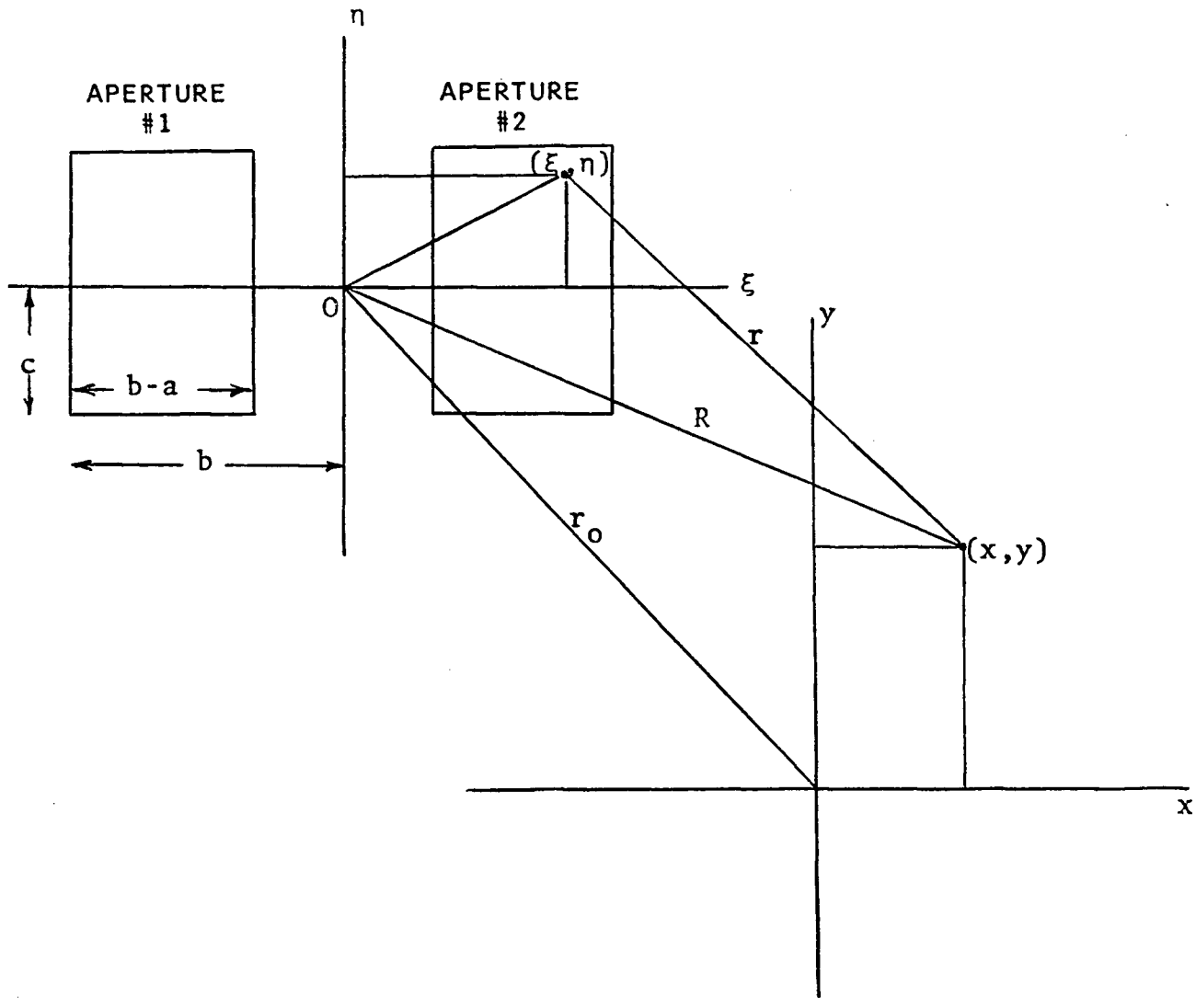

FIG. III-6

FRAUNHOFER DIFFRACTION FROM A DOUBLE RECTANGULAR APERTURE

complex function of position, the square of the modulus of which is proportional everywhere to the intensity of the optical disturbance at that point.

The total disturbance at a point xy in the xy-plane is given by the sum of the contributions, added according to phase, from the source elements $d\xi d\eta$ in the $\xi\eta$-plane. If the optical disturbance in the $\xi\eta$-plane is represented by

$$\phi(\xi\eta) = A(\xi\eta)\exp -i\beta(\xi\eta;t)d\xi d\eta$$

where $A(\xi\eta)$ is the amplitude per unit area
and $\beta(\xi\eta;t)$ is the total phase over the $\xi\eta$-plane
Then the source element $d\xi d\eta$ at $\xi\eta$, in the $\xi\eta$-plane, produces a disturbance at xy, in the xy-plane, given by

$$dB = \frac{A(\xi\eta)}{r/r_o} \exp -i(\beta(\xi\eta;t) - \phi)d\xi d\eta$$

where ϕ is a phase angle resulting from the transit time from the point $\xi\eta$ to the point xy.

$$\phi = 2\pi \frac{r}{\lambda}$$

The total disturbance at xy is given by

$$B(xy) = \int\int_{\substack{\xi\eta \\ \text{plane}}} \frac{A(\xi\eta)}{r/r_o} \exp -i[\beta(\xi\eta;t) - \frac{2\pi r}{\lambda}]d\xi d\eta \qquad (C\text{-}2\text{-}1)$$

From Fig. III-6

$$r^2 = r_o^2 + (x - \xi)^2 + (y - \eta)^2 \qquad (C\text{-}2\text{-}2)$$

and

$$R^2 = r_o^2 + x^2 + y^2 \qquad (C\text{-}2\text{-}3)$$

therefore from eqns. C-2-2 and C-2-3

$$r^2 = R^2 + \xi^2 + \eta^2 - 2(x\xi + y\eta) \qquad (C\text{-}2\text{-}4)$$

completing the square in eqn. C-2-4

$$r^2 = \left[(R^2 + \xi^2 + \eta^2)^{\frac{1}{2}} - \frac{x\xi + y\eta}{(R^2 + \xi^2 + \eta^2)^{\frac{1}{2}}}\right]^2 - \frac{(x\xi + y\eta)^2}{R^2 + \xi^2 + \eta^2}$$

(C-2-5)

Fraunhofer diffraction holds when

$$x,y;\ \xi,\eta \ll R \qquad \text{(C-2-6)}$$

or when

$$\frac{x\xi + y\eta}{R^2 + \xi^2 + \eta^2} \ll 1$$

so

$$r \cong R - \frac{x\xi + y\eta}{R} \qquad \text{(C-2-7)}$$

If $A(\xi\eta)$ and $\beta(\xi\eta;t)$ are assumed to be constant over the $\xi\eta$-plane eqn. C-2-1 can be written

$$B(xy) = \frac{r_o A}{R}\left[\int_{-c}^{c} d\eta \int_{-b}^{-a} d\xi\ \exp -i(\omega_1 t - \frac{2\pi r}{\lambda}) + \int_{-c}^{c} d\eta \int_{a}^{b} d\xi\ \exp -i(\omega_2 t - \frac{2\pi r}{\lambda})\right]$$

(C-2-8)

where ω_1 , ω_2 are the effective angular frequencies of the laser output observed over apertures #1 and #2 respectively. Make a change of variables in the first integral

$$\xi' = -\xi \qquad r' = r(\eta\xi')$$

Eqn. C-2-8 then becomes

$$B(xy) = \frac{r_o A}{R} \int_{-c}^{c} d\eta \int_{a}^{b} d\xi \left[\exp -i(\omega_1 t - \frac{2\pi r}{\lambda}) + \exp -i(\omega_2 t - \frac{2\pi r}{\lambda}) \right]$$

$$B(xy) = \frac{r_o A}{R} \int_{-c}^{c} d\eta \int_{a}^{b} d\xi \left[\cos(\omega_1 t - \frac{2\pi r'}{\lambda}) + \cos(\omega_2 t - \frac{2\pi r}{\lambda}) \right.$$

$$\left. -i(\sin(\omega_1 t - \frac{2\pi r'}{\lambda}) + \sin(\omega_2 t - \frac{2\pi r}{\lambda})) \right]$$

Using the formulae for the addition of sines and cosines

$$B(xy) = \frac{2r_o A}{R} \int_{-c}^{c} d\eta \int_{a}^{b} d\xi \left[\cos(\Omega_1 t - \frac{\pi}{\lambda}(r' + r))\cos(\Omega_2 t - \frac{\pi}{\lambda}(r' - r)) \right.$$

$$\left. -i \sin(\Omega_1 t - \frac{\pi}{\lambda}(r' + r))\cos(\Omega_2 t - \frac{\pi}{\lambda}(r' - r)) \right] \qquad \text{(C-2-9)}$$

where

$$\Omega_1 = \frac{\omega_1 + \omega_2}{2} \quad ; \quad \Omega_2 = \frac{\omega_1 - \omega_2}{2} \qquad \text{(C-2-10)}$$

From eqn. C-2-7 it follows that

$$r' + r = 2(R - \frac{y\eta}{R}) \qquad r' - r = 2\frac{x\xi}{R} \qquad \text{(C-2-11)}$$

Substituting eqns. C-2-11 into eqn. C-2-9 gives

$$B(xy) = \frac{2r_o A}{R} \int_{-c}^{c} d\eta \int_{a}^{b} d\xi \left[\cos(\Omega_1 t + \frac{2\pi}{\lambda}(\frac{y\eta}{R} - R))\cos(\Omega_2 t - \frac{2\pi}{\lambda}\frac{x\xi}{R}) \right.$$

$$\left. -i \sin(\Omega_1 t + \frac{2\pi}{\lambda}(\frac{y\eta}{R} - R))\cos(\Omega_2 t - \frac{2\pi}{\lambda}\frac{x\xi}{R}) \right] \qquad \text{(C-2-12)}$$

The integration of eqn. C-2-12 is straightforward and gives

$$B(xy) = \frac{2r_o A}{R}\frac{\lambda R}{\pi x}\frac{\lambda R}{\pi y} \sin\frac{2\pi yc}{\lambda R} \sin\frac{\pi x}{\lambda R}(b-a)\cos(\frac{\pi x}{\lambda R}(b+a) - \Omega_2 t)$$

$$\cdot \left[\cos(\frac{2\pi R}{\lambda} - \Omega_1 t) + i \sin(\frac{2\pi R}{\lambda} - \Omega_1 t) \right] \qquad \text{(C-2-13)}$$

The intensity of the light in xy-plane is given by

$$I(xy) = B^*B$$

$$I(xy) = 16c^2(b-a)^2\left[\frac{r_o A}{R}\right]^2 \frac{\sin^2\frac{\pi x}{\lambda R}(b-a)}{\left[\frac{\pi x}{\lambda R}(b-a)\right]^2} \quad \frac{\sin^2\frac{2\pi yc}{\lambda R}}{\left[\frac{2\pi yc}{\lambda R}\right]^2} \cdot \cos^2\left[\frac{\pi x}{\lambda R}(b+a) - \Omega_2 t\right]$$

(C-2-14)

Since the light incident on the two apertures is only partially coherent the resultant intensity pattern $I(xy)$ must be modified to allow for the partial coherence. Eqn. C-2-14 can be written

$$I(xy) = 16c^2(b-a)^2\left[\frac{r_o A}{R}\right]^2 \frac{\sin^2\frac{\pi x}{\lambda R}(b-a)}{\left[\frac{\pi x}{\lambda R}(b-a)\right]^2} \quad \frac{\sin^2\frac{2\pi yc}{\lambda R}}{\left[\frac{2\pi yc}{\lambda R}\right]^2} \cdot$$

$$\left[1 - \sin^2\left[\frac{\pi x}{\lambda R}(b+a) - \Omega_2 t\right]\right]$$

The effect of the partially coherent radiation is to reduce the visibility of the interference fringes to the value V, $0 < V < 1$, [34]. Thus

$$I(xy) = 16c^2(b-a)^2\left[\frac{r_o A}{R}\right]^2 \frac{\sin^2\frac{\pi x}{\lambda R}(b-a)}{\left[\frac{\pi x}{\lambda R}(b-a)\right]^2} \quad \frac{\sin^2\frac{2\pi yc}{\lambda R}}{\left[\frac{2\pi yc}{\lambda R}\right]^2} \cdot$$

$$\left[1 - V\sin^2\left[\frac{\pi x}{\lambda R}(b+a) - \Omega_2 t\right]\right] \qquad \text{(C-2-15)}$$

A sketch of the intensity pattern $I(xy)$ for fringe visibility $V \sim 0.4$ is shown in Fig. III-7. From formula C-2-15 it is clear that the fringes are displaced in the positive or negative x-direction at a rate proportional to, and depending on the sign of, $2\Omega_2$.

$$\Omega_2 = \frac{\omega_1 - \omega_2}{2}$$

If the optical path length L is changing at a rate of $\frac{dL}{dt}$, the transit time T is changing at a rate $\frac{dT}{dt} = \frac{1}{c}\frac{dL}{dt}$. If the velocity of light is assumed to be constant, a linear rate of change of the transit time of the light signal imposes a constant d.c. shift on the effective frequency of the light signal of an amount $\Delta\omega = \omega_1 \frac{dT}{dt}$.
Therefore

$$\Delta\omega = \omega_1 - \omega_2 = \frac{\omega_1}{c}\frac{dL}{dt}$$

and

$$\Omega_2 = \frac{\omega_1}{2c}\frac{dL}{dt}$$

The net fringe count for the wavelength λ in an interval $t_1 t_2$ is given by

$$C_\lambda(t_1 t_2) = \frac{1}{2\pi}\int_{t_1}^{t_2} 2\Omega_2(t)dt = \frac{2\omega_1}{4\pi c}\int_{t_1}^{t_2}\frac{dL_\lambda(t)}{dt}\,dt$$

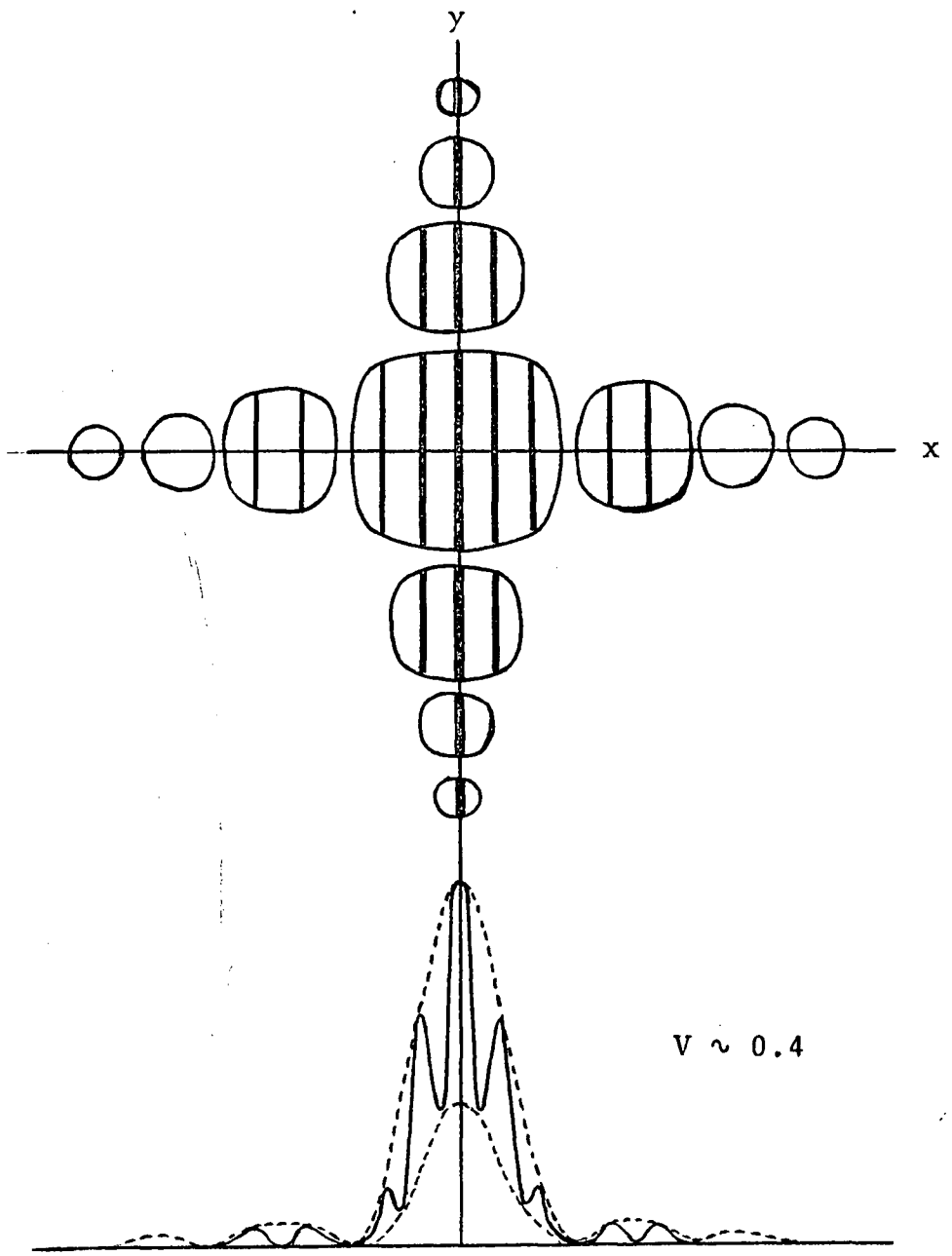

FIG. III-7

INTENSITY PATTERN, I(xy), FROM FRAUNHOFER DIFFRACTION THROUGH A DOUBLE RECTANGULAR APERTURE

FRINGE VISIBILITY $V \sim 0.4$

$$C_\lambda(t_1 t_2) = \frac{1}{\lambda} \left(L_\lambda(t_2) - L_\lambda(t_1)\right)$$

$$\lambda C_\lambda(t_1 t_2) = \delta L_\lambda(t_1 t_2) \qquad \text{(C-2-16)}$$

Eqn. C-2-16 evaluated for λ_1 , λ_2 and λ_3 is seen to be identical with eqns. B-1-11.

3. Fringe Visibility

The coherence length (i.e. the maximum difference in path length that can be introduced between two light signals and still produce observable interference effects) of laser output frequency stabilized to $S_\nu \sim \frac{\delta\nu}{\nu}$ is equal to

$$\ell_{coh} \sim \frac{c}{\delta\nu}$$

A limitation on the distance D over which a free air laser strain meter can operate is simply

$$2D << \ell_{coh}$$

For a laser with a frequency $\sim 10^{14}$ Hz. and a short term frequency stability of one part in 10^{11} the coherence length is of the order of 300 km. Since a short term frequency stability $S_\nu(\tau)$ of one part in 10^{11} is not difficult to achieve over intervals τ of the order of 10^{-3} sec (the transit time of a photon between the end mirrors of a free air laser strain meter) [A-1], it appears that the frequency stability of lasers is ample for the realization of free air laser strain meters of lengths up to 100 km. However the degeneration of phase coherence within the beam due to atmospheric turbulence and the

subsequent decrease of fringe visibility proves to be a more severe limitation on operating distance than coherence length.

The complex coherence function $\gamma_{p_1p_2}(\tau)$ between the optical disturbance at points $p_1 = (\xi_1\eta_1)$ in aperture #1 and $p_2 = (\xi_2\eta_2)$ in aperture #2, Fig. III-8, is defined [35, chapt. 10] as

$$\gamma_{p_1p_2}(\tau) = \frac{\overline{\phi_{p_1}(t+\tau)\,\phi^*_{p_2}(t)}}{[\phi_{p_1}(t)\phi^*_{p_1}(t)\phi_{p_2}(t)\phi^*_{p_2}(t)]^{\frac{1}{2}}} \qquad \text{(C-2-17)}$$

where the bar denotes a time average and where

$$\phi_{p_1} = A(\xi_1\eta_1)\exp -i\,\beta(\xi_1\eta_1;t)\,d\xi d\eta$$

$$\phi_{p_2} = A(\xi_2\eta_2)\exp -i\,\beta(\xi_2\eta_2;t)\,d\xi d\eta \qquad \text{(C-2-18)}$$

are the optical disturbances over the element of area $d\xi d\eta$ surrounding points p_1 and p_2 respectively. Substituting eqns. C-2-18 into eqns. C-2-17 yields

$$\gamma_{p_1p_2}(\tau) = \overline{\exp -i\,[\beta(\xi_1\eta_1;t+\tau) - \beta(\xi_2\eta_2;t)]}\,d\xi d\eta$$

If relative time delay τ between the interfering light signals is small compared to the coherence time $1/\delta\nu$,

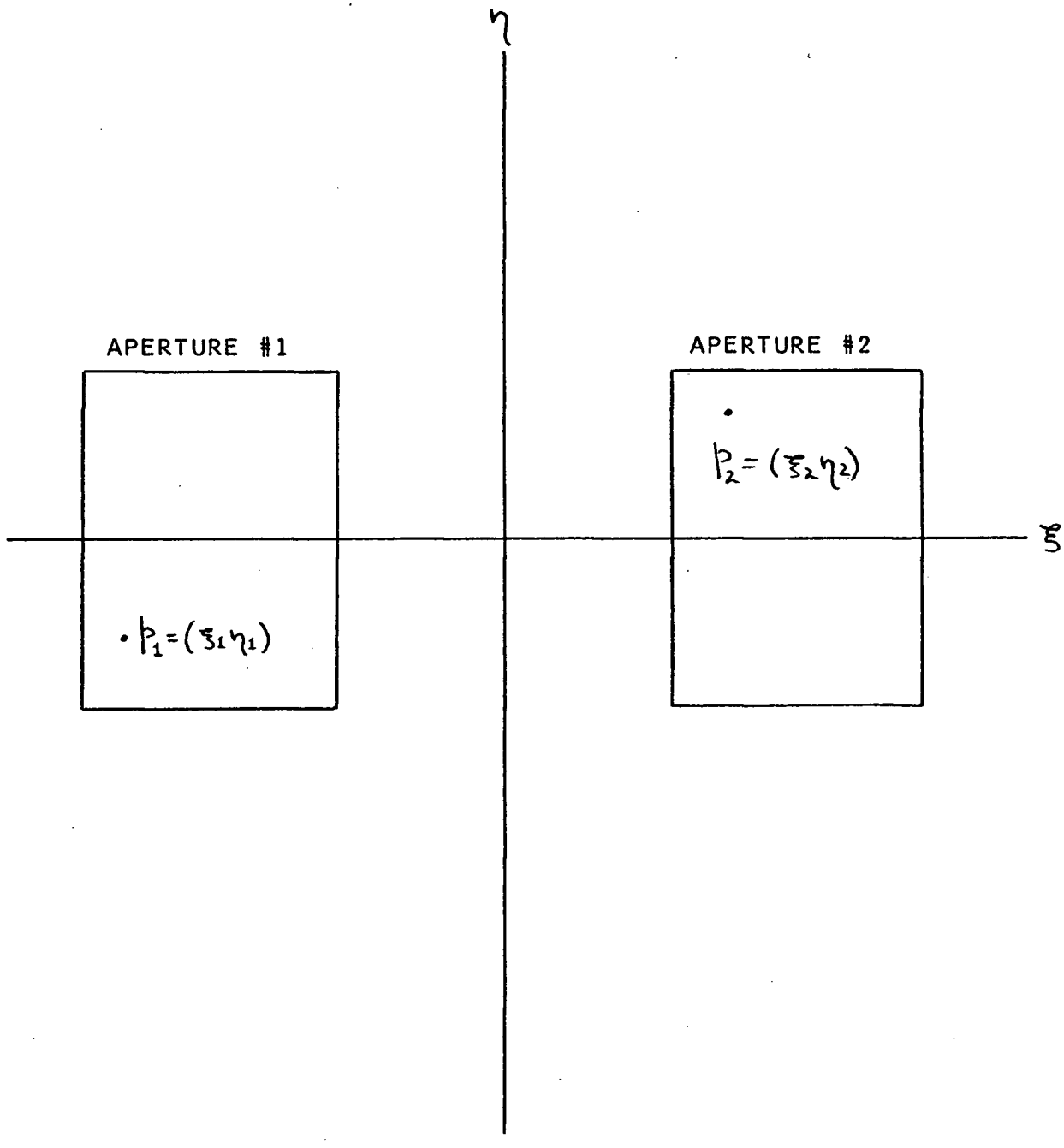

FIG. III-8

COHERENCE BETWEEN APERTURES #1 AND #2

where $\delta\nu$ is the spectral width of the "monochromatic" radiation, then

$$\gamma_{p_1p_2}(\tau) \cong \gamma_{p_1p_2}(o)$$

Since free air laser strain meters must always operate under these conditions, it follows that

$$\gamma_{p_1p_2} = \exp -i\,[\beta(\xi_1\eta_1;t) - \beta(\xi_2\eta_2;t)]d\xi d\eta \qquad \text{(C-2-19)}$$

For purposes of calculating the fringe visibility let

$$\begin{aligned} \beta(\xi_1\eta_1;t) &= \bar{\omega}t \\ \beta(\xi_2\eta_2;t) &= \bar{\omega}t + \theta(\xi\eta;t) \end{aligned} \qquad \text{(C-2-20)}$$

where $\bar{\omega}$ is the mean frequency of the two apertures and $\theta(\xi_2\eta_2;t)$ is a random phase angle at the point $p_2 = (\xi_2\eta_2)$ measured relative to the mean phase angle across the aperture. $\theta(\xi_2\eta_2;t)$ results from the degenerating effects of atmospheric turbulence on the beam. From eqns. C-2-19 and C-2-20

$$\gamma_{p_1p_2} = \overline{\exp -i\,\theta(\xi_2\eta_2;t)}d\xi d\eta$$

A mean complex coherence function, $\langle\gamma\rangle$, for the radiation incident on the two apertures can be calculated by an integral over the source area S of the $\xi\eta$-plane

$$\langle\gamma\rangle = \frac{1}{S} \iint_{\substack{\xi\eta \\ \text{plane}}} \overline{[\cos\theta(\xi_2\eta_2;t) - i\sin\theta(\xi_2\eta_2;t)]d\xi d\eta}$$

where $\langle\cdot\rangle$ indicate an average over the $\xi\eta$-plane. Since $\theta(\xi_2\eta_2;t)$ is not defined outside of aperture #2

$$\langle\gamma\rangle = \frac{1}{2c(b-a)} \overline{\int_{-c}^{c} d\eta \int_{a}^{b} d\xi\, [\cos\theta(\xi_2\eta_2;t) - i\sin\theta(\xi_2\eta_2;t]}$$

Because the phase fluctuations across aperture #2 are random with mean value zero it follows that

$$\overline{\int_{-c}^{c} d\eta \int_{a}^{b} \sin\theta(\xi_2\eta_2;t)d\xi} = 0$$

and

$$V = |\langle\gamma\rangle| = \frac{1}{2c(b-a)} \overline{\int_{-c}^{c} d\eta \int_{a}^{b} \cos\theta(\xi_2\eta_2;t)d\xi}$$

Now

$$\theta(\xi_2\eta_2;t) = \beta(\xi_2\eta_2;t) - \bar{\omega}t$$

where $\beta(\xi_2\eta_2;t)$ is the instantaneous total phase angle at the point p_2 and $\overline{\omega t} = \beta_o$ is the mean phase angle across aperture #2. Hence

$$V = \frac{1}{2c(b-a)} \int_{-c}^{c} d\eta \int_{a}^{b} d\xi \overline{\left(1-\frac{1}{2}(\beta-\beta_o)^2 + \frac{1}{6}(\beta-\beta_o)^4 - \ldots\right)} \qquad \text{(C-2-21)}$$

Interchanging the order of integration and time averaging

$$V = 1 - \frac{1}{2c(b-a)} \int_{-c}^{c} d\eta \int_{a}^{b} d\xi \left[\frac{1}{2}\overline{(\beta-\beta_o)^2} - \frac{1}{6}\overline{(\beta-\beta_o)^4} + \ldots\right]$$

If it is assumed that the dimensions of the diffracting aperture are small enough to allow only small phase deviations across the aperture then

$$V \cong 1 - \frac{1}{2c(b-a)} \int_{-c}^{c} d\eta \int_{a}^{b} d\xi \, \frac{1}{2}\overline{(\beta-\beta_o)^2}$$

If the fringe visibility is required to be larger than a given minimum, V_o , then

$$\frac{1}{2c(b-a)} \int_{-c}^{c} d\eta \int_{a}^{b} d\xi \, \overline{(\beta-\beta_o)^2} \leq 2(1-V_o)$$

$$\langle\overline{(\beta-\beta_o)^2}\rangle \leq 2(1-V_o) \qquad \text{(C-2-22)}$$

If the atmospheric phase fluctuations of the laser output are homogeneous and isotropic then $\langle\overline{(\beta-\beta_o)^2}\rangle$ in eqn. C-2-22 is recognised as the phase structure function $D_{\beta\beta}(\rho)$, [A-2]

$$\langle\overline{(\beta-\beta_o)^2}\rangle = D_{\beta\beta}(\rho)$$

where $\rho = [(\xi_o - \xi_2)^2 + (\eta_o - \eta_2)^2]^{\frac{1}{2}}$. Thus for a fringe visibility of V_o or better

$$D_{\beta\beta}(\rho) \leq 2(1-V_o) \qquad \text{(C-2-23)}$$

Eqn. C-2-23 imposes a restriction on the area of the incoming wavefront, and hence on the dimensions of the rectangular diffracting apertures, acceptable for use in a free air laser strain meter. The area of the incoming wavefront acceptable for interference in a free air laser strain meter, to produce fringes of visibility V_o or greater, must not have linear dimensions exceeding ρ_o , where for $\rho \leq \rho_o$ eqn. C-2-23 is satisfied.

The nature of the phase structure function for laser radiation propagating through a turbulent atmosphere has been investigated by Beckmann [22] and Fried and Cloud [32]. Fried and Cloud have carried out a very thorough analysis starting with an autocorrelation function for atmospheric refractive index fluctuations $C_{\mu\mu}(r)$ whose form is predicted by the

Kolmogoroff theory of turbulence to be

$$C_{\mu\mu}(r) = \left[1 - \frac{1}{2}(r/R_o)^{\frac{2}{3}}\right] \qquad \text{(C-2-24)}$$

where R_o is the "outerscale" of turbulence, they developed a theoretical phase structure function for horizontal propagation of laser output $D_{\beta\beta}(\rho)$

$$D_{\beta\beta}(\rho) = 5.82\ \overline{\mu}^2 k^2 D\ R_o^{-\frac{2}{3}}\ \rho^{\frac{5}{3}} \qquad \text{(C-2-25)}$$

where $k = \frac{2\pi}{\lambda}$ is the wave number of the laser radiation and D is the distance of horizontal propagation, $\overline{\mu}^2$ is the mean square refractive index fluctuations.

Beckmann begins with a gaussian autocorrelation function for refractive index fluctuations

$$C_{\mu\mu}(r) = \exp[-\frac{r^2}{R^2}] \qquad \text{(C-2-26)}$$

where R is the "correlation distance" and proceeds to derive a theoretical phase structure function for horizontal propagation of laser output $D_{\beta\beta}(\rho)$

$$D_{\beta\beta}(\rho) = 4\sqrt{\pi}\ \overline{\mu}^2\ k^2 DR\left[1 - \exp\left(-\frac{\rho^2}{R^2}\right)\right] \qquad \text{(C-2-27)}$$

A comparison of the theoretical predictions of Fried and Cloud with those of Beckmann requires a relationship between the "correlation distance" R, eqn. C-2-26, and the outer scale of turbulence R_o, eqn. C-2-24. When attempting such a comparison a good deal of confusion of definitions is encountered. This difficulty has been pointed out by Strohbehn (24).

According to conventional definitions (23), (24), (31) the parameter R in Beckmann's formula, eqn. C-2-26, corresponds to the "inner scale" of turbulence r_o. For the atmosphere $r_o \sim 1$ cm (19), (25), (32). However both beckmann and Chernov refer to the parameter R as the "correlation distance" and suggest much large values for it. Chernov (26) sets $R = 60$ cm, however this value, based on experimental evidence presented by Liebermann (26, Pp. 5, 8) seems appropriate for sea water and not for the atmosphere. Beckmann claims a value of R appropriate for the atmosphere is $R = 6 \times 10^3$ cm but apparently offers no justification for the use of so large a number. Thus it is clear that whatever is meant by the parameter R in Beckmann's expression for the phase structure function $D_{\beta\beta}(\rho)$, eqn. C-2-27, it is not the inner scale turbulence, r_o.

Possible insight into the nature of the confusion is gained by considering the work of Fried and Cloud. Their theoretical investigations led them to the conclusion that the general phase structure function for horizontal transmission depends in a fairly complicated way on both the inner and outer scales of turbulence, r_o and R_o respectively [32]. However subsequent investigation [40] showed that the dependence on the outer scale of turbulence R_o was most dominant and that the phase structure function could be approximated everywhere to a high degree of accuracy by eqn. C-2-25. Thus Fried and Cloud are able to show that, to a good approximation, the only atmospheric variables needed to describe the phase structure function are the mean square refractive index fluctuations $\overline{\mu^2}$, and the outer scale of turbulence, R_o.

If one assumes this result to be generally true (and Beckmann expresses that hope) then since Beckmann's phase structure function contains only two atmospheric variables, $\overline{\mu^2}$ and R, it is clear that R must be intimately related to the outer scale of turbulence R_o. If the autocorrelation function of Fried and Cloud, based on the Kolmogoroff theory of turbulence, is accepted along with their empirical estimates for R_o then R can be simply related to R_o by defining R to be the distance over which the autocorrelation function of Fried and Cloud decreases to $1/e$ of its value at zero.

If the "correlation distance" of atmospheric refractive index fluctuations R is defined as the distance over which the autocorrelation function drops to $1/e$ then a comparison of Beckmann's results with those of Fried and Cloud can be made by measuring R in units of R_o . From the definition of R and eqns. C-2-24 and C-2-26 it follows that

$$R = [2(1-1/e)]^{\frac{3}{2}} R_o$$

$$R = 1.42\ R_o \qquad \text{(C-2-28)}$$

and Beckmann's eqn. C-2-27 becomes

$$D_{\beta\beta}(\rho) = 5.68\ \sqrt{\pi}\ \overline{\mu}^2 D\ R_o \left[1 - \exp\left(-\frac{\rho^2}{2.03R_o^2}\right)\right] \qquad \text{(C-2-29)}$$

Using Fried and Cloud's results it follows from eqns. C-2-23 and C-2-25 that

$$5.82\ \overline{\mu}^2\ k^2 D R_o^{-\frac{2}{3}}\ \rho^{\frac{5}{3}} \leq 2(1-V_o)$$

which implies

$$\rho \leq \rho_o = \left[\frac{2(1-V_o)\,R_o^{\frac{2}{3}}}{5.82\ \overline{\mu}^2\ k^2 D}\right]^{\frac{3}{5}} \qquad \text{(C-2-30)}$$

Using Beckmann's results it follows from eqns. C-2-23 and C-2-29 that

$$5.68\ \sqrt{\pi}\ \overline{\mu}^2\ k^2 D\ R_o \left[1 - \exp\left(-\frac{\rho^2}{2.03 R_o^2}\right)\right] \leq 2(1-V_o)$$

which implies

$$\rho \leq \rho_o = -2.03\ R_o^2 \log_e \left[1 - \frac{2(1-V_o)}{5.68\ \sqrt{\pi}\ \overline{\mu}^2\ k^2 D\ R_o}\right]^{\frac{1}{2}} \qquad \text{(C-2-31)}$$

Clearly, ρ_o , the largest permissible dimensions for the diffracting apertures, depends on the wave number k and the mean square atmospheric refractive index fluctuations $\overline{\mu}^2$, decreasing monotonically with increasing values of both. Table III-1 shows the resulting values for ρ_o when eqns. C-2-30 and C-2-31 are evaluated for $D = 5 \times 10^5$ cm (5 km.), $R_o = 10^3$ cm and fringe visibility $V_o = 0.5$.

	Fried & Cloud, Eqn. C-2-30		Beckmann, Eqn. C-2-31	
	$\overline{\mu}^2 = 10^{-12}$	$\overline{\mu}^2 = 10^{-10}$	$\overline{\mu}^2 = 10^{-12}$	$\overline{\mu}^2 = 10^{-10}$
$\lambda_1=10\mu$	$\rho_o=0.920$ cm	$\rho_o=0.0583$ cm	$\rho_o=3.19$ cm	$\rho_o=0.319$ cm
$\lambda_2=0.5\mu$	$\rho_o=0.0249$ cm	$\rho_o=0.00158$ cm	$\rho_o=0.159$ cm	$\rho_o=0.0159$ cm
$\lambda_3=0.3\mu$	$\rho_o=0.0136$ cm	$\rho_o=0.000860$ cm	$\rho_o=0.0960$ cm	$\rho_o=0.00960$ cm

TABLE III-1

In their analysis of the effects of a turbulent atmosphere on the propagation of laser output, Fried and Cloud used a model atmosphere whose mean square fluctuation in refractive index were much smaller, in the optical region of the spectrum, than those indicated in table III-1. They preferred $10^{-14} < \overline{\mu}^2 < 10^{-12}$, whereas Beckmann's analysis used $10^{-12} < \overline{\mu}^2 < 10^{-10}$. Beckmann himself points out that $\overline{\mu}^2 \sim 10^{-10}$ is "improbably high" and that $\overline{\mu}^2 \sim 10^{-12}$ is "a more likely value" for the mean square atmospheric refractive index fluctuation. The only "overlap" in the range of mean square refractive index fluctuations that each author feels is applicable to his respective theory is the value $\overline{\mu}^2 \sim 10^{-12}$. The following

values of ρ_o are considered to be representative of the mean of the two theories for fringe visibility 0.5 and $\overline{\mu}^2 \sim 10^{-12}$, moderate-to-intense turbulence.

wavelength	diffracting aperture dimensions
$\lambda_1 = 10\ \mu$	$\rho_o \sim 1$ cm
$\lambda_2 = 0.5\ \mu$	$\rho_o \sim 10^{-1}$ cm
$\lambda_3 = 0.3\ \mu$	$\rho_o \sim 5 \times 10^{-2}$ cm

4. Fringe Counting Rate

The fluctuations in transit time of the whole beam of the laser output appear at the receiver as a modulation u on the operating frequency ω of the laser. If β is the total mean phase averaged across the aperture of the radiation impinging on aperture #2 then

$$\beta = \beta_o + \psi \qquad \text{(C-4-1)}$$

$$\omega' = \omega + u \qquad \text{(C-4-2)}$$

where $\omega' = \frac{d\beta}{dt}$ is the instantaneous frequency, $\omega = \frac{d\beta_o}{dt}$ is the mean frequency and $u = \frac{d\psi}{dt}$ is the modulation frequency. u is a random variable with mean value zero.

From eqn. C-2-10 and C-2-14 it is obvious that the instantaneous fringe counting rate is simply $\omega' - \omega = u$. Thus the fringe counting device of a free air laser strain meter must be able to respond at rates of u or higher.

Beckmann [22] has theoretically investigated the problem of parasitic frequency modulation of laser output induced by passage of the beam through a turbulent atmosphere. Starting with the autocorrelation function for refractive index given by eqn. C-2-26 and assuming that the field of

atmospheric refractive inhomogeneities is "frozen in", that is neglecting turbulent diffusion compared to wind as a means of transporting refractive inhomogeneities, Beckmann divides the vector problem of wind induced frequency modulation into its longitudinal and transverse components.

Beckmann finds the frequency modulation caused by up or downwind components of drift to be insignificant compared to crosswind drift, a result which could be anticipated intuitively.

Beckmann's choice of autocorrelation function for refractive index fluctuations leads to a parasitic modulation u which is gaussian with mean value zero and variance $\overline{u}^2$ given by

$$\overline{u}^2 \text{ crosswind} = \frac{4\sqrt{\pi}\ \overline{\mu}^2\ k^2 D}{1.42 R_o} (v_y^2 + v_z^2) \qquad \text{(C-4-3)}$$

$$\overline{u}^2 \text{ upwind} = 2.84\ \overline{\mu}^2\ k^2 R_o v_x \qquad \text{(C-4-4)}$$

where $\vec{v} = v_x \hat{i} + v_y \hat{j} + v_z \hat{k}$ is the wind velocity. The standard deviations of the frequency modulations are

$$\sigma_{\text{crosswind}} = \left[\frac{4\sqrt{\pi}\ \overline{\mu}^2\ k^2 D}{1.42 R_o} (v_y^2 + v_z^2) \right]^{1/2} \qquad \text{(C-4-5)}$$

$$\sigma_{\text{upwind}} = [2.84\ \overline{\mu}^2\ k^2 R_o v_x]^{1/2} \qquad \text{(C-4-6)}$$

From these results it can be seen that the laser frequency modulation due to crosswind effects is far greater than that due to upwind effects - a result one would anticipate intuitively. From eqn. C-4-5 it can be seen that for a wind velocity of 10 m/sec. , moderate to intense atmospheric turbulence, i.e. $\overline{\mu^2} \sim 10^{-12}$, $D \sim 5$ km and $R_o \sim 10$ m that the standard deviation in the fringe count rate is of the order of 2×10^4 fringes per second. Thus a fringe observation system with a band width of 55 KHz would be able to make free air laser strain meter observations 99% of the time under such conditions. Fringe counters currently operating on conventional laser strain meters have band-widths of up to 1 MHz and would facilitate free air laser strain meter observations under the most disturbed atmospheric conditions imaginable.

D. POWER REQUIREMENTS

The amplitude and phase of laser radiation are complimentary variables in the quantum mechanical sense that the observation of one introduces an uncertainty into the value of the other. The particular uncertainty relationship enjoyed by these variables [36] is

$$\Delta N \Delta \beta \geq 1 \qquad \text{(D-1-1)}$$

where N is the number of photons associated with the laser output available for use in the observation and β is the total phase.

A free air laser strain meter fringe counter capable of counting at a rate of 10^6 fringes per second with an accuracy of $\pm 10^{-2}$ parts of a fringe is effectively making an observation of β with an uncertainty $\Delta\beta \sim 2\pi \times 10^{-2}$ in an interval $\Delta T \sim 10^{-6}$ sec. This observation by eqn. D-1-1, introduces an uncertainty in N of the order $\Delta N \sim 15.9$ Since observing devices in general cannot operate anywhere near the limits of observational accuracy imposed on them by quantum mechanics, the observation of β to an accuracy of $\pm\Delta\beta$ will require N photons where $N >> \Delta N$. In general

$$N = \alpha \ \Delta N$$

The constant α is usually large and depends on the sensitivity and noise characteristics of the observing device. An estimate of the number of photons power requirements for free air laser strain meters can be easily obtained from consideration of the information capacity of radiation detectors.

Counting fringes to an accuracy of $\pm 10^{-2}$ part of a fringe in a cumulative fashion, as required by the operation of a free air laser strain meter, demands, in effect, that the fringe counter be capable of discerning 50 distinct levels of intensity on each fringe. If all levels of intensity on the fringe are assumed "a priori" to be equally probable, the information obtained by the observer upon discovering his observing device to be "focussed" on a given level is

$$- \log_2 \left[\frac{1}{50} \right] = 5.65 \text{ bits}$$

In addition, to facilitate cumulative fringe counting, the observing device must be able to extract a sign (+ ve or - ve) for each observed level to indicate whether the fringe motion which brought the observing device to that position on the fringe was to the left or to the right. This observation requires an additional one bit per level. In this manner the observation of each distinct level of the fringe intensity furnishes 6.65 bits of information to the observer.

Thus cumulative fringe counting at a rate of 10^6

fringes per second to an accuracy of $\pm 10^{-2}$ part of a fringe requires an information channel capacity of 3.33×10^{8} bits per second.

Jones [37] has investigated the information efficiency of various radiation detectors and has found them to vary widely in efficiency from 10^{-1} bits per photon for the 1P21 photomultiplier tube, 7.2×10^{-3} bits per photon for the human eye, to 2.0×10^{-5} bits per photon for the 6849 image orthicon tube. The information efficiency of the radiation detectors employed in laser strain meters should be in the upper end of this range of values since the observing devices are at liberty to exploit photoamplifying schemes such as those used in photomultiplier tubes. A suggested value for the information efficiency of the photodetectors of laser strain meters is therefore 10^{-2} bits per photon.

[Although Jones' analysis strictly only applies to radiation from non-laser sources the use of his figures in this thesis is a prudent and conservative choice since the use of laser sources with their very low inherent noise characteristics can only be expected to improve these figures.]

Thus cumulative fringe counting to the nearest 10^{-2} part of a fringe at a rate of 10^{6} fringes per second requires a flux of 3.33×10^{10} photons per second incident on the radiation detectors. The geometry of the diffracting apertures and the placement of the radiation detectors of a free air laser

strain meter could probably be arranged so that the radiation detectors intercept 0.1% of the total number of photons entering the apertures. Since half of these photons must enter through aperture #2 it follows that the operation of a free air laser strain meter requires a flux of 1.67×10^{13} photons per second incident on the second aperture from the distant retro reflector.

The area of the second aperture is of the order of $\rho_o^2(\lambda)$ therefore the photon flux at the second aperture must be of the order of

$$I(\lambda) \sim \frac{1.67 \times 10^{13}}{\rho_o^2(\lambda)} \quad \frac{\text{photons}}{\text{cm}^2 \text{ sec}} \qquad \text{(D-1-2)}$$

If it is assumed that the laser radiation diverges at an angle $\theta(\lambda)$, then after propagating a distance d it is spread over an area $A(\lambda)$

$$A(\lambda) = \frac{\pi}{4} \theta(\lambda)^2 d^2 \quad \text{cm}^2 \qquad \text{(D-1-3)}$$

An estimate for the angle of divergence $\theta(\lambda)$ can be obtained by assuming the beam diverges at its diffraction limit in which case

$$\theta(\lambda) = \frac{1.22\lambda}{d_o} \qquad \text{(D-1-4)}$$

where λ is the wavelength of the radiation in question and d_o is the diameter of the exit pupil of the laser.

If is assumed that the diameter of the exit pupil of the laser is $d_o = 1$ cm then evaluation $\theta(\lambda)$ for $\lambda_1 = 10\,\mu$, $\lambda_2 = 0.5\,\mu$, $\lambda_3 = 0.3\,\mu$ it follows that

$$\theta(\lambda_1) = 1.22 \times 10^{-3} \text{ rad}$$

$$\theta(\lambda_2) = 6.1 \times 10^{-5} \text{ rad}$$

$$\theta(\lambda_3) = 3.66 \times 10^{-5} \text{ rad} \quad .$$

It has been pointed out by Bender [43] that atmospheric scattering places an upper limit on the degree of collimation achievable in a laser beam of roughly 10^{-5} rad . However given that the diffraction limit of the laser system exceeds 10^{-5} rad it appears practicable to design an optical system capable of achieving collimation very near the diffraction limit. Laser theodolites used in construction are advertized which have achieved an azimuthal collimation of 6×10^{-5} rad at $0.6328\,\mu$. This even exceeds the "diffraction limit" as calculated by the above

formula however it is achieved at the expense of rather poor elevation collimation. For these reasons it seems reasonable to retain the above calculated values as representative of the angle of divergence of the beams.

If E is the power output of the laser in watts, then the photon flux of the beam at a distance D from the exit pupil is

$$I(\lambda) = \frac{E}{A(\lambda)\ h\nu} \times 10^7 \ \frac{\text{photons}}{\text{cm}^2\ \text{sec}} \qquad \text{(D-1-5)}$$

where h is Planck's constant $h = 6.63 \times 10^{-27}$ erg-sec. and $\nu = c/\lambda$ is the operating frequency of the laser.

Let $E_o(\lambda)$ be the power output required (in the absence of atmospheric attenuation and fluctuations) to supply the necessary flux $I(\lambda)$ (given by eqn. D-1-2), at the second diffracting aperture of a free air laser strain meter. Thus from eqns. D-1-2 and D-1-5

$$E_o(\lambda) = \frac{1.67\ A(\lambda)\ h\nu}{\rho_o^2(\lambda)} \times 10^6 \ \text{watts}$$

Substituting for $A(\lambda)$ and for ν

$$E_o(\lambda) = \frac{1.67\pi\ \theta^2(\lambda)\ D^2\ hc}{\rho_o^2(\lambda)} \times 10^6 \text{ watts} \qquad \text{(D-1-6)}$$

If $D = 5 \times 10^5$ cm (5 km)

$c = 3 \times 10^{10}$ cm/sec

$\lambda_1 = 10^{-3}$cm(10μ) $\quad \theta(\lambda_1) = 1.22\times10^{-3}$rad $\quad \rho_o(\lambda_1) = 1$ cm

$\lambda_2 = 5\times10^{-5}cm(0.5\mu)$ $\quad \theta(\lambda_2) = 6.1\times10^{-5}$rad $\quad \rho_o(\lambda_2) = 10^{-1}$cm

$\lambda_3 = 3\times10^{-5}cm(0.3\mu)$ $\quad \theta(\lambda_3) = 3.66\times10^{-5}$ rad $\quad \rho_o(\lambda_3) = 5\times10^{-2}$cm

Then

$$E_o(\lambda_1) = 390 \times 10^{-3} \text{ watts}$$

$$E_o(\lambda_2) = 1.94 \text{ watts} \qquad \text{(D-1-7)}$$

$$E_o(\lambda_3) = 4.66 \text{ watts.}$$

In estimating the above power requirements no allow-

ance has been made for atmospheric absorption or fluctuations in intensity due to atmospheric turbulence. Atmosphere absorption at these frequencies is less than 1% per thousand feet [38] . Thus atmospheric attenuation of the power of the laser output as a function of distance D can be expressed as

$$E(\lambda) = E_o(\lambda) \exp -\alpha \frac{D}{D_o} \qquad \text{(D-1-8)}$$

where $D_o \sim 3.1 \times 10^4$ cm (1000 ft) and $\alpha \sim 0.01$.

Internal fluctuations in intensity of the beam, however, require a considerable increase in power over $E_o(\lambda)$ to be overcome. Beckmann [22] has shown that the logarithm of the relative amplitude of the beam, A/A_o , is a random variable gaussian distributed about zero with standard deviation.

$$\sigma_{\log A/A_o} = \left[\frac{64\sqrt{\pi}\,\overline{\mu^2}\,D^3}{3R_o^3} \right]^{1/2} \qquad \text{(D-1-9)}$$

Since the intensity $I \propto A^2$ and $\log A/A_o = 2 \log I/I_o$ it follows that the relative intensity of the beam is log-normally distributed about zero with standard deviation

$$\sigma_{\log I/I_o} = 2\left[\frac{64\sqrt{\pi}\,\overline{\mu^2}\,D^3}{3R_o^3}\right]^{1/2} \qquad \text{(D-1-10)}$$

From these results it follows that for random fluctuations in the intensity I

$$I \geq I_o \exp - 5.15\left[\frac{64\sqrt{\pi}\,\overline{\mu^2}\,D^3}{3R_o^3}\right]^{1/2} \qquad \text{(D-1-11)}$$

for 99.5% of the time.

Combining eqns. D-1-6 , D-1-8 , and D-1-11 it follows that for a 99.5% confidence level the required power is

$$E(\lambda) = \frac{1.67\pi\,\theta^2(\lambda)D^2hc}{\lambda\,\rho_o^2(\lambda)} \times 10^6 \exp\left[5.15\left[\frac{64\sqrt{\pi}\overline{\mu^2}D^3}{3R_o^3}\right]^{1/2} + 2\frac{\alpha D}{D_o}\right] \text{watts}$$

(D-1-12)

Thus if

$$D = 5 \times 10^{5} \text{ cm}$$

$$\overline{\mu^2} = 10^{-12}$$

$$R_o = 10^{3} \text{ cm}$$

$$\alpha = 0.01$$

$$D_o = 3.1 \times 10^{4} \text{ cm}$$

$$h = 6.63 \times 10^{-27} \text{ ergs-sec}$$

$$c = 3 \times 10^{10} \text{ cm/sec}$$

$\lambda_1 = 10\mu$	$\theta(\lambda_1) = 1.22 \times 10^{-3}$ rad	$\rho_o(\lambda_1) = 1$ cm
$\lambda_2 = 0.5\mu$	$\theta(\lambda_2) = 6.1 \times 10^{-5}$ rad	$\rho_o(\lambda_2) = 10^{-1}$ cm
$\lambda_3 = 0.3\mu$	$\theta(\lambda_3) = 3.66 \times 10^{-5}$ rad	$\rho_o(\lambda_3) = 5 \times 10^{-2}$ cm

It follows that the required laser powers are:

$$E(\lambda_1) = 1.19 \text{ watts}$$

$$E(\lambda_2) = 5.92 \text{ watts}$$

$$E(\lambda_3) = 14.2 \text{ watts}$$

CHAPTER IV
CONCLUSIONS

A. SUMMARY OF RESULTS

The research presented in this thesis indicates that laser strain meters capable of making sampled measurements of earth strain, accurate to the limit of the frequency stability of the laser, while operating through uncontrolled atmosphere over distances of several kilometers are indeed feasible with existing technology.

The observing device, here-in called a "free air laser strain meter", would consist of three frequency stabilized lasers, appropriately spaced in the spectrum, whose outputs are combined into a single beam and directed through the atmosphere to a distant retroreflector. The combined return beam would be separated according to wavelength and portions the size of a "coherence region" would be directed into three double rectangular interferometers where it interferes with a portion of the beam direct from the respective laser. At each interferometer a means of cumulative fringe counting is provided. The cumulative fringe counts in an interval Δt are used to compute the net fluctuation in geometrical ray-path length in the interval. A series of continuous consecutive observations of the fluctuations in geometrical ray-path length can be averaged over an interval $\Delta\tau$ to remove the atmospheric fluctuations and reveal any tectonic changes in length that have taken place between the end mirrors of the laser strain meter.

The dispersive nature of the atmosphere to electromagnetic radiation of optical frequencies facilitates a mathematical separation of the "geometrical" and "refractive" contributions to the fluctuations in optical path length. In fact if $U(t_1t_2)$ is the geometrical fluctuation in ray-path length in the interval $\Delta t = t_2 - t_1$ and $V(t_1t_2)$, $W(t_1t_2)$ are so-called refractive contributions then

$$\begin{pmatrix} L_{\lambda_1}(t_1t_2) \\ L_{\lambda_2}(t_1t_2) \\ L_{\lambda_3}(t_1t_2) \end{pmatrix} = \begin{pmatrix} 1 & f(\lambda_1) & g(\lambda_1) \\ 1 & f(\lambda_2) & g(\lambda_2) \\ 1 & f(\lambda_3) & g(\lambda_3) \end{pmatrix} \begin{pmatrix} U(t_1t_2) \\ V(t_1t_2) \\ W(t_1t_2) \end{pmatrix}$$

where

$$L_{\lambda_1} = \lambda_1 \, C_1(t_1t_2)$$

$$L_{\lambda_2} = \lambda_2 \, C_2(t_1t_2)$$

$$L_{\lambda_3} = \lambda_3 \, C_3(t_1t_2)$$

λ_1 , λ_2 , λ_3 are the wavelengths "in vacuo" of the laser output and $C_{\lambda_1}(t_1t_2)$, $C_{\lambda_2}(t_1t_2)$, $C_{\lambda_3}(t_1t_2)$ are the respective cumulative fringe counts in the interval Δt . The elements of the matrix of coefficients are derived from the formula for atmospheric refractive index

$$n = 1 + f(\lambda)F(P,T) + f(\lambda)g(p,T)$$

The accuracy of present day knowledge of the refractive index

formula and contemporary cumulative fringe counting abilities facilitate measurement of tectonic motions to an accuracy of roughly ±1 % or better.

The relationship between the confidence level of the free air laser strain meter observations and the averaging time for the atmospheric geometrical ray-path fluctuations was derived

$$\eta(|\xi'|) = \operatorname{erf}\left[\frac{2\,|h_k|\,r_o}{\sqrt{2}\,s\,\bar{\mu}^2\,\ell_o\,D}\sqrt{\frac{3\,\Delta\tau^3}{32\pi\,\Delta t}}\right]$$

Solved explicitly for $\Delta\tau$ this gives

$$\Delta\tau = \left[\frac{32\pi\,\Delta t}{3}\right]^{1/3}\left[\frac{s\,\bar{\mu}^2\,\ell_o\,D|\xi'|}{2|h_k|\,r_o}\right]^{2/3} \quad \text{sec.}$$

These results indicate that a tectonic motion of $|h_k| = 1$ cm/year between reflectors a distance $D = 5$ km apart can be detected with a 99% confidence level ($|\xi'| = 2.58$) and a signal-noise ratio $s = 2$ in the presence of moderate-to-intense atmospheric turbulence $\bar{\mu}^2 \sim 10^{-12}$ in about $\Delta\tau = 39$ minutes of observation time.

Free air laser strain meters appear to be theoretically capable of measuring changes in the regional ambient strain state of parts in 10^{12} in the presence of weak atmospheric turbulence and parts in 10^{10} in the presence of moderate-to-intense atmospheric turbulence. In each case the free air laser strain meter appears to be theoretically capable of measuring earth strain up to the limit of the laser frequency stability for the corresponding observation interval.

The intensity distribution $I(xy)$ from the double rectangular Fraunhofer diffraction pattern cast by laser radiation of frequency ω_1 and wavelength λ passing through apertures of dimensions $2c$, $b - a$, is

$$I(xy) = \frac{\sin^2 \frac{\pi x}{\lambda R}(b-a)}{\left[\frac{\pi x}{\lambda R}(b-a)\right]^2} \frac{\sin^2 \frac{2\pi yc}{\lambda R}}{\left[\frac{2\pi yc}{\lambda R}\right]^2} \left[1-V \sin^2\left[\frac{\pi x}{\lambda R}(b+a)-\Omega_2 t\right]\right]$$

where $\Omega_2 = \frac{\omega_1 - \omega_2}{2}$, $u = \omega_1 - \omega_2$ is an effective frequency modulation of the radiation incident on the second aperture as a result of its journey through a turbulent atmosphere. V is the fringe visibility. The fringe count rate Ω_2 is proportional to the rate of change of optical path length L

$$\Omega_2 = \frac{\omega_1}{c} \frac{dL}{dt}$$

and thus cumulative fringe counting for an interval Δt actually measures the net change in optical path length in units of λ .

The effective band width required of a fringe counter for a free air laser strain meter to have a 99% operating capability is

$$u_{\text{bandwidth}} = 2.57 \left[\frac{4\sqrt{\pi}\ \overline{\mu^2}\ k^2 D}{1.42\ R_o} (v_y^2 + v_z^2) \right]^{1/2} \text{Hz.}$$

where $k = \frac{2\pi}{\lambda}$; v_y , v_z are components of wind velocity transverse to the strain meter axis, R_o is the outer scale of turbulence and $\overline{\mu^2}$ is the mean square refractive index fluctuation.

Thus it is seen that a fringe counter with a megacycle band width is adequate for free air laser strain meter observations in the presence of intense atmospheric turbulence and high

winds over distances of several kilometers.

To insure high fringe visibility it is necessary to restrict the diffracting aperture to small dimensions $\rho \leq \rho_o$ where ρ_o is the dimension of a coherence patch. If V_o is the minimum acceptable fringe visibility then two theoretical expressions for ρ_o have been derived.

$$\rho_o = \left[\frac{2(1-V_o) R_o^{2/3}}{5.82\ \overline{\mu^2}\ k^2\ D} \right]^{3/5} \quad \text{cm.}$$

$$\rho_o = -2.03\ R_o^2\ \ln \left[1 - \frac{2(1-V_o)}{5.68\ \pi\ \overline{\mu^2}\ k^2\ DR_o} \right]^{1/2} \quad \text{cm.}$$

the difference in these two formulae being the choice of autocorrelation function for refractive index variations.

For a minimum fringe visibility of $V_o = 0.5$ and observations made over 5 km in the presence of moderate-to-intense atmospheric turbulence the following values of ρ_o were calculated

$\lambda_1 = 10\mu$ $\qquad$ $\rho_o(\lambda_1) \sim 1$ cm

$\lambda_2 = 0.5\mu$ $\qquad$ $\rho_o(\lambda_2) \sim 10^{-1}$ cm

$\lambda_3 = 0.3\mu$ $\qquad$ $\rho_o(\lambda_3) \sim 5 \times 10^{-2}$ cm

The restriction on aperture size implies a minimum restriction on required laser power. Information efficiencies of present day photo detectors are of the order of 10^{-2} bits/photon. Cumulative fringe counting at rates of a megacycle with accuracies of $\pm 10^{-2}$ fringe implies a channel capacity of 3.33×10^{8} bits/second and requires a flux of roughly 1.67×10^{13} photons/sec into the second diffracting aperture.

Atmospheric attenuation of laser power can be expressed as

$$E(\lambda) = E_o(\lambda) \exp -2\left(\frac{\alpha D}{D_o}\right)$$

where $\alpha \sim 0.01$ and $D_o \sim 3.1 \times 10^{4}$ cm .

Internal fluctuations in intensity I of the laser beam about its mean intensity I_o due to atmospheric turbulence are such that

$$I \geq I_o \exp - 5.15 \left[\frac{64\sqrt{\pi}\ \overline{\mu^2}\ D^3}{3\ R_o^3}\right]^{\frac{1}{2}}$$

for 99.5% of the operating time.

Combining the effects of atmospheric attenuation and intensity fluctuations it follows that sufficient operating power for free air laser strain meter observations is provided

by a laser whose output is

$$E(\lambda) = \frac{1.67\pi\,\theta^2(\lambda)\,D^2hc}{\lambda\,\rho_o^2(\lambda)} \times 10^6 \exp\left[5.15\left[\frac{64\sqrt{\pi}\,\overline{\mu^2}D^3}{3\,R_o^3}\right]^{1/2} + \frac{2\alpha D}{D_o}\right] \text{ watts}$$

where $\theta(\lambda)$ is the angle of spread of the laser beam, h is Planck's constant and c is the velocity of light.

For observations over $D = 5$ km with diffraction limited laser beams and in the presence of intense atmospheric turbulence the following laser powers are required

$\lambda_1 = 10\mu$ $\quad E(\lambda_1) \sim 1.19$ watts

$\lambda_2 = 0.5\mu$ $\quad E(\lambda_2) \sim 5.92$ watts

$\lambda_3 = 0.3\mu$ $\quad E(\lambda_3) \sim 14.2$ watts

B. APPLICATIONS OF FREE AIR LASER STRAIN METERS

1. Tectonic Research

The successful operation of free air laser strain meters would provide geophysicists in both the field of tectonics and the field of geodesy with a tool of unusual capabilities and as such would be recognized as a major advance.

As a research tool in tectonics, free air laser strain meters are able to directly observe many long term tectonic processes with unprecedented accuracy and ease. Such observations along with the gross geological feature of the earth are among the essential elements to be accounted for by theories of earthquake mechanism, mountain building, ocean floor spreading and continental drift. The observation and measurement of such phenomena by free air laser strain meters could play an important role in the development of such theories.

Free air laser strain meter observations could be of crucial importance in resolving many problems in tectonics. Measurements made across the rift valleys of the world particularly in East Africa, the Middle East and Iceland as well as between islands straddling an oceanic ridge would yield information of some considerable importance to the development of current theories of tectonics.

2. Earthquake Prediction

A major goal of earthquake engineering research is the prediction of earthquakes, hours, days or even weeks in advance. A major parameter used in evaluating earthquake precursors is the combined state of regional strain. Experience in California [8] with geodimeter distance measurement between points straddling known faults show "an extremely high rate of movement prior to and during the earthquake with some relaxation following, Fig. IV-1. This suggests that large movements and high rates of movement a few hours or minutes prior to an earthquake may provide an effective criterion for short-range earthquake warnings. Continuous or near continuous monitoring of suspected sites would be necessary to provide this kind of forecast".

Current efforts to use strain precursors to study earthquake and faulting mechanisms involves the use of geodimeters to accurately measure the distance between two points set in the ground on repeated occasions, often separated by months, and account for any changes in length observed in terms of tectonic activity. The accuracy of geodimeter distance measurement is between one part in 10^6 and one part in 10^7 and as such is an order of magnitude less than the precision required to investigate, in detail, the earthquake precursor parameter of earth strain [9]. In addition geodimeters lack the long term stability needed to conduct continuous measurements of earth strain build up.

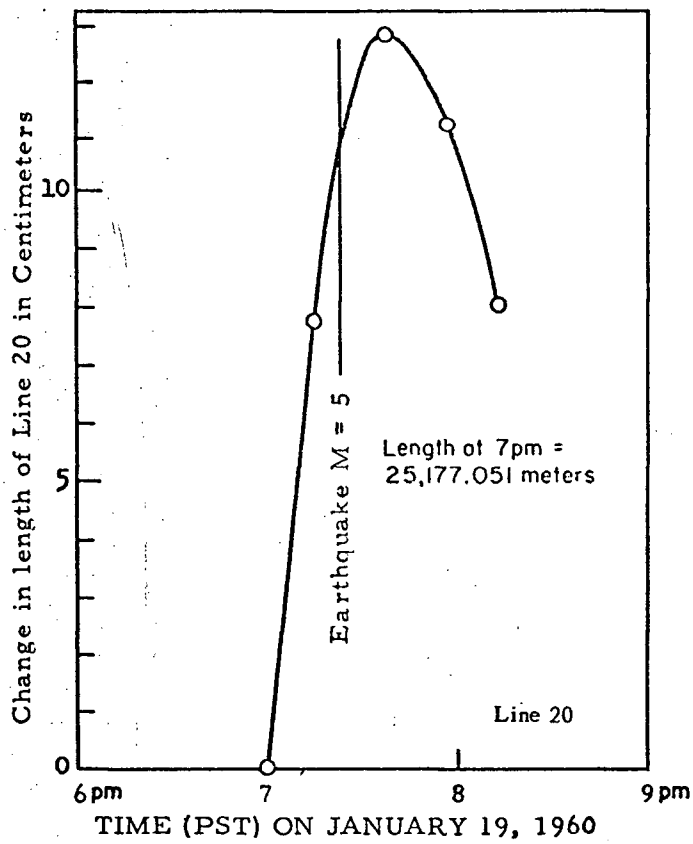

FIG. IV-1

EXAMPLE OF OBSERVED EARTHQUAKE STRAIN PRECURSOR

Researchers in the United States of America have developed the Geodetic Laser Survey System (GLASS) capable of making distance measurements accurate to several millimeters over distances of up to 40 km. This corresponds to an ability to measure strain precursors of about 5 parts in 10^8.

The research presented in this thesis indicates that free air laser strain meters could make strain measurements a factor of 10^2 to 10^4 more accurately than GLASS over a distance of 5 km. Providing laser power was available larger observing distances would result in proportionately higher strain sensitivities. The free air laser strain meter derives its advantage in sensitivity from the fact that it

a) interferes photons and not a modulated light signal

b) directly observes the change in distance δD without measuring the distance D. In so doing it retains the same absolute sensitivity to changes in distance over its entire range of operating abilities.

The ability of a free air laser strain meter to make consecutive observations of changes in the ambient regional strain at intervals of a few minutes makes it ideally suited to the purpose of earthquake prediction. In addition the potentially high strain sensitivity, 10^{-10} - 10^{-12}, of the

free air laser strain meter holds hope for prediction of teleseismic events. Strain precursors of teleseismic events have been observed up to half an hour before a teleseismic event [15]. Theoretical predictions for the magnitude of such strains be approximately in the range 10^{-9} - 10^{-12}, [17]. Smylie [41] has recently calculated, for a "real earth" model, the theoretical displacement fields resulting from faulting within the earth. Knowledge of such displacement fields coupled with a world-wide or continental wide network of laser strain meters may lead to an effective system of earthquake prediction. As a result one can reasonably look forward to the day when "earthquake warnings" (similar to hurricane warnings) will be issued resulting in the saving of thousands of lives each year.

3. Engineering

Contemporary trends toward larger man made structures raises more complex problems regarding structural stability and integrity of dams, bridges, and buildings.

Dams, for example, are subjected to large isostatic readjustments. Such motions often involve displacements of inches or feet and will force deformation within the structure itself.

Standard engineering methods of surveying to establish such motions are clearly less sensitive and convenient than the use of a free air laser strain meter. A retro reflector mounted on the structure (dam, bridge, or building) will facilitate remote sensing of the deformation. In this way quick answers can be obtained to such questions as internal deformations of the structure, displacements in the surrounding land mass, and the interplay between the two.

APPENDIX A-1

A-1. THE GAS LASER

1. Operating Characteristics

The principles of operation of gas lasers are discussed extensively by various authors [10] in contemporary textbooks and journals of optics. For this reason only those characteristics of gas lasers pertinent to the operation of laser strain meters will be introduced in the following discussion.

The gas laser oscillator is just one of several types of laser oscillators capable of generating coherent electromagnetic radiation at optical wavelengths. Basically, a gas laser consists of a plasma tube filled with a mixture of gases and excited by an electrical discharge. The gas mixture is selected to sustain a population inversion among the atoms of the gas populating the excited atomic or molecular energy levels. Under these conditions a photon emitted by the spontaneous decay of an atom in the highly populated higher energy state has a larger probability of stimulating the emission of another such photon than of being absorbed by an atom in a lower energy state. The result is a cascading, avalanche-like emission of stimulated photons, which rapidly becomes highly directional, aligned parallel to the plasma tube, lasting as long as the population inversion is maintained. The ends of the plasma tube are brewster windows producing an output of linearly polarized radiation.

The conversion of a "laser", which acts as an optical amplifier, to a "laser oscillator" with definite modes of oscillation requires feedback. This is provided simply by placing mirrors at each end of the plasma tube creating an optical resonant cavity. Output from the laser oscillator is obtained by making one mirror partially reflecting. For purposes of this thesis the distinction between a laser and a laser oscillator will be dropped and the word "laser" will be used to refer to a "gas laser oscillator".

The radiation field in a laser cavity is sustained in discrete modes defined by the cavity dimensions and labelled TEM_{mnq} ; in a similar manner to the modes in a microwave resonator. The numbers m , n and q define the number of modes in the standing electromagnetic wave in the x, y and z-directions respectively; where z is taken to be parallel to the axis of the plasma tube. The configurations of the electromagnetic field in x-y directions are called spatial modes with m and n being typically in the range 0 to 3. The configurations of the electromagnetic field in the z-direction are called temporal modes with q being $\sim 10^6$. The disparity in the magnitude of the subscripts m , n and q has resulted in a notation convention for describing laser modes only in terms of the spatial subscripts; TEM_{mn} .

For temporal mode resonance the length L between the end mirrors of the laser cavity must be an integral number of half wavelengths λ of the laser radiation

$$\lambda = \frac{2L}{q} \text{ cm.} \qquad \text{(A-1-1)}$$

This corresponds to a frequency of laser oscillation ν

$$\nu = \frac{cq}{2L} \text{ Hz.} \qquad \text{(A-1-2)}$$

where c is the velocity of light in the laser medium. The frequency separation between temporal modes corresponding to consecutive values of q is $\Delta\nu_L$

$$\Delta\nu_L = \frac{c}{2L} \text{ Hz.} \qquad \text{(A-1-3)}$$

In general as many temporal modes of oscillation as can be accommodated under the doppler broadened gain profile will be operating simultaneously in a laser, Fig. A-1-1. Since each temporal mode (being at a slightly different frequency from its neighbour) will produce an independent set of interference fringes it is desirable for purposes of laser interferometry to eliminate all but one temporal mode. This

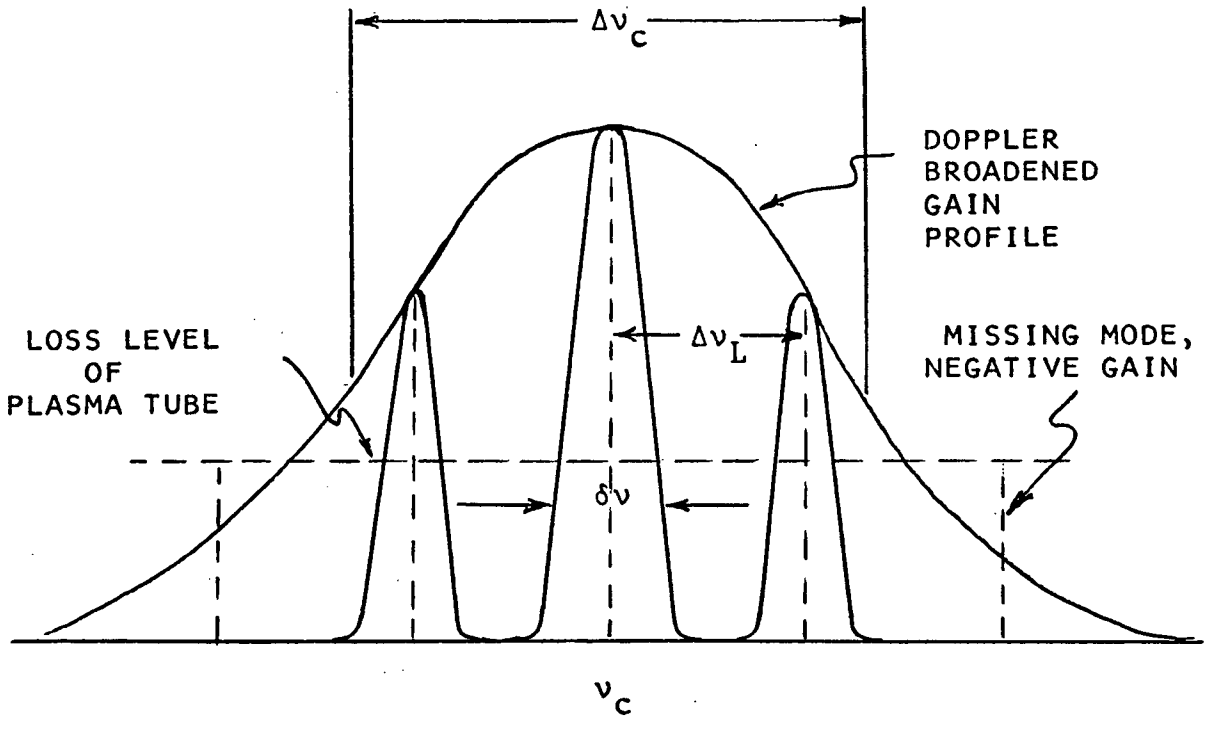

FIG. A-1-1

FREQUENCY DISTRIBUTION OF LASER OUTPUT

is usually accomplished by both shortening the length of the laser cavity and consequently increasing $\Delta\nu_L$ until only one mode appears; and raising the loss level of the plasma tube until all modes but the one near ν_c, the centre frequency of the gain profile, exhibit gain of less than one. When this is achieved the laser is said to operate in a unimodal fashion. Unimodal lasers with very large power outputs are difficult to construct, however, unimodal TEM_{oo} lasers with power output up to 10 watts are available commercially.

The spatial modes of the laser oscillation determine the intensity distribution across the output beam. The spatial modes present in a laser oscillation are controlled by the shape and alignment of the optical resonator as well as the nature of the edge losses present in the plasma tube. For purposes of laser interferometry the TEM_{oo} mode is desirable. This mode does not contain any phase shifts in the electromagnetic field across the output beam. The TEM_{oo} mode also offers the advantage of smallest spot size and lowest angular divergence of the output beam for a given size of exit pupil. The output beam of a unimodal laser operating in the TEM_{oo} mode has a gaussian intensity distribution with plane or spherical fronts of constant phase.

2. Frequency Stability

The stability of the frequency of oscillation of laser output is a matter of prime importance in laser interferometry since frequency stability is synonymous with wavelength stability. The frequency stability of a laser $S_\nu(\tau)$ is given by

$$S_\nu(\tau) = \frac{\delta\nu(\tau)}{\nu} \qquad \text{(A-1-4)}$$

where $\delta\nu(\tau)$ is the range of frequency over which the output of a laser varies in time τ when operating at a frequency ν. The frequency stability of a laser is characterized by a long-term and a short-term stability depending on whether τ is greater or less than some characteristic time, usually of the order of hours. A quantity closely related to frequency stability and of equal importance in laser interferometry is frequency resettability, R_ν, which describes the accuracy with which the frequency ν_o can be reproduced after the laser is perturbed and readjusted.

$$R_\nu = \frac{\overline{\nu - \nu_o}}{\nu} \qquad \text{(A-1-5)}$$

where $\overline{\nu - \nu_o}$ is the average deviation of a number of settings from the desired frequency ν_o.

The ultimate short term frequency stability of a laser is determined by the natural spectral width, $\delta\nu$, of the atomic transition occurring in the laser. This line width has been calculated by Schawlow and Townes [11] to be

$$\delta\nu = \frac{8\pi\ h\ \nu\ (\Delta\nu_c)^2}{W}\ \text{Hz}. \qquad \text{(A-1-6)}$$

where $\Delta\nu_c$ is the spectral width at half intensity of the doppler broadened spectral line of the laser transition, W is the output power of the laser and h is Planck's constant. This equation predicts a frequency spread of about 10^{-2} Hz. or a maximum frequency stability $S_\nu(\tau)_{max} \sim 10^{-16} - 10^{-17}$ for typical optical lasers [12]. However the frequency stability achieved in practice is limited by the Q of the optical cavity to values several orders of magnitude less than the theoretical maximum.

Since the practical limit on laser frequency stability is the Q of the optical resonator, laser frequency stability depends almost entirely on the stability of the cavity dimensions. The principle causes of laser frequency fluctuation are changes in ambient pressure and temperature and detuning due to external mechanical and acoustical vibrations. Passive methods of frequency stabilization such as mechanical and thermal isolation and the use of invar spacers between the

mirrors are inadequate for accurate laser interferometry and for such purposes active methods of frequency stabilization are used.

Active frequency stabilization systems all employ a cavity length control element (usually a piezoelectric crystal) on which one of the cavity mirrors is mounted. The control element is driven by a servo signal whose magnitude and polarity correspond to the magnitude and sign of the deviation of the laser frequency from the desired frequency. The various active frequency stabilizing systems differ one from the other in the technique by which the error signal is derived. In general, schemes for stabilizing lasers fall into two classes; those in which the error signal is derived from the laser itself (self-stabilizing) and those in which the error signal is derived from an external reference cell (externally stabilized).

In the self-stabilizing scheme an a.c. voltage is applied to the piezoelectric crystal which, by varying the cavity dimensions, frequency modulates the laser. Frequency modulation is accompanied by an amplitude modulation of the beam intensity by virtue of the shape of the gain profile. The beam amplitude modulation is in phase with the applied voltage for frequencies $\nu > \nu_c$ and opposed in phase for frequencies $\nu < \nu_c$. The output beam intensity is monitored

by a photodiode and phase detected producing an error signal which when applied to the control element will keep the laser frequency ν near ν_c , the centre frequency of the gain profile.

The sensitivity of this method of frequency stabilization suffers from the disadvantage of being dependent on the shape of the gain profile near ν_c , which can be badly flattened by the Lamb dip resulting in a low sensitivity to frequency drifts. Nevertheless this frequency stabilization scheme is able to stabilize laser oscillations to two parts in 10^9 for many days [13] and allow a resettability of several parts in 10^9 [12].

One of the most successful external stabilization schemes involves resonant absorption of part of the linearly polarized laser output in an absorbing cell; the absorption profile of which has been Zeeman split by the application of an axial magnetic field [13]. The absorption cell medium becomes dichroic; preferentially absorbing right hand circularly polarized light for frequencies $\nu > \nu_c$ and preferentially absorbing left hand circularly polarized light for frequencies $\nu < \nu_c$. An error signal is derived by alternately sampling the LHCP and RHCP output from the absorber using a KDP electro optic switch driven by a square wave generator and requiring that both outputs be of equal

intensity. This error signal applied to the length control element keeps the laser frequency ν near ν_c . This system is theoretically capable of long term frequency stabilities of two parts in 10^{12} and has achieved frequency stabilization of four parts in 10^{10} for eight minutes [13].

Vali [39] has pointed out that the utilization of resonant absorption in a narrow molecular rotation-vibration line of methane at 3.39μ has been used to frequency stabilize a laser resulting in a resettability of better than one part in 10^{11} and possible frequency stability of one part in 10^{12}.

Other methods involving the use of the dispersive properties of the inverted population to construct a frequency discriminator are used to stabilize lasers. These methods have resulted in laser frequency stabilities of one part in 10^{10} for a period of eight hours during which for periods of a minute or so the laser was frequency stabilized to one part in 10^{12}.

The very short term ($\tau \sim 1 - 10^{-3}$ sec.) frequency stability of lasers is investigated by heterodyning two similar frequency stabilized lasers together since no direct means of counting at optical frequencies exists. Such experiments reveal beat frequencies of 1-20 Hz. over periods ranging from a few tens of milliseconds to a few seconds indicating that for periods of this order laser frequencies can be stabilized to one part in 10^{13} [12].

APPENDIX A-2

A-2. THE REFRACTIVE INDEX OF THE ATMOSPHERE

1. Formula for Refractive Index

The quantum theory of atomic and molecular polarizability coupled with the classical theory of electromagnetism yield the Lorentz-Lorenz relation which gives the refractive index n of a dielectric in terms of its specific refractivity $R(\lambda)$ and its density ρ .

$$\frac{n_\lambda^2 - 1}{n_\lambda^2 + 2} = R(\lambda)\rho \qquad \text{(A-2-1)}$$

The specific refractivity is considered to be invariant under changes in density for a given dielectric and to be a function only of the wavelength of the incident radiation λ . If the dielectric is a homogeneous, single component fluid then

$$R(\lambda) = \frac{4\pi}{3} \frac{N_o\, \alpha(\lambda)}{M} \qquad \text{(A-2-2)}$$

where N_o is Avogadros number, M is the molecular weight of the material and $\alpha(\lambda)$ is its molecular polarizability. If the dielectric consists of several components then

$$\frac{n_\lambda^2 - 1}{n_\lambda^2 + 2} = \sum_i R_i(\lambda)\rho_i \qquad \text{(A-2-3)}$$

where $R_i(\lambda)$ is the specific refractivity of the i^{th} component and ρ_i is the partial density of the i^{th} component.

Although the earth's atmosphere contains many gaseous components the Lorentz-Lorenz relation is capable of giving the atmospheric refractive index to accuracies of parts in 10^{10} if the summation in eqn. 3-3 is terminated at $i=3$, [20]. Thus

$$\frac{n_\lambda^2 - 1}{n_\lambda^2 + 2} = R_1(\lambda)\rho_1 + R_2(\lambda)\rho_2 + R_3(\lambda)\rho_3 \qquad \text{(A-2-4)}$$

where R_1, R_2 and R_3 are the specific refractivities of CO_2-free "air", water vapour, and carbon dioxide respectively and ρ_1, ρ_2 and ρ_3 are their respective partial densities*.

If the amount of CO_2 present in the atmosphere is assumed to be constant at 0.035 molar % then the atmospheric refractive index can be expressed as

$$\frac{n_\lambda^2 - 1}{n_\lambda^2 + 2} = R_1'(\lambda)\rho_1' + R_2(\lambda)\rho_2 \qquad \text{(A-2-5)}$$

where $R_1'(\lambda)$ is the specific refractivity of dry "air" and

---

*"Air" is defined as a mixture of gases containing 78.09 molar % N_2, 20.95 molar % O_2, 0.93 molar % Ar, 0.03 molar % CO_2 whereas "atmosphere" refers to that mixture of gases surrounding the planet earth. The specific refractivities of N_2, O_2 and Ar are so similar they are all included in the first term, $R_1(\lambda)$.

ρ_1' is the corresponding partial density. The assumption of constant CO_2 content in the freely circulating atmosphere is supported by experimental evidence. The variability of CO_2 content in atmospheric samples has been found to be less than a few thousandths of one percent from its normal value of 0.035 molar % [21].

An empirical formula for atmospheric refractive index corresponding to eqn. 3-5 is given by Owens [20] as

$$n_\lambda = 1 + \mu_\lambda$$

$$n_\lambda = 1 + f(\lambda)F(P,T) + g(\lambda)G(p,T) \qquad \text{(A-2-6)}$$

where the dispersion factors $f(\lambda)$ and $g(\lambda)$ are given by

$$f(\lambda) = \left[2371.4 + \frac{683939.7}{130 - 1/\lambda^2} + \frac{4547.3}{38.9 - 1/\lambda^2}\right] \times 10^{-8} \qquad \text{(A-2-7)}$$

$$g(\lambda) = \left[6487.31 + \frac{58.058}{\lambda^2} - \frac{0.71150}{\lambda^4} + \frac{0.08851}{\lambda^6}\right] \times 10^{-8} \qquad \text{(A-2-8)}$$

and the density factors $F(P,T)$ and $G(p,T)$ are given by

$$F(P,T) = \frac{P}{T}\left[1 + P\left(57.90 \times 10^{-8} - \frac{9.3250 \times 10^{-4}}{T} + \frac{0.25844}{T^2}\right)\right] \qquad \text{(A-2-9)}$$

$$G(p,T) = \frac{p}{T}\left[1 + p\left(1 + 3.7 \times 10^{-4}\, p\right)\left(-2.37321 \times 10^{-3} + \frac{2.23366}{T} - \frac{710.792}{T^2} + \frac{7.75141 \times 10^{4}}{T^3}\right)\right] \qquad \text{(A-2-10)}$$

and λ = wavelength of light in microns

T = temperature of atmosphere in °K

P = partial pressure of dry air in millibars

p = partial pressure of water vapour in millibars.

The deviations from unity of the atmospheric refractive index is represented by μ and is measured in μ-units. One μ-unit is a refractive index deviation of 10^{-6}. Formula 3-6 gives the absolute value of the refractive index accurate to one part in 10^9 over the range

$$2302\ \text{Å} < \lambda < 20{,}586\ \text{Å}$$

$$0 < P < 4000 \text{ mb.}$$

$$0 < p < 100 \text{ mb.}$$

$$240°K < T < 330°K$$

2. Statistical Properties of the Atmospheric Refractive Index

The earth's atmosphere is in a state of turbulent motion. The values of wind velocity as well as the atmospheric pressure, temperature, and humidity undergo irregular fluctuations in space and time which cause random spatial and temporal fluctuations in the atmospheric refractive index n . The atmospheric refractive index n can be considered to be a random field dependent on the three cartesian spatial coordinates x , y , z and time τ . If $\vec{R} = x\hat{i} + y\hat{j} + z\hat{k}$ is the position vector relative to cartesian axes ox , oy , and oz with unit vectors $\hat{i}$, $\hat{j}$, and $\hat{k}$ respectively then from eqn. A-2-6

$$n(\vec{R},\tau) = 1 + \mu(\vec{R},\tau)$$

A complete statistical description of $n(\vec{R},\tau)$ is given by the set of joint probability density functions $\beta_i(\mu(\vec{R}_1)\mu(\vec{R}_2)\ldots\mu(\vec{R}_i);\ \tau_1\ ,\ \tau_2\ldots\tau_i)$ $i = 1, 2, 3,\ldots$ where $\beta_i(\mu(\vec{R}_1)\mu(\vec{R}_2)\ldots\mu(\vec{R}_i);\ \tau_1\ ,\ \tau_2\ldots\tau_i)$ is defined as the probability that all $\mu(\vec{R}_i)$ be in the range μ to $\mu + d\mu$ at times τ_i respectively. A complete statistical description of most random processes thus involves an infinite set of such functions. In practice an incomplete but computationally useful description of a random process results if "i" is allowed to assume values $i = 1,2$; corresponding to $\beta_1(\mu(\vec{R}_1);\ \tau_1)$ and $\beta_2(\mu(\vec{R}_1)\mu(\vec{R}_2);\tau_1\ \tau_2)$

Moments of various orders corresponding to density functions β_1 and β_2 are defined

$$\overline{\mu^n(\vec{R}_1\ \tau_1)} = \int_0^\infty \mu^n(\vec{R}\tau)\beta_1(\mu(\vec{R}_1);\tau_1)d\mu$$

$$\overline{\mu^n(\vec{R}_1\ \tau_1)\mu^m(\vec{R}_2\ \tau_2)} = \int_0^\infty\int_0^\infty \mu^n(\vec{R}_1\ \tau_1)\mu^m(\vec{R}_2\ \tau_2)\beta_2(\mu(\vec{R}_1)\mu(\vec{R}_2);\tau_1\tau_2)d\mu_1 d\mu_2$$

Again from a practical standpoint the most important of these are the lowest order moments

$$\overline{\mu(\vec{R}_1\ \tau_1)} = \int_0^\infty \mu(\vec{R}_1\tau)\beta_1(\mu(\vec{R}_1);\tau_1)d\mu \qquad \text{(A-2-11)}$$

$$\overline{\mu(\vec{R}_1\ \tau_1)\mu(\vec{R}_2\ \tau_2)} = \int_0^\infty\int_0^\infty \mu(\vec{R}_1\ \tau_1)\mu(\vec{R}_2\ \tau_2)\beta_2(\mu(\vec{R}_1)\mu(\vec{R}_2);\tau_1\ \tau_2)d\mu_1\ d\mu_2$$

(A-2-12)

which are the mean value $\bar{\mu}$ and the auto covariance $\overline{\mu^2}$ as a function of space and time respectively.

If the atmospheric refractive index fluctuations are considered to be homogeneous and isotropic the statistical description of them is invariant with respect to translations and rotations of the coordinate axes. If the atmospheric

refractive index fluctuations are considered to be stationary their statistical description is invariant with respect to translations in time. The assumption of isotropy permits the vector $\vec{R}$ appearing in eqns. A-2-11 and A-2-12 to be replaced by its modulus R .

$$\mu(R_1\tau_1) = \int_0^\infty \mu(R,\tau)\beta_1(\mu(R_1);\tau_1)d\mu \qquad \text{(A-2-13)}$$

$$\mu(R_1\tau_1)\mu(R_2\tau_2) = \int_0^\infty \int_0^\infty \mu(R_1\tau_1)\mu(R_2\tau_2)\beta_2(\mu(R_1)\mu(R_2);\tau_1\tau_2)d\mu_1\, d\mu_2 \qquad \text{(A-2-14)}$$

The assumptions of homogeniety and stationarity permit one to arbitrarily set $R_1 = 0$ $\tau_1 = 0$ and to define variables $r = R_2 - R_1$ and $t = \tau_2 - \tau_1$. Thus

$$\bar{\mu} = \int_0^\infty \mu(R_1\tau_1)\beta_1(\mu(R_1);\tau_1)d\mu \qquad \text{(A-2-15)}$$

and

$$\overline{\mu(R_1\tau_1)\mu(R_2\tau_2)} = B(R_2 - R_1),\ (\tau_2 - \tau_1))$$

$$\overline{\mu(R_1\tau_1)\mu(R_2\tau_2)} = B(r,t) \qquad \text{(A-2-16)}$$

The auto covariance normalized by division by the variance of the refractive index fluctuations $\overline{\mu^2}$ gives the auto-correlation function $c(r,t)$

$$c(r,t) = \frac{1}{\overline{\mu^2}} B(r,t) \quad . \qquad \text{(A-2-17)}$$

The assumptions of homogeniety, isotropy and stationarity of atmospheric refractive index fluctuations requires some scrutiny. Clearly the real atmosphere conforms to none of these ideal descriptions. The atmosphere is characterized spatially by large vertical and horizontal gradients in pressure, temperature, and humidity; and temporally by seasonal and daily variations in these same parameters. However for calculating the effect of atmospheric turbulence on the propagation of laser output, particularly the effect on the phase coherence, the assumptions are justified.

Kolmogorov has pointed out and experiment has verified [23, p. 79] that the small scale components of turbulence tend toward homogeniety and isotropy. The assumptions of homogeniety and isotropy are justified since it is the small scale turbulence which will be the primary cause of degeneration of phase coherence in the laser signal [24]. The larger scales of turbulence will tend to deflect the beam as a whole while preserving the structure of the phase fronts. While the statistical description of atmospheric turbulence is admittedly time dependent and hence

non-stationary on a time scale of days, the assumption of stationarity is justified on the short time scales involved in the investigation of phase coherence in the laser signal. The transit time of a photon along a free air laser strain meter of length 3 km is of the order of 10^{-5} sec and the statistics of atmospheric refractive index fluctuations are very nearly stationary over such short time intervals. Assuming the autocorrelation function for atmospheric refractive index fluctuations is a single parameter function of r, $C_{\mu\mu}(r)$, it remains only to assign a specific dependence on r and to define the parameter in physical terms. While it has been shown experimentally [24] that there does not exist a refractive index autocorrelation function valid for all atmospheric conditions several theoretical predictions concerning the nature of the refractive index autocorrelation function have been made. Chernov [20, p. 29] presents a simple proof that any refractive index autocorrelation function $C_{\mu\mu}(r)$ must exhibit the property that

$$\left.\frac{d\, C_{\mu\mu}(r)}{dr}\right|_{r=0} = 0 \qquad \text{(A-2-18)}$$

This is a necessary consequence of the fact that the atmospheric refractive index is a continuous and differentiable function of position. The Kolmogoroff theory of turbulence predicts a

refractive index autocorrelation function [32] $C_{\mu\mu}(r) = 1-b(r/R_o)^{\frac{2}{3}}$ where b is a constant and R_o is the outer scale of turbulence. While this autocorrelation function and others such as $C_{\mu\mu}(r) = \exp - (r/R_o)$ violate the condition required at $r=0$ they are used by many authors who consider them to be adequate representations of atmospheric refractive index fluctuations. Tatarski [25] has shown the atmospheric parameters of pressure, temperature and humidity behave approximately in which case the autocorrelation functions of the atmospheric refractive index and wind velocity are the same [24] except for a constant of proportionality. However, the autocorrelation function of the velocity distribution in a homogeneous turbulent medium tends to be gaussian [23, p. 94] and so for this reason as well as mathematical simplicity some authors assume the autocorrelation for atmospheric refractive index fluctuations to be gaussian

$$C_{\mu\mu}(r) = \exp - (r^2/r_o^2)$$

APPENDIX A-3

A-3. MATHEMATICAL APPENDIX

A-3-1

Given

$$P_\theta(\beta) = \frac{1}{\sqrt{2\pi\theta^2}} \exp\left[-\frac{\beta^2}{2\theta^2}\right] \qquad -\infty \leq \beta \leq \infty$$

to calculate $P_{\theta^2}(\gamma)$ $\qquad 0 \leq \gamma \leq \infty$

If

$$p\{a \leq \theta \leq b\} = \int_a^b P_\theta(\beta)d\beta \qquad 0 < a < b$$

then

$$p\{a \leq \theta^2 \leq b\} = p\{\sqrt{a} \leq \theta \leq \sqrt{b}\} + p\{-\sqrt{b} \leq \theta \leq -\sqrt{a}\}$$

$$p\{a \leq \theta^2 \leq b\} = \int_{-\sqrt{a}}^{-\sqrt{b}} P_\theta(\beta)d\beta + \int_{-\sqrt{b}}^{-\sqrt{a}} P_\theta(\beta)d\beta$$

make a change of variables: in the first integral let $\beta = \gamma^{1/2}$

in the second integral let $\beta = -\gamma^{1/2}$

$$p\{a \leq \theta^2 \leq b\} = \int_a^b \frac{P_\theta(\sqrt{\gamma})d\gamma}{2\sqrt{\gamma}} - \int_b^a \frac{P_\theta(-\sqrt{\gamma})}{2\sqrt{\gamma}}\,d\gamma$$

$$p\{a \leq \theta^2 \leq b\} = \int_a^b \frac{P_\theta(\sqrt{\gamma})d\gamma}{2\sqrt{\gamma}} + \int_a^b \frac{P_\theta(-\sqrt{\gamma})}{2\sqrt{\gamma}}\,d\gamma$$

$$\int_a^b P_{\theta^2}(\beta)\,d\beta = \int_a^b \frac{P_\theta(\sqrt{\gamma}) + P_\theta(-\sqrt{\gamma})}{2\sqrt{\gamma}}\,d\gamma$$

$$P_{\theta^2}(\beta) = \frac{P_\theta(\sqrt{\beta}) + P_\theta(-\sqrt{\beta})}{2\sqrt{\beta}} \qquad 0 \leq \beta \leq \infty$$

$$P_{\theta^2}(\beta) = \frac{1}{\sqrt{2\pi\beta^2\overline{\theta^2}}} \exp\left[-\frac{\beta^2}{2\overline{\theta^2}}\right] \qquad 0 \leq \beta \leq \infty$$

and

$$P_{\phi^2}(\beta) = \frac{1}{\sqrt{2\pi\beta^2\overline{\phi^2}}} \exp\left[-\frac{\beta^2}{2\overline{\phi^2}}\right] \qquad 0 \leq \beta \leq \infty$$

A-3-2

Given $$P_{\theta^2}(\beta) = \frac{1}{\sqrt{2\pi\beta^2\overline{\theta^2}}} \exp\left[-\frac{\beta^2}{2\overline{\theta^2}}\right] \qquad 0 \leq \beta \leq \infty$$

$$P_{\phi^2}(\beta) = \frac{1}{\sqrt{2\pi\beta^2\overline{\theta^2}}} \exp\left[-\frac{\beta^2}{2\overline{\theta^2}}\right] \qquad 0 \leq \beta \leq \infty$$

$$\alpha^2 = \theta^2 + \phi^2$$

to calculate $P_{\alpha^2}(\xi)$.

Now $\overline{\alpha^2} = \overline{\theta^2} + \overline{\phi^2}$ and if the atmospheric turbulence is isotropic $\overline{\theta^2} = \overline{\phi^2} = \frac{\overline{\alpha^2}}{2}$.

Substituting $\beta^2 = \nu$ in $P_{\theta^2}(\beta)$

and $\beta^2 = \eta$ in $P_{\phi^2}(\beta)$

results in

$$P_{\theta^2}(\nu) = \frac{1}{\sqrt{\pi\overline{\alpha^2}\nu}} \exp\left[-\frac{\nu}{\overline{\alpha^2}}\right]$$

$$P_{\phi^2}(\eta) = \frac{1}{\sqrt{\pi\overline{\alpha^2}\eta}} \exp\left[-\frac{\eta}{\overline{\alpha^2}}\right]$$

Now $P_{\alpha^2}(\xi) = P_{\theta^2}(\nu) \otimes P_{\phi^2}(\eta)$

where "⊛" symbolized convolution.

$$P_{\alpha^2}(\xi) = \int_{-\infty}^{\infty} P_{\theta^2}(\lambda) P_{\phi^2}(\xi - \lambda) d\lambda$$

$$P_{\alpha^2}(\xi) = \int_{0}^{\xi} P_{\theta^2}(\lambda) P_{\phi^2}(\xi - \lambda) d\lambda$$

since $P_{\theta^2}(\nu) \equiv 0 \quad$ for $\quad \nu < 0$

$P_{\phi^2}(\eta) \equiv 0 \quad$ for $\quad \eta < 0$

$$P_{\alpha^2}(\xi) = \frac{1}{\pi\alpha^2} \int_{0}^{\xi} \frac{1}{\sqrt{\lambda(\xi-\lambda)}} \exp\left[-\frac{\xi}{\alpha^2}\right] d\lambda$$

$$P_{\alpha^2}(\xi) = \frac{\left[-\frac{\xi}{\alpha^2}\right]}{\pi\,\overline{\alpha^2}} \int_{0}^{\xi} \frac{d\lambda}{\sqrt{\lambda(\xi-\lambda)}}$$

the integral can be easily shown to equal π by completing the square

$$\int_{0}^{\xi} \frac{d\lambda}{\sqrt{\lambda(\xi-\lambda)}} = \int_{0}^{\xi} \frac{d\lambda}{\sqrt{\xi^2/4 - (\lambda-\xi/2)^2}}$$

let $\lambda' = \lambda - 3/2$

$$\int_0^{\xi} \frac{d\lambda}{\sqrt{\lambda(\xi-\lambda)}} = \int_{-\xi/2}^{\xi/2} \frac{d\lambda'}{\xi/2\sqrt{1 - \frac{4\lambda'^2}{\xi^2}}}$$

let $u = \frac{4\lambda'^2}{\xi^2}$

$$\int_0^{\xi} \frac{d\lambda}{\sqrt{\lambda(\xi-\lambda)}} = \int_{-1}^{1} \frac{\xi/2\ du}{\xi/2\sqrt{1-u^2}} = \sin^{-1}u \Big|_{-1}^{1} = \pi$$

$$P_{\alpha^2}(\xi) = \frac{1}{\alpha^2} \exp\left[-\frac{\xi}{\alpha^2}\right]$$

A-3-3

$$\text{If} \qquad P_{\Delta\varepsilon}(\beta) = \frac{1}{\ell_o\overline{\alpha^2}} \exp\left[-\frac{\beta}{\ell_o\overline{\alpha^2}}\right]$$

The Laplace Transform of $P_{\Delta\varepsilon}(\beta)$ is given by

$$Q_{\Delta\varepsilon}(s) = \int_o^\infty e^{-s\beta} P_{\Delta\varepsilon}(\beta)d\beta$$

$$Q_{\Delta\varepsilon}(s) = \frac{1}{\ell_o\overline{\alpha^2}} \int_o^\infty \exp\left[-\beta\left(s + \frac{1}{\ell_o\overline{\alpha^2}}\right)\right] d\beta$$

$$Q_{\Delta\varepsilon}(s) = \frac{1}{\ell_o\overline{\alpha^2}} \left[\frac{\exp - \beta\left(s+\frac{1}{\ell_o\overline{\alpha^2}}\right)}{s + \frac{1}{\ell_o\overline{\alpha^2}}}\right]_o^\infty$$

$$Q_{\Delta\varepsilon}(s) = \frac{1}{\ell_o\overline{\alpha^2}} \left[\frac{1}{s + \frac{1}{\ell_o\overline{\alpha^2}}}\right]$$

A-3-4

If x is a random variable, gaussian distributed with parameters 0 and 1, then x has probability density function

$$P_x(\beta) = \frac{1}{\sqrt{2\pi}} \exp\left[-\frac{\beta^2}{2}\right]$$

The probability that $-a \leq x \leq a$ is given by

$$p(-a \leq x \leq a) = 2\int_0^a P_x(\beta)d\beta$$

$$p(-a \leq x \leq a) = \frac{2}{\sqrt{2\pi}}\int_0^a \exp\left[-\frac{\beta^2}{2}\right]d\beta$$

By definition

$$\text{erf } z = \frac{2}{\sqrt{\pi}}\int_0^z \exp[-\beta^2]d\beta$$

by the change of variables $\beta' = \beta/\sqrt{2}$ it is clear that

$$p(-a \leq x \leq a) = \text{erf}\left[\frac{a}{\sqrt{2}}\right]$$

APPENDIX A-4

A-4. GEOPHYSICAL AND ATMOSPHERIC PARAMETERS

The magnitudes assigned the various geophysical and atmospheric parameters used in this thesis are subject, in some instances, to considerable debate. The following discussion is presented as an attempt to justify the values chosen for computation in this thesis.

1) "D" - The distance D over which the tectonic observations are to be made was arbitrarily set at 5 km. D = 5 km. was chosen in the hope that it was large enough to ensure observations of regional, as opposed to local, tectonic movements. D = 5 km. is large enough in most cases for observing stations straddling a fault zone to be set back from the area of active faulting and thus each be situated on relatively large and stable geologic platforms.

2) "$|h_k|$"- The choice of $|h_k|$ = 1 cm/year was made on the basis of evidence [8] that this figure is typical of fault motion on major fault systems. It is also typical of projected continental drift velocities.

3) "s" - The choice of a signal-to-noise ratio S = 2 is entirely arbitrary.

4) "Δt" - The appropriate magnitude for Δt can be described as the smallest time interval possible (to ensure rapid data acquisition) over which the atmospheric ray-paths can be considered uncorrelated. An estimate of Δt can be obtained from the frequency of scintillation of light sources observed

through an uncontrolled atmosphere. The power spectra of such fluctuations in light intensity have been determined experimentally under a variety of atmospheric conditions. These power spectra all show a broad peak extending from 5 Hz - 250 Hz (25, p. 220), (30). Since the temporal fluctuations in images viewed through a turbulent atmosphere shown no appreciable fourier components with periods longer than 2×10^{-1} sec this value was chosen for the magnitude of Δt . The magnitude of Δt is not very critical in determining the observation interval $\Delta\tau$ since $\Delta\tau \propto \Delta t^{1/3}$.

5) Turbulence scales - A good deal of confusion persists in the literature regarding "scales of turbulence". To begin with, the "inner (outer) scale of turbulence" is usually vaguely defined (31) as a measure of, but not necessarily equal to, the dimensions of the smallest (largest) inhomogenieties present in the velocity field. There is a generally accepted practice of associating the inner and outer scales of turbulence with the so-called "micro-scale" and "integral scale" derived mathematically from the spatial autocorrelation function C(r) for the field.

The micro scale, λ , is the intercept on the r-axis of a parabola fitted to the autocorrelation function at the origin

$$-\frac{1}{\lambda^2} = \left.\frac{d^2 C(r)}{dr^2}\right|_{r=0}$$

Physically, the micro scale must exist for reasons of continuity but many analytical autocorrelation functions such as the exponential do not have a "micro scale".

The "integral scale", L_o, is defined as the value of r which is numerically equal to the integral of the autocorrelation function from zero to infinity.

$$L_o = \int_0^\infty C(r)\, dr$$

Physically, the integral scale is expected to exist since correlation functions approach zero for large values of the argument.

The guassian autocorrelation function is an analytical autocorrelation function widely used in theoretical work because of its mathematical manageability

$$C(r) = \exp\left[-\frac{r^2}{R^2}\right] .$$

The parameter R is usually referred to as the correlation distance - the value of r at which the autocorrelation function has dropped to $1/e$ of its value at the origin. Unfortunately the gaussian autocorrelation function is blessed with the curious mathematical property that its micro scale is larger than its integral scale and the association between the inner and outer scales of turbulence and the micro- and integral scales respectively cannot be made when gaussian autocorrelation functions are used.

6. "r_o" - Since the smallest scale of turbulence present in the atmosphere has been determined by radar scattering and other methods to vary from several millimeters (25) to several centimeters (32) a value of $r_o = 1$ cm was chosen for ease of computation. The magnitude of r_o is not a critical factor in determining the observation time $\Delta\tau$ since $\Delta\tau \propto r_o^{-2/3}$.

7. "ℓ_o", "R_o" - The magnitude of the parameter ℓ_o, the straight line segments used to approximate the curved ray-path, is difficult to estimate. The mathematical analysis presented in this thesis is valid under the assumption $r_o \ll \ell_o \ll D$. Since $r_o \sim 1$ cm and $D \sim 10^6$ cm a mathematically convenient choice for ℓ_o is 10^3 cm or 10 meters. However there are physical reasons for this choice of ℓ_o as well.

It would obviously be physically reasonable to equate ℓ_o with the outer scale of turbulence, R_o . In most physical problems, e.g. fluid flow through a pipe, the outer scale of turbulence is defined by obvious physical constraints,e.g. the inner diameter of the pipe. The atmosphere is a turbulent fluid confined by only one wall, the surface of the earth; thus one expects the size of the largest units of turbulence to depend on altitude, h .

Fried and Cloud (32) present a graph of experimentally determined values of R_o vs. h . They claim an empirical fit to the data is given by

$$R_o = \sqrt{b\,h}$$

h is in meters
b = 4 meters .

Thus assigning $\ell_o = R_o = 10$ meters is consistent with a laser beam propagating parallel to the ground at an average height of 25 meters. This is physically reasonable for a free air laser strain meter making observations over a distance of 5 km. The calculated observing interval $\Delta\tau$ only depends on $\ell_o^{2/3}$.

8. " $\overline{\mu^2}$" - The mean square fluctuations in atmospheric refractive index as a function of height h (meters) above sea level based on microwave refractometer observations is given empirically by Fried and Cloud (32) as

$$\overline{\mu^2} = 1.2 \times 10^{-12} \exp\left[-\frac{h}{h_o}\right] \qquad h_o = 1600 \text{ m} \quad .$$

Because of the effects of water vapour, present at microwave frequencies, but greatly reduced at optical frequencies, Fried and Cloud prefer an alternative formula

$$\overline{\mu^2} = 6.7 \times 10^{-14} \exp\left[-\frac{h}{h_o}\right] \qquad h_o = 3200 \text{ m} \quad .$$

which, they claim, agrees more closely with values for $\overline{\mu^2}$ derived astronomically.

Beckmann (22) chooses larger values for $\overline{\mu^2}$ and uses $10^{-12} < \overline{\mu^2} < 10^{-10}$. Beckmann points out, however, that $\overline{\mu^2} = 10^{-10}$ is an "improbably high value" and considers $\overline{\mu^2} = 10^{-12}$ to be "a more likely value".

Consortini et al (44) have recently published data derived from fluctuations in laser beams transmitted over a

horizontal path which reveal measured mean square refractive index fluctuations between 7×10^{-14} and 2×10^{-13}.

Thus for purposes of this thesis $10^{-14} < \overline{\mu^2} < 10^{-12}$. Weak atmospheric turbulence corresponds to $\overline{\mu^2} = 10^{-14}$ and moderate-to-intense atmospheric turbulence corresponds to $\overline{\mu^2} = 10^{-12}$.

LIST OF SYMBOLS

P	partial pressure of dry air [m.m. Hg]
T	atmospheric temperature [°K]
p	partial pressure of water vapour [m.m. Hg]
x,y,z	cartesian spatial coordinates, $r = (x^2 + y^2 + z^2)^{1/2}$
$\hat{i},\hat{j},\hat{k}$	unit vectors along axes ox , oy , oz
t	absolute time
τ	relative time measured from the beginning of the free air laser strain meter observations
D	distance over which strain measurements are to be made through the uncontrolled atmosphere
h_k	linear approximation to the rate of change of distance between the ends of the strain meter in the k^{th} averaging interval
Δt	sampling interval of the fluctuations in atmospheric ray-path length, equal to the correlation time for light rays passing through the uncontrolled atmosphere
$\Delta\tau$	averaging interval for suppression of atmospheric fluctuations in ray-path to reveal tectonic changes in distance
s	signal noise ratio of the free air laser strain meter observations
$\lvert\xi'\rvert$	confidence parameter of free air laser strain meter observations, $0 \leq \xi' \leq \infty$.
$\eta(\lvert\xi'\rvert)$	confidence level of free air laser strain meter observations, $\eta(\lvert\xi'\rvert) = \mathrm{erf}(\lvert\xi'\rvert/\sqrt{2})$, $0 \leq \eta(\lvert\xi'\rvert) \leq 1$
$\overline{\mu^2}$	mean square refractive index fluctuation
r_o	inner scale of atmospheric turbulence
R_o	outer scale of atmospheric turbulence
$S(t)$	arc length of atmospheric ray-path at time t

ℓ_o straight line segment, a series of which are used to approximate the atmospheric ray-path. ℓ_o is equal in magnitude to the outer scale of turbulence

$U(\Delta t)$ the net fluctuation in geometric ray-path length in the interval Δt .

$X(\tau)$ the fluctuation in geometric ray-path length as a function of time τ

ℓ curve parameter for mathematical representation of atmospheric ray-path. ℓ is proportional to distance travelled parallel to the x-axis.

$\varepsilon(t)$ the extra distance, over the straight line distance, travelled by a photon when traversing the ray-path between the end mirrors of a free air laser strain meter

δS fluctuation in geometrical ray-path length

$\alpha(\ell)$ total angle between the direction of the ray and the x-axis

λ wavelength in vaccuo of laser radiation

$k = \frac{2\pi}{\lambda}$ wavenumber of laser radiation

ν frequency of laser radiation

$\omega = 2\pi\nu$ angular frequency of laser radiation

ξ, η coordinates in the plane of the rectangular diffracting apertures

x, y coordinates in the plane of the fringe observation

V fringe visibility

β total phase of laser radiation

ρ spatial variable in a plane normal to the direction of propagation of the laser beam

$D_{\beta\beta}(\rho)$ phase structure function

$C_{\mu\mu}(r)$ autocorrelation function of refractive index fluctuations

V_o minimum acceptable fringe visibility

ρ_o maximum allowable dimensions for diffracting apertures

$\vec{v} = v_x\hat{i} + v_y\hat{j} + v_z\hat{k}$ wind velocity

h Planck's constant

c velocity of light

$\theta(\lambda)$ angle of divergence of laser beam

D_o 1% power attenuation distance for laser beam propagating through the atmosphere. $D_o \sim 3.1 \times 10^4$ cm.

BIBLIOGRAPHY

1. WELLS, H. G.; A Short History of the World. The MacMillan Co., New York, 1922.

2. JACOBS, J. A., RUSSELL, R. D., WILSON, J. T.; Physics and Geology, McGraw Hill Inc., Toronto, 1959.

3. GOLD, T.; Radio Method for the Precise Measurement of the Rotation Period of the Earth. Science, v. 157, 302-304, July 21, 1967.

4. BERGSTRAND, E.; The Geodimeter System - A Short Discussion of its Principal Function and Future Development. J. Geophys. Res., v. 65, No. 2, 404-409, February 1960.

5. OWENS, J.C.; A Review of Atmospheric Dispersion Measurements in Geodesy and Meteorology. Paper presented at the Conference on "Refraction Effects in Geodesy and Electronic Distance Measurement." University of New South Wales, Sydney, Australia, November 5-8, 1968.

6. BENDER, P. L. and OWENS, J. C.; Correction of Optical Distance Measurements for the Fluctuating Atmospheric Index of Refraction. J. Geophys. Res., v. 70, No. 10, 2461-2462, May 1965.

7. THOMPSON, M. C.; Space Averages of Air and Water Vapour Densities by Dispersion for Refractive Correction of Electro-Magnetic Range Measurements. J. Geophys. Res., v. 73, No. 10, 3097-3102, May 1968.

8. HOFMANN, R. B.; Geodimeter Fault Movement Investigations in California. Publication of the Department of Water Resources, State of California, U.S.A., Bulletin No. 116-6.

9. FOWLER, R. A.; Earthquake Prediction from Laser Surveying. N.A.S.A. Report SP-5042, Scientific and Technical Information Division, Office of Technology Utilization, National Aeronautical and Space Administration, Washington, D.C., 1968.

10. BLOOM, A. L.; Gas Lasers. John Wiley and Sons, Inc., New York, 1968.

11. SCHAWLOW, A. L. and TOWNES, C. H.; Infrared and Optical Masers. Phys. Rev., v. 112, No. 6, 1940-1949, December 15, 1958.

12. BIRNBAUM, G.; Frequency Stabilization of Gas Lasers. Proc. I.E.E.E., v. 55, No. 6, 1015-1025, June 1967.

13. WHITE, A. D.; Frequency Stabilization of Gas Lasers. I.E.E.E., J. Quantum Electronics, v. QE-1, No. 8, 349-357, November 1965.

14. VALI, V.; Measuring Earth Strains by Laser. Scientific American, v. 221, No. 6, 89-95, December 1969.

15. VALI, V.; Strains Recorded on a High Magnification Interferometric Seismograph. Nature, v. 220, 1018-1020, December 7, 1968.

16. VALI, V., KROGSTAD, R. S., MOSS, R. W.; Observation of Earth Tides Using a Laser Interferometer. J. Applied Phys., v. 37, No. 2, 580-582, February 1966.

17. PRESS, F.; Displacements, Strains, and Tilts at Teleseismic Distances. J. Geophys. Res., v. 70, No. 10, May 15, 1965.

18. HONKASLO, T.; Measurement of Standard Baselines with the Väisälä Light Interference Comparator. J. Geophys. Res., v. 65, No. 2, 457-460, February 1960.

19. ERICKSON, K. E.; Long-Path Interferometry through an Uncontrolled Atmosphere. J. Opt. Soc. America, v. 52, No. 7, 781-788, July 1962.

20. OWENS, J. C.; Optical Refractive Index of Air: Dependence on Pressure, Temperature, and Composition. Applied Optics, v. 6, No. 1, 55-58, January 1967.

21. TILTON, L. W.; Standard Conditions for Precise Prism Refractometry. J. Res. Nat. Bureau of Standards, v. 14, 393-418, April 1935.

22. BECKMANN, P.; Signal Degeneration in Laser Beams Propagated through a Turbulent Atmosphere. J. Res. Nat. Bureau of Standards, v. 69-A, No. 4, 629-640, April 1965.

23. LUMLEY, J. L. and PANOFSKY, H. A.; The Structure of Atmospheric Turbulence. John Wiley & Sons, Inc., New York, 1964.

24. STROHBEHN, J. W.; The Feasibility of Laser Experiments for Measuring Atmospheric Turbulence Parameter. J. Geophys. Res., v. 71, No. 24, 5793-5808, December 15, 1966.

25. TATARSKI, V. I.; Wave Propagation in a Turbulent Medium. Translated by R. A. Silverman, Dover Books Inc., New York, 1961.

26. CHERNOV, L. A.; Wave Propagation in a Random Medium. Translated by R. A. Silverman, Dover Books Inc., New York, 1960.

27. CHANDRASEKHAR, S.; Stochastic Problems in Physics and Astronomy. Reviews of Modern Physics, v. 15, No. 1, 1-89, January 1943.

28. Handbook of Mathematical Functions. M. Abramowitz and I. Stegun Ed., Dover Publications Inc., New York, 1965.

29. GRADSHTEYN, I. S. and RYZHIK, I. M.; Tables of Integrals Series and Products. Translated by A. Jeffrey, Academic Press, New York, 1965.

30. DEITZ, P. H.; Optical Method for Analysis of Atmospheric Effects on Laser Beams. Proc. Symposium on Modern Optics, Polytechnic Institute of Brooklyn, 757-774, March 1967.

31. ROUSE, H.; Advanced Mechanics of Fluids. P. 282, John Wiley and Sons Inc., 1959.

32. FRIED, D. L. and CLOUD, J. D.; Atmospheric Turbulence and Its Effect on Laser Communication Systems. 2nd Report, Electro-optical Laboratory Technical Memorandum #91, North American Aviation Inc., Space and Information Systems Division, June 15, 1964.

33. WANG, M. C., and UHLENBECK, G. E.; On the Theory of the Brownian Motion. Rev. Modern Phys., v. 17, Nos. 2 and 3, 323-342, April-July 1945.

34. LONGHURST, R. S.; Geometrical and Physical Optics. 2nd Ed., p. 104, Longmans, London Inc., 1967.

35. BORN, M. and WOLFE, E.; Principles of Optics. Chapt. 10, 3rd Rev. ed., Pergamon Press, New York, 1965.

36. DE BROGLIE, L.; New Perspectives in Physics. Chapt. 1, Basic Books Inc., New York, 1962.

37. JONES, R. C.; Information Capacity of Radiation Detectors. J. Op. Soc. America, v. 52, No. 11, 1193-1200, November 1962.

38. ASHFORD, R. D.; personal communication.

39. VALI, V.; Some Earth Strain Measurements with Laser Inferometer. Earthquake Displacement Fields and the Rotation of the Earth, 206-216, D. Reidel Pub. Co., Holland, 1970.

40. CLOUD, J. D. and FRIED, D. L.; The Significance of the Inner Scale of Turbulence to the Phase Structure Function. Electro-optical Laboratory Technical Memorandum #120, North American Aviation, Inc., Space and Information Systems Division, July 1964.

41. SMYLIE, D. E.; personal communication.

42. GANGI, A. F.; Error Analysis of a Laser Strain Meter. Earthquake Displacement Fields and the Rotation of the Earth, 217-229, D. Riedel Pub. Co., Holland, 1970.

43. BENDER, P. L.; Laser Measurements of Long Distances. Proc. J.E.E.E., v. 55, No. 6, 1039-1045, June 1967.

44. CONSORTINI, A., RONCHI, L., STEFANUTTI, L.; Investigation of Atmospheric Turbulence by Narrow Laser Beams. Applied Optics, v. 9, No. 11, 2543 - 2547, November 1970.